University of Padova

Department of *Surgery, Oncology and Gastroenterology*

PhD COURSE IN
ONCOLOGY AND SURGICAL ONCOLOGY
XXIX CYCLE

IDENTIFICATION OF A HLA-A*0201-RESTRICTED IMMUNOGENIC EPITOPE FROM THE UNIVERSAL TUMOR ANTIGEN DEPDC1

Coordinator: Prof. Paola Zanovello

Supervisor: Prof. Antonio Rosato

Tutor: Dr. Roberta Sommaggio

PhD Candidate: Anna Tosi

INDEX

SUMMARY

The identification of universal tumor-specific antigens (TSA) shared between multiple patients and/or multiple tumors is of great importance to overcome the practical limitations of personalized cancer immunotherapy. Recent studies support the involvement of DEPDC1 in many aspects of cancer traits, such as cell proliferation, anti-apoptosis and cell invasion, suggesting that it may play key roles in the oncogenic process. In this study, we report that DEPDC1 expression is up-regulated in several types of human tumors, and closely linked to a poorer prognosis; therefore, it might be regarded as a novel universal oncoantigen potentially suitable for targeting many different cancers. In this regard, we report the identification of an immunogenic DEPDC1-derived epitope restricted for the HLA-A*0201 molecule, which is able to induce cytotoxic T lymphocytes (CTL) exerting a strong and specific functional response *in vitro* in response not only to peptide-loaded cells but also to triple negative breast cancer (TNBC) cells endogenously expressing the DEPDC1 protein. Such CTL are also therapeutically active against human TNBC xenografts *in vivo* upon adoptive transfer in immunodeficient mice. Overall, these data provide evidences that this DEPDC1-derived antigenic epitope can be exploited as a new tool for the development of immunotherapeutic strategies for HLA-A*0201 patients with TNBC, and potentially many other cancers. Moreover, we plan to employ an approach of multiplexing digital pathology to study the intimate relationships that adoptively transferred lymphocytes can establish with TNBC cells in tumor-bearing mice, as further advances in immunotherapy approaches require a detailed understanding of cell dynamics within the tumor microenvironment. The benefits of multispectral immunohistochemistry, combined with the development of software for quantitation, are making this methodology an increasingly powerful tool in the analysis and characterization of tissue and cellular processes, supporting diagnostic potential in order to improve therapies.

RIASSUNTO

L'identificazione di antigeni tumore-specifici universali condivisi tra più pazienti e/o tra più tumori diversi, è di grande importanza per superare le limitazioni pratiche dell'immunoterapia oncologica personalizzata. Il coinvolgimento di DEPDC1 in molti aspetti del processo tumorale, come, ad esempio, nella proliferazione cellulare, nell'anti-apoptosi e nell'invasione cellulare, è stato supportato da lavori pubblicati di recente, suggerendo che tale proteina possa svolgere ruoli chiave nel processo oncogeno. In questo studio riportiamo che l'espressione di DEPDC1 è sovra-regolata in molti tipi di tumori umani, e strettamente collegata ad una prognosi avversa; per questo motivo DEPDC1 può essere considerato come un nuovo antigene tumorale universale potenzialmente adatto per il *targeting* di molti tumori diversi. A questo proposito, riportiamo l'identificazione di un epitopo immunogenico derivato da DEPDC1 ristretto per la molecola HLA-A*0201, capace di indurre linfociti T citotossici (CTL) esercitanti una forte e specifica risposta funzionale *in vitro*, in risposta non solo a cellule caricate con il peptide ma anche in risposta a cellule di tumore al seno triplo negativo (TNBC) che esprimono in modo endogeno la proteina DEPDC1. Tali CTL sono anche attivi in modo terapeutico *in vivo,* in seguito al loro trasferimento adottivo in topi immunodeficienti, nei confronti di xenotrapianti di cellule di TNBC umane. Complessivamente, questi dati forniscono evidenze a supporto dell'uso di questo epitopo antigenico derivante da DEPDC1 come un nuovo strumento per lo sviluppo di strategie immunoterapeutiche per pazienti HLA-A*0201 con TNBC, e potenzialmente con molti altri tipi di tumore. Inoltre, poiché ulteriori miglioramenti negli approcci di immunoterapia necessitano di una comprensione dettagliata delle dinamiche cellulari all'interno del microambiente tumorale, programmiamo di usare un approccio di *multiplexing digital pathology* per studiare le strette relazioni che i linfociti adottivamente trasferiti possono stabilire con le cellule di TNBC in topi portanti il tumore. I benefici dell'immunoistochimica multispettrale, combinati con lo sviluppo di software per la quantificazione, stanno rendendo questa metodologia un strumento sempre più potente nell'analisi a nella caratterizzazione di processi tessutali e cellulari, supportando il potenziale diagnostico con lo scopo di migliorare le terapie.

INTRODUCTION

1. Cancer and the immune system

Immunology, long considered not to be a critical discipline to understand cancer mechanisms, has provided today new important evidences for a comprehensive view of tumor biology. Until recently, investigations into the nature of cancer focused strictly on the cancer cells and on cancer as a genetic disease, while nowadays there is an increased emphasis on studying cancer as a systemic disease; this has led to move the focus to the host and to the microenvironment in which the cancer grows, such as the immune system. As a result, in 2011 a new picture of cancer has emerged: cancer is considered to be able to modify or reprogram its cellular metabolism, to maintain its genome instable and mutable, to avoid immune destruction, and, finally, to induce the chronic inflammation that promotes its growth rather than elimination [1]. The last two hallmarks highlight the newly recognized dual interaction between cancer and the immune system.

The first indication that the immune system can recognize and reject tumors, a concept known as cancer immunosurveillance, came from animal models in which tumors were rejected. In particular, mice lacking an intact immune system were shown to be more susceptible to carcinogen-induced and spontaneous cancers, as compared with their immunocompetent counterparts [2]. Studies of cancer-immune system interactions revealed that every known innate and adaptive immune effector mechanism participates in tumor recognition and control [3]. The first few transformed cells are detected by NK cells through specific ligands on surface of tumor cells. This leads initially to their destruction, and then to the uptake and processing of their fragments by the macrophages and dendritic cells that in turn, are activated to secrete inflammatory cytokines, such as Interferon-γ (IFN-γ). The tumor cell-derived peptides are then presented to $CD8^+$ and $CD4^+$ T cells on the Human Leucocyte Antigen (HLA) class I and II, respectively. The activation of T lymphocytes leads to the production of additional cytokines that further promote activation of innate immunity, and support the expansion and production of tumor-specific cytotoxic T cells (CTL) and antibodies by B lymphocytes. B cells secrete specific antibodies causing the lysis or the phagocytosis of cells that display tumor antigens, while CTLs use their T cell receptor (TCR) to specifically recognize small cell-derived peptides presented on cell surface bound to MHC class I molecules, and release cytotoxic molecules and cytokines that kill the tumor

cells and activate nearby immune cells. $CD4^+$ helper T cells promote the activation of both B cells and CTLs. In this way, the adaptive immune system can eliminate remaining tumor cells and, importantly, can generate an immune memory to specific tumor components that prevent tumor recurrence. On the other hand, immunity shapes the intrinsic nature of developing tumors through the immunological pressure afforded by cancer immunosurveillance. The combination of the host-protective and the tumor-sculpting functions of the immune system during the tumor development is termed cancer immunoediting [4]. This process can have at least three different but related outcomes: elimination, equilibrium and escape [5] (Figure 1). A highly immunogenic tumor in a immunocompetent individual will results in optimal stimulation of the innate immune system leading to the production of immunostimolatory cytokines, acute inflammation and activation of a large number of T and B cells, which make possible a prompt elimination of the arising tumor. A less immunogenic tumor leads to the survival of some cancer cells that nevertheless remain under immunosurveillance. Into this dynamic equilibrium phase, the slow growth of the tumor would be accompanied by repeated activation of the immune system and the elimination of some tumor cells, followed by further cycles of tumor regrowth and immune-mediated destruction. During this period of Darwinian selection, many of the original escape variants of the tumor cells are destroyed, but new variants arise, carrying different mutations that provide resistance to the immune attacks. The equilibrium phase is the longest of the three processes and could last life-long, or be disturbed by changes in the tumor that allow it to avoid immunosurveillance (i.e. the loss of tumor antigens or co-stimolatory molecules [6]) or changes in the immune system that weak the tumor surveillance (i.e. factors secreted by tumor cells that inhibit T cells, such as TGF-β). The tumor escape is caused also by an increase of immunosuppressive cells, such as regulatory T cells (Treg), myeloid-derived suppressor cells (MDSC), immunosuppressive cytokines derived from Treg, MDSC and tumor cells, and co-inhibitory molecules that inhibit the T cell activation, such as CTLA-4 and PD-1 [7]. This results in a clinically observable malignant disease.

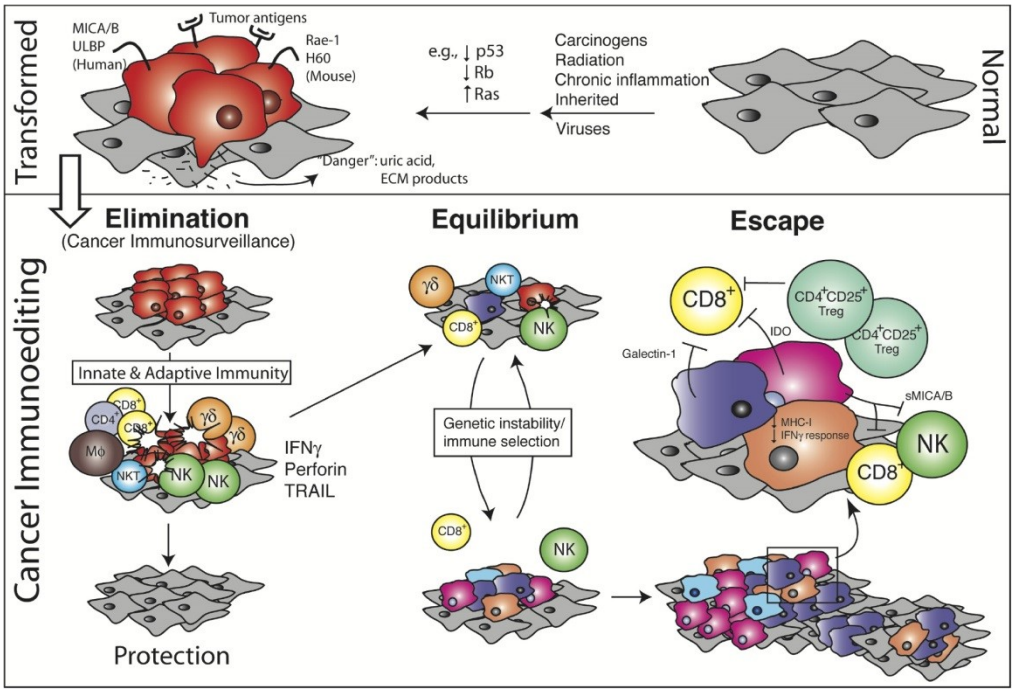

Figure 1. The three phases of the cancer immunoediting process. Normal cells (gray) subject to common oncogenic stimuli ultimately undergo transformation and become tumor cells (red) (top). Even at early stages of tumorigenesis, these cells may express distinct tumor-specific markers and generate proinflammatory "danger" signals that initiate the cancer immunoediting process (bottom). Image from Dunn et al. *Immunity*, 2004.

2. Tumor antigens

Effectors of adaptive immunity, such as $CD4^+$ helper T cells, $CD8^+$ cytotoxic T cells and antibodies specifically target tumor antigens. The molecular nature of antigens recognized by CTL on tumors was revealed in 1989, when Lurquin et al. showed that a mouse tumor-specific CTL population recognized a peptide derived from a self-protein, mutated in cancer cells [8]. This observation led to the concept that MHC class I molecules continuously display on the cell surface peptides of 8 to 10 amino acids that are derived from a wide variety (if not all) of intracellular proteins processed by the proteasome (the so called "antigen processing pathway") [9]. In tumors, some of these peptides originate from altered or aberrantly expressed proteins, thereby marking the cells for CTL recognition and killing through the release of cytotoxic molecules and cytokines that stimulate the activation of adjacent immune cells [10] (Figure 2).

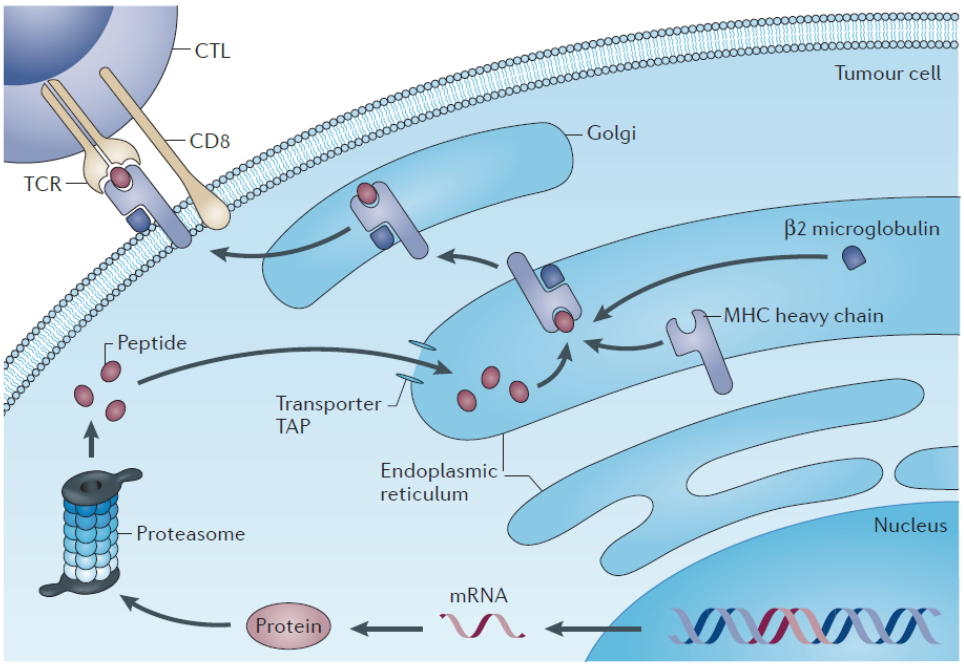

Figure 2. Processing of tumor antigens that are recognized by CD8+ T cells. Image from Coulie et al. *Nature Reviews Cancer*, 2014.

Tumor antigens have been tested as vaccines, targets for monoclonal antibodies and targets for adoptively transferred cytotoxic T cells. To be safe and efficient, immunotherapy strategies should elicit efficient T cell responses against antigenic peptides that are present on tumor cells but not on healthy cells, in order to avoid autoimmune side effects [11]. Such cancer rejection epitopes may be derived from two classes of antigens: a first one is formed by Tumor-Associated Antigens (TAA), which are highly overexpressed in tumors but can also be found in normal tissues; the second class is formed by Tumor-Specific Antigens (TSA), which are exclusively expressed in tumor tissues (Figure 3).

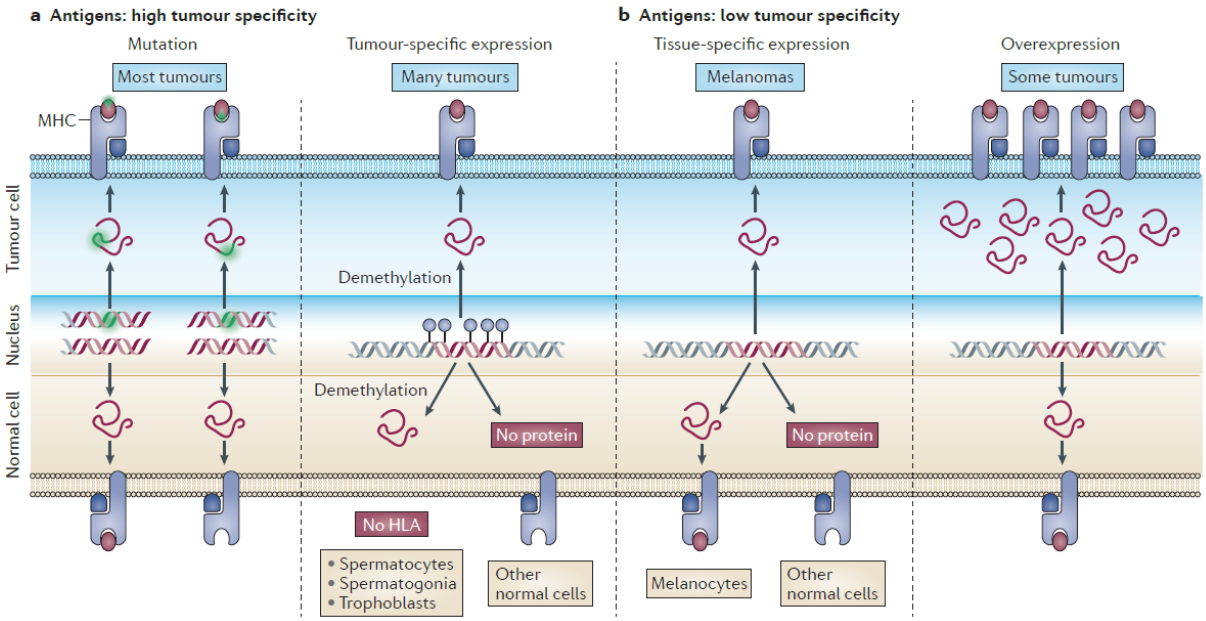

Figure 3. Classes of human tumor antigens that are recognized by T lymphocytes. Image from Coulie et al. *Nature Reviews Cancer*, 2014.

2.1 Tumor-associated antigens (TAA)

This category of antigens comprises differentiation antigens and antigens derived from genes that are overexpressed in tumors [12].

- **Differentiation antigens.** Differentiation antigens are derived from proteins that are expressed only in a given type of tumor and in the corresponding healthy tissue. Most of differentiation antigens identified thus far are present on melanoma cells, in which the corresponding protein is often involved in melanin biosynthesis or melanosome biogenesis [13]. Interestingly, spontaneous responses to peptides derived from proteins such as tyrosinase [14], gp100 [15], Melan-A/MART-1 [16] or gp75/TRP1 [17] are frequent in melanoma patients and healthy donors [18], suggesting that central tolerance to these antigens is not complete. T cell responses to differentiation antigens can lead to vitiligo, a partial skin depigmentation often observed in melanoma patients and generally associated with a good prognosis [19]. Peptides were also identified from the prostate specific antigen (PSA) and the prostatic acidic phosphatase, two proteins expressed in normal prostate and tumor prostate tissues [20,21]. Moreover, the carcinoembryonic antigen (CEA) is often highly expressed in colorectal cancer and

other epithelial tumors but is also present at lower level in a variety of normal epithelial cells of the intestinal tract [22]. Antigens of this group are not tumor-specific, so their use as targets for cancer immunotherapy may result in autoimmunity towards the corresponding normal tissue, if not removed, as the case of PSA [23].

- **Overexpressed antigens.** Overexpression of proteins in tumors may provide an opportunity for a specific T cell response, as a threshold level of antigen expression on the cell surface is required for recognition by T cells. However, the reliability of the quantification of their amounts on the surface of cancer cells versus normal cells is difficult to define [24]. Examples of peptides derived from overexpressed genes include those derived from the inhibitor of apoptosis protein Survivin [25], the wild-type p53 protein [26], the oncogene and growth factor receptor ERBB2 (HER2/NEU), which is overexpressed in many epithelial tumors including ovarian and breast carcinoma [27]. Peptides are also derived from the protein Wilms tumor 1 (WT1), a transcription factor expressed at 10- to 1000-fold higher levels in leukemic versus normal cells [28]. In leukemia patients receiving an allogenic hematopoietic cell transplant, followed by an infusion of donor-derived CTL recognizing the WT1-derived HLA-A2-restricted peptide, a decrease in the number of leukemic cells was observed, without evidence of autoimmune toxicity [29]. As overexpressed antigens are shared by numerous tumors, they represent attractive targets for the development of immunotherapy; however, their use is not devoid of the risk of developing autoimmune reactions due to the low but still detectable expression of the corresponding genes in healthy tissues.

2.2 Tumor-specific antigens (TSA)

There are three classes of antigens with a tumor-specific expression pattern [12]: antigens derived from viral proteins, from point mutations, and encoded by cancer-germline genes. As compared with tumor-associated antigens, TSA have been postulated to be of particular relevance to tumor control, as the quality of T cell pool that is available for these antigens is not affected by central T cell tolerance [30].

- **Viral antigens.** Viruses are at the origin of several types of cancers, for example cervical carcinoma, nasopharyngeal carcinoma, hepatocarcinoma and some leukemias [31]. Vaccines containing long Human papilloma virus peptides (HPV) recently emerged as a promising therapeutic modality for HPV-related cancers, as they increase the number and activity of HPV-16-specific $CD4^+$ and $CD8^+$ T cells [32].

- **Antigens encoded by mutated genes.** Many CTL isolated from the blood or tumors of cancer patients were found to recognize antigens that arise from point mutations in ubiquitously expressed genes [33]. In most cases, the mutation changes one amino acid in the peptide sequence, either enabling the peptide to bind to the MHC class I molecule or creating a new antigenic determinant that is recognized by the CTL. In some cases, the mutation causes a frameshift leading to the production of a new antigenic peptide [34]. The CDK4 gene mutation, for example, affect the binding of CDK4 to its inhibitor p16/INK4a receptor, favoring uncontrolled cell division [35]. In most cases, however, these mutations are passenger mutations (mutations that have no effect on the fitness of the tumor but may be associated with a clonal expansion) and the corresponding antigenic peptides are unique to the tumors in which they were identified. Tumors with a high mutation rate, such as melanoma or lung carcinoma, have more mutated antigens and therefore they are more immunogenic [36]. Another oncogenic process involves chromosomal translocations. In this case, the breakpoints can code for chimeric peptides that can be processed in the tumor cells and presented on HLA molecules. Such peptides from BCR-ABL or ETV6-AML1 fusion proteins are recognized by T cells in leukemic patients [37,38].

- **Cancer-germline genes.** This class of tumor-specific antigens are expressed in a wide variety of cancer types but not in normal tissues except in testicular germline and placenta trophoblastic cells, and include the melanoma-antigen encoding (MAGE) [39], BAGE [40] and GAGE [39] gene families, all located on the X chromosome. Their tumor-specific pattern expression results from the demethylation of their promoter sequence, as part of a genome-wide demethylation that takes place in male germ cells and in some advanced cancers [41]. Because male germline cells and trophoblastic cells do not display MHC class I molecules on their surface [42], they cannot display antigens to T

cells. This class of antigens appear to be strictly tumor-specific and their use as immunotherapeutic targets in cancer vaccination or in adoptive T cells transfer should not be deleterious to the patient.

3. Cancer immunotherapy

Immunotherapy, which aims to enhance the cancer patient's immune system by improving its ability to recognize the tumor or providing a missing immune effector function, is a treatment approach that holds promise of a life-long cure [43]. The most convincing evidence for existence of antitumor activity came from clinical trials performed in the late 1980s. These trials showed that some metastatic melanoma and renal cell carcinoma patients experienced dramatic tumor regressions in response to treatment with the cytokine interleukin (IL)-2, which was known to have no direct tumoricidal capacity but was instead a potent activator of cytotoxic T lymphocytes [44]. Although most patients progressed on IL-2 therapy, almost 15% of patients had objective responses, and half of these went on to be completely cured [45,46]. These results led the US Food and Drug Administration (FDA) to approve IL-2 in the late 1990s as the first bona fide immunotherapy for the treatment of cancer patients. They also inspired several research studies over the past two decades, to develop alternative immunotherapies with better safety and efficacy and to improve the understanding of IL-2 mechanism of action. Over the last decade, great efforts have been dedicate to the development of interventions that mediate antineoplastic effects by initiating a novel or boosting an existing immune response against neoplastic cells [47,48]. This intense wave of preclinical and clinical investigation culminated with the approval of various immunotherapeutic interventions for use in humans. Clinical studies are being initiated at an ever accelerating rate to test the safety and efficacy of various immunotherapeutic regimens in cancer patients, either alone or combined with other antineoplastic agents [49]. The hopes generated by these approaches are immense, and several other forms of immunotherapy are expected to obtain regulatory approval within the next few years (Figure 4).

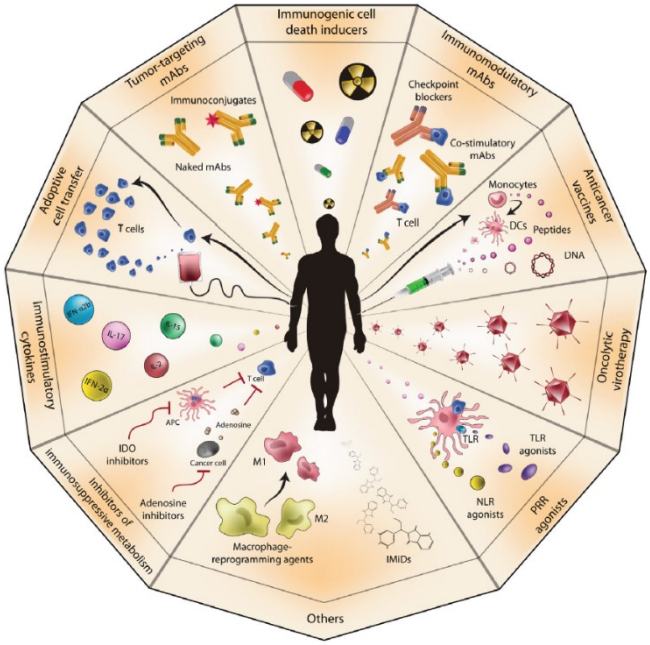

Figure 4. Anticancer immunotherapy. Image from Galluzzi et al. *Oncotarget,* 2014.

Anticancer immunotherapies are generally classified as “active” or “passive” based on their ability to activate the host immune system against cancer cells. In this way, anticancer vaccines and checkpoint inhibitors exert anticancer effects only upon the engagement of the host immune system, constituting clear examples of active immunotherapy [50,51]. Conversely, tumor-targeting monoclonal antibodies (mAbs) and adoptively transferred T cells are considered passive forms of immunotherapy, as they are endowed with intrinsic antineoplastic activity [52,53]. An alternative classification of immunotherapeutic anticancer regimens is based on antigen-specificity: thus, while tumor-targeting mAbs are widely considered antigen-specific interventions, immunostimolatory cytokines or checkpoint blockers activate anticancer immune responses of generally broad specificity.

3.1 Active immunotherapy

- **DC-based immunotherapy.** Several forms of DC-based immunotherapy have been developed, most of which involve the isolation of patient- or donor-derived circulating monocytes and their amplification, differentiation and maturation *ex vivo* [54]. More often, autologous DCs are re-infused into cancer patients upon exposure to a source of

TAAs, including TAA-derived peptides [55], mRNAs coding for one or more specific TAAs [56], expression vectors coding for one or more specific TAAs [57], bulk cancer cell lysates [58] or bulk cancer cell-derived mRNA [59]. As an alternative, DCs are allowed to fuse *ex vivo* with inactivated cancer cells, generating the dendritomes [60]. The rationale behind of these approaches is that DCs loaded *ex vivo* with TAA or TAA-coding molecules, become able to prime TAA-targeting immune responses upon reinfusion in cancer patients. TAA are fused to mAbs, polypeptides or carbohydrates that selectively bind to DCs [61,62], encapsulated in DC-targeting immunoliposomes [63] or encoded by DC-specific vectors [64]. Sipuleucel-T (also known as Provenge) was the first therapeutic DC-based cancer vaccine approved in 2010 by FDA for the therapy of asymptomatic or minimally symptomatic metastatic castration-refractory prostate cancer [65]. Sipuleucel-T consist of autologous professional antigen-presenting cells (APCs) activated with a fusion protein (PA2024) between the prostatic acid phosphatase and the immunostimolant GM-CSF. Despite an overall survival benefit of 4.1 months was demonstrated compared to placebo, the challenge of producing sufficient vaccine for the target population and the costs of this treatment led the producing company (Dendreon) to stop production and bankruptcy [66].

- **Peptide- and DNA-based anticancer vaccines.** A successful therapeutic cancer vaccine activates the cancer patient's immune system, resulting in eradication or long-term control of disease. A vaccine typically consists of a full-length recombinant TAAs or peptides in an immunogenic formulation (adjuvants which promote DC maturation) administered to cancer patients, most often intramuscularly, subcutaneously or intradermally [67,68]. In this way, resident DCs (or other APCs) acquire the ability to present the TAA-derived epitopes while maturing, hence priming a robust TAA-specific immune response. The mechanisms underlying the priming of anticancer immune responses by peptide-based vaccines, and therefore their efficacy, depend (at least in part) on their size. Thus, while short peptides (8-12 amino acids) are designed to directly bind to MHC molecules expressed on the surface of APCs, long peptides (25-30 residues) must be endocytosed, processed and presented by APCs for eliciting an immune response [50]. Normally, the therapeutic activity of long peptides is superior to the short counterparts, especially when they include epitopes recognized by both CTL

and $CD4^+$ helper T cells, or when conjugated to efficient adjuvants [69]. A peculiar type of peptide-based vaccines include autologous tumor lysates complexed with immunostimulatory chaperons. However, generating personalized anticancer vaccines is associated with considerable costs [70].

DNA-based anticancer vaccines are based on TAA-coding constructs, naked or vectored by viral particles, non-pathogenic bacteria or yeast cells, and transform APCs or muscular cells that become a source of such TAA [71]. A particularly interesting approach in this context is represented by oncolytic viruses genetically altered to code for the TAA, called oncolytic vaccines [72]. The most successful cancer vaccine to date is the vaccination against human papilloma virus (HPV) [73] to prevent the cervical cancer.

- **Immunostimolatory cytokines.** Various attempts have been made to harness the biological potency of specific cytokines to elicit novel or reinvigorate pre-existent tumor-targeting immune responses [74]. The administration of most of the immunostimolatory cytokines alone to cancer patients, is however associated with little, if any, clinical activity, and hence they are generally used as adjuvants [75]. Notable exceptions are the use of interferon (IFN)-α2b (Intron A), currently approved by the FDA for the therapy of hairy cell leukemia (HCL), AIDS-related Kaposi's sarcoma, follicular lymphoma, multiple myeloma, melanoma and cervical intraepithelial neoplasms [76], and the use of IL-2 (Proleukin), which has, as single agent, therapeutic activity in patients with metastatic renal cell carcinoma or malignant melanoma [77].

- **Immunomodulatory mAbs.** This class of mAbs are able to interact with soluble or cellular components of the immune system, altering their functions [78]. There are four general strategies: (1) the inhibition of immunosuppressive receptors expressed by activated T lymphocytes, such as cytotoxic T lymphocyte-associated protein 4 (CTLA4) [79] and programmed cell death 1 (PD-1) [80]; (2) the inhibition of the principal ligands of these receptors, such as the PD-1 ligand (PD-L1) [81]; (3) the activation of co-stimolatory receptors expressed on the surface of immune effector cells, such as tumor necrosis factor receptor superfamily [82]; (4) the neutralization of immunosuppressive factors released in the tumor microenvironment, such as transforming growth factor β1 (TGFβ1) [83]. The first of these approaches, commonly referred as "checkpoint blockade",

has been shown to induce robust and durable responses in cohorts of patients with a variety of solid tumors [84]. The anti-CTLA4 mAb Ipilimumab (Yervoy) was licensed by the FDA in 2011 for use against unresectable or metastatic melanoma [85], while the anti-PD-1 mAb Pembrolizumab (Keytruda) was approved by FDA in 2014 for the treatment of advanced or unresectable melanoma patients who fail to respond to other therapies [86]. Preclinical data suggest that combining checkpoint blockers with co-stimulatory mAb has better antineoplastic effects [87].

3.2 Passive immunotherapy

- **Tumor-targeting mAbs.** This form of anticancer immunotherapy is the best characterized and perhaps the most widely employed in the clinic [88]. There are at least five functionally distinct tumor-targeting mAbs variants: (1) naked mAbs that inhibit signaling pathways required for the survival or progression of neoplastic cells, but not of their non-malignant counterparts, such as the epidermal growth factor receptor (EGFR)-specific mAb Cetuximab, which is approved by the FDA for the treatment of head and neck cancer and colorectal carcinoma [89,90]; (2) naked mAbs that activate potentially lethal receptors expressed only on the surface of malignant cells, such as Tigatuzumab (CS-1008), a specific mAb for a member of tumor necrosis factor receptor superfamily (TRAILR2) that is currently under clinical development [91]; (3) immune conjugates, i.e. TAA-specific mAbs coupled to toxins or radionuclides, such as Gemtuzumab ozogamicine, an anti-CD33 calicheamicin conjugate currently approved for use in acute myeloid leukemia patients [92]; (4) naked TAA-specific mAbs that opsonize cancer cells and hence activate antibody-dependent cell-mediate cytotoxicity (ADCC) [93], antibody-dependent cellular phagocytosis [94], and complement-dependent cytotoxicity (CDC) [95], such as the CD20-specific mAb Rituximab, which is currently approved for the treatment of B-cell lymphomas, chronic lymphocytic leukemia and non-Hodgkin lymphoma [96,97]; (5) and finally the so called “bispecific antibodies” formed by chimeric proteins consisting of two single-chain variable fragments from distinct mAbs, one targeting a TAA and one specific for a T cell surface antigen (for example Blinatumomab, a CD19- and CD3 bispecific antibody recently approved for the therapy

of Philadelphia chromosome-negative precursor B-cell acute lymphoblastic leukemia) [98].

The selection of tumor antigens suitable for antibody targeting and therapy, requires a comprehensive analysis of their expression on tumor and normal tissue, and their biologic role in tumor growth. If the mAb has to bind to cell surface receptors to activate or inhibit signaling, or to promote the ADCC or CDC, the antigen-mAb complex should not be rapidly internalized. Whether this is the case, the Fab and Fc regions have more chances to appropriately engage surface receptors, and immune effector cells and/or complement proteins, respectively. In contrast, the internalization is desirable for antibodies delivering toxins into cancer cell and for antibodies that downregulate cell surface receptors [99].

- **Adoptive cell therapy (ACT).** Cancer immunotherapy using T cells represents a prominent form to treat malignant diseases and has multiple advantages compared to other immunotherapies: (1) T cell responses are specific and can distinguish cancerous from healthy tissue; (2) T cells responses are robust, they undergo up to 1,000-fold clonal expansion after the activation; (3) T cell response can traffic to the site of antigen expression, suggesting a mechanism for eradication of distant metastases; (4) T cell responses have memory, and thus maintain therapeutic effect for many years after initial treatment. ACT is conceptually distinct from dendritic cell-based approaches (which de facto constitute cellular vaccines without an intrinsic anticancer activity [100]) and allogenic hematopoietic stem cell transplantation (which can be employed for the therapy of hematopoietic tumors [101]) as it involves the isolation and expansion of autologous circulating or tumor-infiltrating lymphocytes from patient's blood or tumor, their activation *ex vivo* against defined tumor antigens and their subsequent re-administration to the lymphodepleted patients, most often in combination with immunostimolatory agents such as massive doses of IL-2 [52]. Rosemberg and colleagues demonstrated that the infusion of autologous *ex vivo* expanded tumor-infiltrating lymphocytes (TIL) can induce objective clinical responses in metastatic melanoma [102]. While these results represented a stunning breakthrough in melanoma treatment, the protocol could not be applied to patients who lacked readily detectable T cell responses, or to cancers in which TIL culture remained a challenge. For example, both

breast and colon cancers have been found to contain TILs; however, their antigen specificities are still incompletely defines, and a significant proportion of those lymphocytes has suppressive rather than anti-tumor activity [103]. Recently, sufficient TILs were isolated from cholangiocarcinoma patients to induce remission, but responses to epithelial cancers cells remained rare [104]. Tumor-specific T cell clones can be generated from repeated antigen-specific stimulation of patient-derived or donor-derived T cells *in vitro* [105]. For example, a recent pilot study explored the use of allogenic $CD8^+$ T cells with activity against WT1 in leukemia patients. Clones were generated by leukapheresis of HLA-matched donor cells and repeated stimulation with autologous peptide-pulsed dendritic cells over several months. Adoptively transferred lymphocytes remained long-term detectable in patient blood, and transient responses were observed in 2/11 of these high relapse-risk patients, with stable disease observed in 3 others [29]. Similar approaches have been used in melanoma [106] and ovarian cancer [107]. Genetic engineering improved the therapeutic potential of ACT endowing peripheral blood lymphocytes (PBLs) with features such as a unique antigen specificity [108], an increased proliferative potential and persistence *in vivo* [109], an elevated tumor-infiltrating capacity [110], and higher cytotoxicity [111].

The specificity of T cells can be altered prior to re-infusion by genetically modifying them to express a high-affinity TAA-specific T cell receptor (TCR) [112], or a chimeric antigen receptor (CAR), a transmembrane protein composed of the TAA-binding domain of an immunoglobulin linked to one or more immunostimolatory domains of T cell signaling molecules [113]. Several clinical trials have already demonstrated the therapeutic potential of T cells expressing transgenic TCR or CAR, in particular for patients affected by hematological malignancies [114]. In spite of promising preclinical findings, the adoptive transfer of purified natural killer cells to cancer patients has been associated with limited therapeutic activity [115,116]. Conversely, a subset of natural killer T lymphocytes called “cytokine-induced killer (CIK) cells” was first discovered in the 1990s and can be generated from lymphocytes by the timed addition of IFN-γ, a mAb directed against CD3 (OKT3) and IL-2 *in vitro* [117]. Compared to standard lymphokine-activated killer (LAK) cells, numerous studies have demonstrated that CIK cells possess enhanced cytotoxic anti-tumor activity against different tumor cells both *in vitro* and *in vivo* [118]. Furthermore, our laboratory demonstrated for the first time that

CIK cells express CD16 in a donor-dependent manner, and that the concurrent administration of therapeutic mAbs leads to a significant improvement of their antitumor activity, triggering a potent ADCC activity [119]. Collectively, although no ACT protocol is currently approved by the FDA, adoptive cell therapy represents a powerful approach to expand the benefits of cancer immunotherapy to non-responsive patients and non-immunogenic tumors, which represent the majority of human cancers.

4. DEPDC1

In 2007, Kanehira et al. [120] identified and characterized a novel gene, *DEPDC1* (DEP domain containing 1) significantly overexpressed in the great majority of bladder cancer cells, but not expressed in normal human tissues, except the testis. The up-regulation of DEPDC1 was found in other several types of human cancers including multiple myeloma, breast cancer, hepatocellular carcinoma, lung adenocarcinoma and glioblastoma [121–125]. Furthermore, a high expression of DEPDC1 is also associated with worse prognosis in patients with multiple myeloma and hepatocellular carcinoma [121,125]. Recent studies demonstrated that DEPDC1 is upregulated also in breast cancer brain metastasis compared with non-neoplastic tissues [126]. Located in 1p31.2, DEPDC1 has two transcriptional variants, denoted as DEPDC1 isoform 1 (DEPDC1-V1: GeneBank Accession AB281187) and DEPDC1 isoform 2 (DEPDC1-V2: GeneBank Accession AB281274) consisting of 5318 and 4466 nucleotides that encode 811 and 527 amino-acid proteins (93.1 KDa and 61.5 KDa, respectively). The DEPDC1-V1 variant consists of 12 exons while DEPDC1-V2 isoform lacks exon 8 (852 nucleotides). Both variants contain a highly conserved DEP domain, and interact in the nucleus with the zing finger transcription factor ZNF224 [120] (Figure 5).

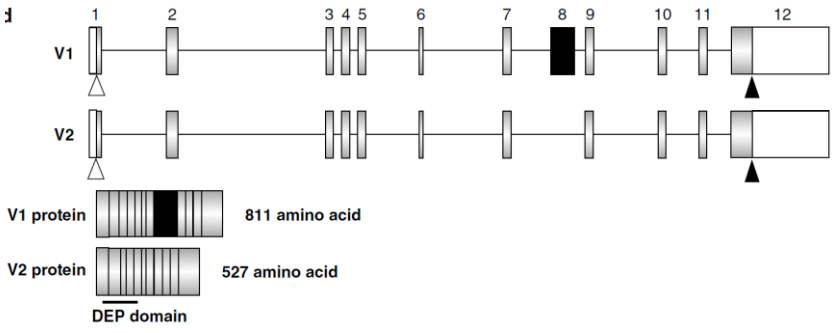

Figure 5. Genomic and protein structures of the two variants of DEPDC1 (DEPDC1-V1 and DEPDC1-V2). Gray boxes indicate coding regions, and white boxes indicate non-coding regions.

Black box indicates DEPDC1-V1-specific exon 8 (852 bp). The DEP domain is underlined (16-104 amino acids). Image from Kanehira et al. *Oncogene*, 2007.

Proteins containing the DEP (Dishevelled, EGL-10, Pleckstrin) domain have been reported to regulate a broad range of cellular functions including a large number of signaling proteins. The DEP domain is a module of approximately 90 amino acids first identified in *Drosophila Melanogaster* Dishevelled, known to be an adaptor in the Wnt signaling [127], in *C. Elegans* EGL-10, a negative regulator of G-protein coupled receptors signaling [128], and in mammalian Pleckstrin, which modulates signaling in platelets and neutrophils [129]. Although DEPDC1 contains a highly conserved DEP domain, its biological functions and pathophysiologic roles in growth of human cancer cells are poorly known, with nowadays only few published reports showing its role in apoptosis and mitotic progression. In bladder cancer, DEPDC1 is associated in the nucleus with the transcriptional repressor ZNF224 to inhibit the transactivation of A20, which normally inhibits the phosphorylation of IκB-α (the inhibitor of NF-κB) and subsequently blocks its ubiquitination and proteasomal degradation [130]. The suppression of A20 transcription results in NF-kB activation and translocation in the nucleus where it mediates the activation of anti-apoptotic pathways [131] (Figure 6).

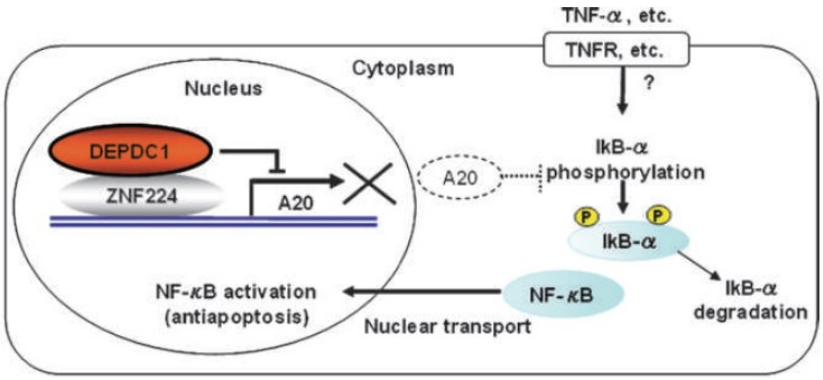

Figure 6. Schematic presentation of the DEPDC1-ZNF224 complex signaling pathway for bladder cancer cells. Image from Harada et al. *Cancer Res.* 2010.

In addition, studies using HeLa cells showed that DEPDC1 was highly expressed in the mitotic phase of the cell cycle, and that its knock down resulted in remarkable mitotic defects such as abnormal multiple nuclei and multipolar spindle structures accompanied by the up-regulation of

the A20 gene, as well as cycle-related genes [132]. Recent studies have shown that DEPDC1 plays key roles in the regulation of MCL1, a member of anti-apoptotic BCL-2 family proteins [133], and seems to be a downstream molecule in the MELK-signaling pathway [134], which is reported to be upregulated in various types of human cancer and is known to be associated with cancer progression, maintenance of stemness and poor prognosis [135,136]. In endometrial endometrioid carcinoma (EEC), a novel Protocadherin-DEPDC1-caspase signaling regulatory axis was suggested to contribute to EEC development and progression through the inhibition of apoptosis, which in turn leads to increase of tumor cells growth [133]. Moreover, DEPDC1 itself has a significant function in cancer cells growth/survival, as its siRNA-mediated knock-down suppressed tumor cells growth and increase the number of apoptotic cells in bladder cancer and multiple myeloma [120,121]. DEPDC1 knock down in myeloma cells also resulted in increased expression of mature plasma cell markers and therefore it could contribute to the plasmablast features of multiple myeloma cells found in some patients with adverse prognosis, blocking the differentiation of malignant plasma cells and promoting cell cycle [121]. Collectively, these studies support the involvement of DEPDC1 in many aspects of cancer traits, such as cell proliferation, anti-apoptosis and cell invasion, suggesting that it may play key roles in tumorigenesis and might serve as novel target for the diagnosis and/or treatment of cancers. Besides, a DEPDC1-derived peptide vaccine restricted for the HLA-A*2402 molecule has been shown to effectively induce peptide-specific cytotoxic T lymphocytes in 66.7% (4/6) of advanced bladder cancer patients, leading to a stable disease and increase of overall survival without any adverse effect [137]. Moreover, a phase I clinical trial of a five-peptide cancer vaccine (five HLA-A*2402-restricted TAA epitope peptides from KOC1, TTK, URLC10, DEPDC1 and MPHOSPH1) combined with chemotherapy in patients positive for HLA-A*2402 with locally advanced, metastatic, and/or recurrent gastrointestinal, lung or cervical cancer is now ongoing. Preliminary results have shown that treatment was well tolerated without any therapy-associated adverse events above grade 3, and that TAA-specific T cell responses induced by vaccine were significantly associated with longer survival [138].

5. Triple-negative breast cancer

Triple-negative breast cancers (TNBCs) are characterized by the lack of estrogen receptor (ER), progesterone receptor (PR) and human epidermal growth factor receptor type 2 (HER2) expression [139]. TNBC is an aggressive cancer that occur in approximately 15% of all patients with

breast cancer [140], with an higher incidence in young and African American women [141]. Women with triple-negative breast cancer do not benefit from hormonal treatments or molecularly targeted therapies such as Tamoxifen or Trastuzumab, because they lack the appropriate targets for these drugs. Although sensitive to chemotherapy, early relapse is more likely in patients with TNBC than with other breast cancer subtypes [142], and visceral metastasis, including brain and lung metastasis, is commonly seen [143], all features that reflect the intrinsically adverse prognosis associated with the disease.

6. Digital pathology and multispectral imaging

Pathology has significantly changed over the last decades and, as a result of the technological developments in molecular pathology and genetics, aims to become quantitative and to provide more information about protein expression on a cellular level in tissue sections. The advent of digital imaging and computer analysis methods started a new era in pathology, beginning in research and moving slowly but steadily into clinical practice. Therapies like ipilimumab and nivolumab have shown the potential for approaches that direct the patient's own immune system against tumors [144]. The complex repertoire of immune cells infiltrating many primary tumors are considered to be indicative of a spontaneous host immune response to tumor antigens [145]; therefore, the idea that the T cell environment in primary tumors could have a prognostic value and might also be of predictive significance is now increasingly spreading. Studies performed in solid tumors have shown that infiltration of the tumor by T cells, especially $CD3^+$ and $CD8^+$ T cells, is associated with good prognosis [146,147,148]. On the other hand, adverse effects of TILs are also documented, such as the presence of large numbers of regulatory T cells or myeloid-derived suppressor cells that clearly correlate with poor survival [149]. However, further advances in the understanding of microenvironment role on tumor progression/regression will require a detailed characterization of the location and status of immune cells in the tumor landscape and their interaction with tumor cells. To address this issue, methods which provide phenotyping of immune and cancer cells combined with the cytoarchitectonics of the tumor become necessary. Until recently it was difficult, if not impossible, to phenotype immune cells in solid tumors while maintaining cellular spatial relationships and morphological context. Both flow cytometry and next-generation sequencing can phenotype cells, but only in disaggregated tissues, and standard pathological analyses can deliver morphology without being able to analyze complex phenotypes.

Standard immunohistochemistry methodologies can be used on tissue sections to visualize or quantify one marker at a time, but standard methods cannot capture the complex, multimarker phenotypes needed to analyze the subsets of immune cells that are important in cancer immunology [150]. To address this issue, multispectral quantitative digital pathology imaging approach allows the visualization and quantification of biomarkers and protein expression *in situ*. This technique enables the development of multiplexed immune cell and protein expression profiling assays for cellular phenotyping in the tumor and tumor microenvironment of standard formalin-fixed paraffin-embedded (FFPE) tissue sections, maintaining the tissue architecture and the morphology [151]. This provides spatial information that can lead to a better understanding of the distribution, the role, the types and the density of immune cells within primary tumors or metastasis. Vasaturo et al. [152] used the multispectral approach to quantify $CD3^+$ T cells infiltration in primary tumors of metastasized patients using the ratio of intratumoral versus peritumoral T cell densities (I/P ratio). The authors showed that patients with longer survival had higher number of infiltrating T cells than patients with shorter survival, confirming that I/P ratio was the strongest predictor of survival in a multivariate analysis. Studies in breast cancer revealed that in patients not achieving a pathologic complete response after neoadjuvant chemotherapy, the density of both $CD8^+$ and $CD4^+$ infiltrates in the stroma were significantly greater than in the tumor. Conversely, for patients achieving a pathologic complete response, no significant difference in densities of stromal and intratumoral $CD8^+$ or $CD4^+$ was observed, suggesting that T cell infiltration from the stroma into the tumor is critical for successful neoadjuvant chemotherapy in breast cancer [153]. With similar approaches, Oguejiofor at al. demonstrated that stromal infiltration of $CD8^+$ T cells is associated with improved clinical outcome in HPV-positive oropharyngeal squamous carcinoma [154].

6.1 Fluorescent multiplex immunohistochemistry with Tyramide Signal Amplification (TSA)

Multispectral immunohistochemistry (mIHC) technique enables the simultaneous detection of up to six immunohistochemically labeled proteins, plus counterstain, onto single FFPE tissue sections, saving valuable tissues and enabling full contextual exploration of multiple cell types and functional states, and cell-to-cell interactions that are difficult or impossible to obtain with other methods [155]. mIHC is based on detection via indirect immunofluorescence involving primary and secondary antibodies to facilitate signal amplification. In the protocol, an HRP-

conjugated secondary antibody binds to an unconjugated primary antibody specific for the target/antigen of interest, and the detection is ultimately achieved with a fluorophore-conjugated tyramide molecule that serves as the substrate for HRP. Activated tyramide forms covalent bonds with tyrosine residues on the protein of interest and is permanently deposited on the antigen site. This can markedly enhance the level of signal amplification, and the permanent nature of the tyramide-antigen binding allows for heat-mediated removal of primary/secondary antibody pairs, while preserving the antigen-associated fluorescence signal, making this process amenable to multiple rounds of staining in a sequential fashion (Figure 7). Importantly, one of the key advantages of this method is that multiple primary antibodies of the same species can be used without the concern for crosstalk.

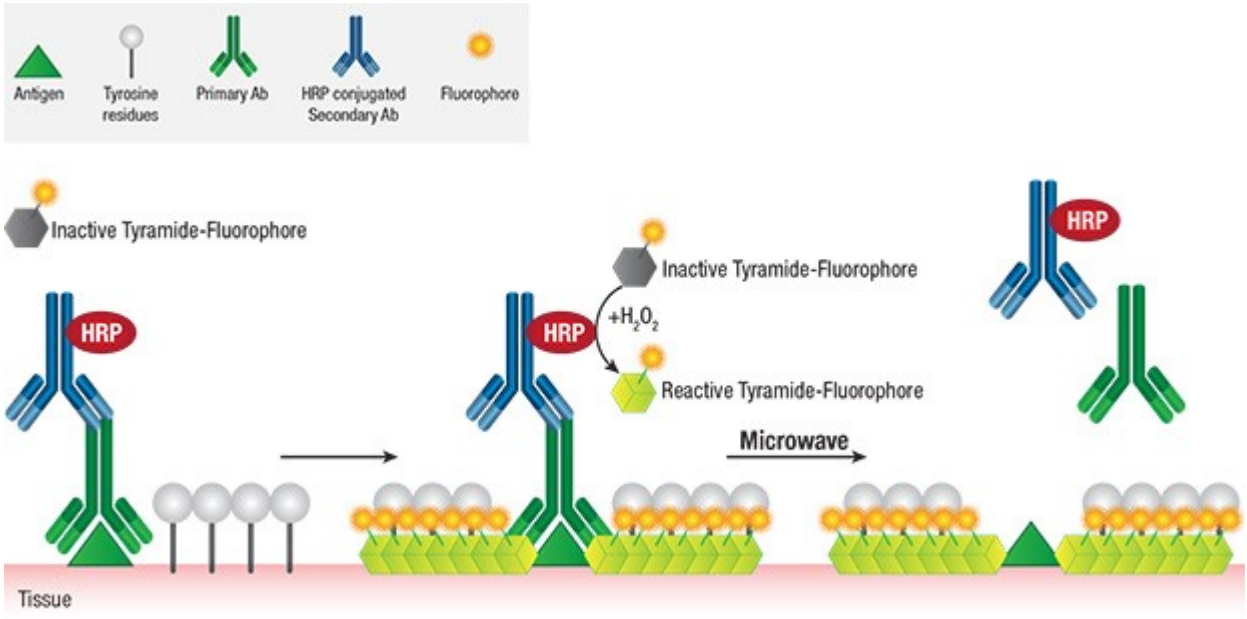

Figure 7. Basic principles of tyramide-based fluorescent mIHC.

The mIHC workflow incorporates three essential elements:

- Multiplex staining of FFPE tissue slides, even with multiple antibodies raised in the same species. The approach involves detection with TSA-reactive fluorophores that covalently label the epitope, followed by microwave treatment (MWT) for removal of primary and secondary antibodies, of any non-specific staining and reduction of tissue

auto-fluorescence. The TSA signal is largely unaffected by MWT and antibody removal. After MWT, another round of staining can be performed for additional target detection without risk of antibody cross-reactivity.

- Multispectral imaging eliminates fluorophore crosstalk and interference from tissue auto-fluorescence, allowing precise measurement of each fluorescence signal within a tissue sample. A critical aspect of multispectral imaging and an essential component for obtaining quantitative results is the generation of correct spectral libraries for each fluorophore, including any background or intrinsic signal such as melanin or tissue autofluorescence, which means the correct separation of all the fluorescence signals within the sample. Once correct spectral signatures are present, the individual images corresponding to the intensity contributions of each fluorophore are extracted from the multispectral data set using linear unmixing [156].
- Image analysis software that determines the intensity values per-cell and per-subcellular compartment. This information is used in combination with user-trainable machine learning algorithms to phenotype cells, recognize morphologic regions of the tissue (e.g. tumor and stroma), and provide cell counts and densities within each region, together with the per-cell quantitation of many markers simultaneously.

AIM OF THE STUDY

In recent years, the field of cancer immunotherapy has considerably expanded with the development of several new treatment options, including cancer vaccines, adoptive cell transfer, CAR T-cell therapy, immune checkpoint inhibitors and monoclonal antibodies [157]. For the majority of patients, monotherapy may be relatively ineffective, and thus a combination of multiple therapeutic approaches may be required [158]. Recent studies demonstrated that immune checkpoint inhibitors can generate and/or amplify an immune response against mutated antigens [159,160]. Accordingly, the combination therapy with immune checkpoint inhibitors and cancer vaccine or adoptive transfer of enriched populations of neoantigen-reactive T cells, may function synergistically to induce more effective antitumor immune responses [161]. However, therapeutic developments targeting clonal neoantigens in order to design personalized immunotherapies to treat patients with advanced cancer are typically unwieldy, time-consuming and expensive [162]. Thus, the identification of universal TSA shared by multiple patients and/or multiple tumors is of great importance to overcome the practical limitations of personalized cancer immunotherapy. Furthermore, the identification and selection of TSA playing a key role in tumor cell proliferation and survival are considered crucial to overcame the immune escape, as they downregulation or loss is expected to impair tumor progression [163]. One promising universal TSA could be DEPDC1, as studies show its almost ubiquitous expression in cancer, and support its involvement in many aspects of cancer traits, such as cell proliferation, anti-apoptosis and cell invasion, suggesting that it may play key roles in the tumorigenesis process.

In this study, we focused our attention on TNBC since no hormonal treatments or targeted therapies are currently available, as cancer cells lack the appropriate targets for these drugs [164]. In this regard, the identification of new potential targets for immunological interventions could offer a therapeutic option and result in improved clinical outcomes for this aggressive and deadly form of breast cancer.

Therefore, the aim of the PhD project was the identification of potential immunogenic DEPDC1-derived epitopes presented in the context of the HLA-A*0201 allele, being this latter the most common MHC-class I subtype in Caucasian population [165], to be used for the development of new immunotherapeutic strategies for HLA-A*0201 patients with TNBC. However, in order to enhance the therapeutic potential of antigen-specific cytotoxic T lymphocytes directed against tumor cells,

a detailed understanding of the tumor microenvironment including the characterization of the immune cells phenotype and their local distribution and cell-to-cell interactions, becomes crucial. For this purpose, I spent three months in Paris in the laboratory of Prof. Jerome Galon, one of the pioneers of the digital pathology applied to cancer-immunology for patient stratification according to the immune status of tumor microenvironment. During this period, I gained confidence with novel multispectral immunohistochemistry (mIHC) technologies, which allow the visualization and quantification of different cell phenotypes simultaneously in the same FFPE tissue section, maintaining the tissue architecture and the morphology. Exploiting this expertise, we will be able to investigate the relationships established between adoptively transferred cytotoxic T lymphocytes and triple negative breast cancer cells, both in tumor-bearing mice and in humans.

MATERIALS AND METHODS

1. cDNA microarrays analysis

The Oncomine database, a repository for published cancer-profiling cDNA microarray data [166] (http://www.oncomine.org), was explored for DEPDC1 mRNA expression in various human tumors, and in the corresponding non-neoplastic tissues. Statistical analysis of the differences in DEPDC1 expression was accomplished through the use of the ONCOMINE algorithms, which allow multiple comparisons among different studies [167,168]. The fold change and gene rank were defined as "all", whereas the data type was restricted to mRNA. Only studies with results achieving a $P<0.05$ were considered.

2. Western blot

Total cell extracts from tumor cells were obtained with a buffer containing 50 mM Tris HCl pH 7.5, 2 mM EDTA, 150 mM NaCl, 1% NP-40 and 1% protease inhibitor cocktail (Roche Biochemical Reagents). Protein concentration was determined by BCA Protein Assay Micro Kit (Serva Electrophoresis). Lysates were resolved by SDS-sample buffer [4% sodium dodecyl sulfate (SDS), 200 mM Tris HCl pH 6.8, 3% β-Mercaptoethanol, 6% glycerol and 0.6% Bromophenol Blue, all from Sigma-Aldrich], boiled for 5 minutes before loading in NuPage Novex 4-12% Bis-Tris Midi Protein gels (Invitrogen), and then transferred to the nitrocellulose membrane (PerkinElmer). DEPDC1 expression was assessed in non-neoplastic samples using a commercially available tissue microarray (ProSci) containing nine human normal tissues (bladder, breast, cervix, kidney, ovary, placenta, prostate, testis and uterus. Western blot analysis was performed according to standard procedures using a rabbit anti-DEPDC1 polyclonal antibody (1:500, Abcam) and HRP-conjugated goat anti-rabbit IgG (diluted 1:3000, Abcam) secondary antibody. The membrane was developed with ECL detection reagents (ThermoFisher Scientific) and visualized using chemiluminescence. Signal intensity was measured by a Bio-Rad XRS chemiluminescence detection system (Lyfe Science Group).

3. Cell lines

The following cell lines were used in this study: the human triple negative breast cancer (TNBC) cell line MDA-MB-231 (HLA-A*0201^{+}), and the related derivatives MDA-MB-231 shDEPDC1 and MDA-MB-231 shCTRL that are stably transduced with a short hairpin RNA (siRNA) for DEPDC1 silencing or a control siRNA, respectively; the human TNBC cell line MDA-MB-468; MCF-7, a human breast cancer cell line; the human bladder cancer cell line SW-780; U87MG, a human glioblastoma cell line; HeLa, a human cervix adenocarcinoma cell line; HCT-15, a human colorectal adenocarcinoma cell line; MKN-45, a human gastric cancer cell line; K562, a human chronic myelogenous leukemia cell line; HepG2, a human hepatocellular carcinoma cell line; A549, a human lung carcinoma cell line; A375, a human melanoma cell line; SKOV-3, a human ovarian carcinoma cell line; T3M4, a human pancreatic adenocarcinoma cell line; PC-3, a human prostate carcinoma cell line; the human embryonic kidney cell line 293 (HLA-A*0201^{-}) and 293-A2 (stably expressing the HLA-A*0201 molecule upon transfection); the T2 cells (HLA-A*0201^{+}), a TAP-deficient human hybrid B/T lymphoblastic cell line; the mouse fibroblast cell line NIH 3T3 and NIH 3T3-A2 (stably expressing HLA-A*0201 upon retroviral transduction, see below). Cells were maintained in DMEM (MDA-MB 231, MDA-MB-468, MCF-7, SW-780, U87MG, HeLa, HepG2, A549, A375, 293 and NIH 3T3) or RPMI 1640 (HCT-15, MKN-45, K562, SKOV-3, T3M4, PC3, T2) medium (EuroClone) supplemented with 10% Fetal Bovine Serum (FBS, Gibco), 2 mM L-Glutamine, 10 mM HEPES, 100 U/ml Penicillin and 100 U/ml Streptomycin (all from Lonza), at 37°C in a 5% CO_2 atmosphere.

4. Peptide selection and synthesis

Several 9-mer HLA-A*0201 binding motifs from DEPDC1 protein sequence were selected based on a integration of their score using the HLA peptide binding prediction algorithms available at BIMAS (http://www-bimas.cit.nih.gov/molbio/hla_bind/)[169], NetMHC (http://www.cbs.dtu.dk/services/NetMHC/)[170] and NetCTL (http://www.cbs.dtu.dk/services/NetCTL/)[171] websites. A total of 10 HLA-A*0201-restricted peptides were chosen. The DEPDC1-derived HLA-A*2402-restricted peptide EYYELFVNI served as negative control in the T2 stabilization assays. All peptides were synthesized by CRIBI (Padova, Italy) with a purity of 98% verified by mass spectrometry analysis. The peptide SLYNTVATL (HIV-1 p17 Gag, aa 77-85; named Gag-$17_{77\text{-}85}$) was used as negative control in functional assays, as it was

previously described as an optimal HLA-A2-restricted CTL epitope [172–174]. The HLA-A2-restricted peptide ELAGIGILTV (Melan-A/MART-1 analogue, aa 26-35*A27L; named Melan-$A_{26\text{-}35*A27L}$) was used for the generation of Melan-A-specific T cells for *in vivo* experiments [175].

5. T2 stabilization assay

Binding and stabilization of HLA-A*0201 molecule by DEPDC1-derived peptides was evaluated using T2 cells [176]. T2 cells were stripped in 0.131 M citric acid, 0.066 M Na_2HPO_4 (pH 3.3) for 45 sec, washed and resuspended in serum-free culture media. A total of $2x10^5$ cells were incubated with 3 µg/ml β2-microglobulin (Sigma-Aldrich) and 100 µg/ml peptide in a final volume of 500 µl for 4 hours at 37°C. Cells were then washed and stained with the FITC-conjugated HLA-A*0201 monoclonal antibody BB7.2 (Biolegend) before cytometry evaluation (FACSCalibur, BD Biosciences). Stabilization was calculated by dividing the Mean Fluorescence Intensity (MFI) of peptide-pulsed T2 cells with the MFI of T2 cells loaded with a negative control peptide (EYYELFVNI) with no predicted binding affinity to HLA-A*0201 [177].

6. Generation of peptide-specific T cells from healthy donors

$CD8^+$ T cells and monocyte-derived dendritic cells (DCs) were obtained from peripheral blood of HLA-A*0201 positive healthy donors. Peripheral blood mononuclear cells (PBMCs) were isolated by Ficoll-Plaque PLUS (GE Healthcare) density gradient centrifugation, and then separated by adherence to plastic culture flasks (Falcon) for 1.5 hours at 37°C in 5% CO_2 to enrich the monocyte fraction. Non-adherent cells were collected and purified for $CD8^+$ T cells using MACS CD8 microbeads (Miltenyi Biotec) according to manufacturer's instructions. Isolated $CD8^+$ T cells were cryopreserved until further use. The adherent fraction was differentiated into mature dendritic cells by culture in RPMI 1640 supplemented with 8% Human AB serum (HS; Aurogene), 2 mM L-Glutamine, 10 mM HEPES, 100 U/ml Penicillin, 100 U/ml Streptomycin and 50 µM 2β-mercaptoethanol for 7 days with the addition of 1000 U/ml granulocyte-macrophage colony-stimulating factor (GM-GSF) and 500 U/ml IL-4 (PeproTech). After 5 days, 1 µg/ml of LPS was added, and the DC's mature phenotype at day 7 was confirmed by flow cytometry analysis of the expression of CD14 (clone TUK4; Miltenyi), CD83 (clone HB15; Miltenyi), CD86 (clone FM95; Miltenyi), CD80 (clone L307.4; BD Biosciences), CCR7 (clone G043H7; BioLegend), HLA-ABC (clone

W6/32; BioLegend) and HLA-DR (clone L243; BioLegend) markers. Mature DCs were pulsed with 20 µg/ml of synthesized peptides in presence of 3 µg/ml β2-microglobulin (Sigma) in RPMI 1640 medium supplemented with 3% HS at 37°C for 4 hours. These peptide-pulsed DCs were then irradiated (55 Gy) and mixed at 1:10 ratio with autologous $CD8^+$ T cells on 24 well plates (Falcon) in a final volume of 2 ml of complete medium supplemented with 8% HS, 10 ng/ml IL-7 (PeproTech) and 20 U/ml rhIL-2 (Proleukine, Novartis). After 2 days, half of medium was replaced with fresh medium supplemented with 100 U/ml IL-2. On days 7, 14 and 21, T cells were restimulated with the autologous peptide-pulsed DCs as described above (Figure 8).

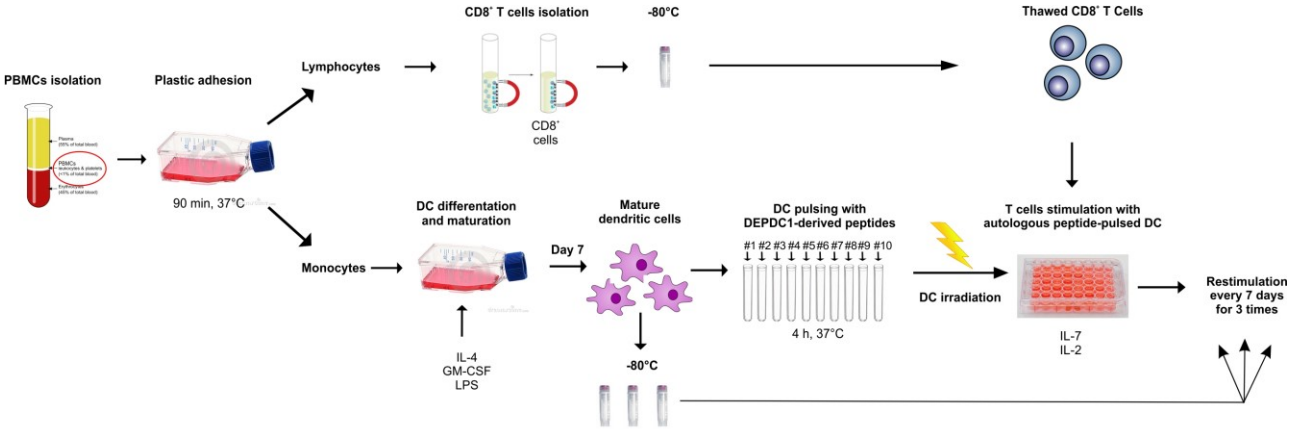

Figure 8. *Ex vivo* protocol for the generation of peptide-specific T cells from healthy donors peripheral blood.

7. Generation of EBV-transformed B cell lines (LCL)

For LCL generation, $10x10^6$ fresh PBMC from HLA-A*0201 healthy donors were infected with supernatant from the B95-8 EBV producer cell line (ATCC), as previously reported [178]. The day after, 0.7 µg/ml Cyclosporin A (Sigma-Aldrich) was added and cells were plated at $1x10^5$ cells per well in flat-bottomed 96-well plates containing RPMI 1640 medium (EuroClone) supplemented with 10% Fetal Bovine Serum (FBS, Gibco), 2 mM L-Glutamine, 10 mM HEPES, 100 U/ml Penicillin and 100 U/ml Streptomycin (all from Lonza).

8. Intracellular cytokine staining for interferon-γ (IFN-γ) detection

IFN-γ production by DC/peptide-stimulated T cell cultures was measured by intracellular cytokine staining after blocking the cellular secretion using BD Cytofix/Cytoperm kit, according to the

manufacturer's instructions. HLA-A*0201 positive LCL or tumor target cell lines were used as stimulators. LCL cells were pulsed overnight with each peptide (10 μg/ml), washed and incubated at 1:1 ratio with peptide-specific CTLs stimulated 3 times with autologous peptide-pulsed DCs. The Gag-$17_{77\text{-}85}$ peptide served as negative control, while phorbol 12-myristate 13-acetate (PMA; 40 ng/ml)/ionomycin (4 μg/ml) (Sigma Aldrich) as positive control. After 1 hour, cellular cytokine secretion was blocked by the addiction of GolgiStop (2 μM) and the incubation was allowed to continue for 5 hours at 37°C. Cells were then stained with APC-conjugated anti-CD8a antibody (clone RPA-T8; BioLegend), washed and fixed. After permeabilization, cells were stained with a PE-conjugated anti-IFN-γ antibody (clone B27; BioLegend) for 30 minutes at 4°C, and flow cytometry analysis was performed (FACSCalibur, BD Biosciences).

9. MHC-biomonomer and MHC-tetramer preparation

The synthesis of MHC-peptide tetrameric complexes is based on the use of prokaryotic expression systems for MHC class I heavy chain and β2-microglobulin [JM109(DE3), Promega]. The MHC heavy chain (HLA-A*0201) was modified by substitution of the transmembrane and cytosolic domains with a signal sequence containing a biotinylation site for the enzyme BirA. The MHC heavy chain, β2m and epitope peptide (DEPDC1#5 or Melan-$A_{26\text{-}35*A27L}$ peptides) were subjected to a refolding *in vitro* in Tris-HCl pH 8, L-Arginin-HCl, NaEDTA, oxidized glutathione and reduced glutathione (Sigma-Aldrich). The complex was isolated through dialysis, concentrated and purified by HPLC to separate monomers from unconjugated components. Monomers were then enzymatically biotinylated by the enzyme BirA. The biomonomers obtained were purified and subsequently quantified with a spectrophotometer. The tetramers were finally assembled with phycoerythrin (PE)-conjugated extravidin (Sigma-Aldrich) to be detect by flow cytometry. The MHC-tetramers obtained were stored at 4°C. The efficiency of tetramerization and hence the correct volume of extravidin-PE to add was verified by ELISA. Briefly, 96-well plates (Maxisorb, NUNC) were coated overnight at room temperature (RT) with rabbit anti-human β2 microglobulin antibody (1:5000 in PBS 1X; Genetex), which recognizes β2 microglobulin of free biomonomers. The coating was then removed and the assay buffer (AB: PBS 1X, 2% BSA, pH 7.4) was added for 1 hour at RT to saturate the aspecific sites. After three washes with wash buffer (WB: Tris HCl 50 mM, 0.2% Tween 20, pH 7.4), serial dilutions starting from 1 μg/ml of tetramers or the corresponding biomonomers were added for 1 hour at RT. The biomonomer solutions were used

as positive controls. The plates were then washed three times with WB and Poly-Horseradish Peroxidase-Streptavidin antibody (1:15000 in AB; Endogen) was added for 1 hour at RT. After three washes with WB, OPD solution (*o*-Phenylenediamine dihydrochloride, Sigma-Aldrich) was added for 3 minutes for the detection of peroxidase activity. The reaction was finally stopped with HCl 3N and the absorbance was read at 490 nm in the ELISA plate reader (Victor X4 Multilabel Plate Reader; PerkinElmer).

10. Peptide-specific T cell characterization

T cells generated *in vitro* were characterized using the following fluorochrome-conjugated monoclonal antibodies: APC-conjugated CD3 (clone UCHT1), CD28 (clone CD28.2) and CD8 (clone RPA-T8; all Biolegend); FITC-conjugated CD16 (clone 3G8; Biolegend) and CCR7 (clone G043H7; Biolegend) and CD11a (clone HI111 RUO; BD Biosciences); PerCP-Cy5.5-conjugated CD56 (clone B159; BD Biosciences) and CD45RA (clone HI100; Biolegend); BV421-conjugated CD8 (clone RPA-T8; BD Biosciences); APC-H7-conjugated CD4 (clone RPA-T4; BD Biosciences); PE-conjugated CD4 (clone RPA-T4), CD44 (clone BJ18), CD62L (clone DREG-56) and CD83 (clone HB15e; all Biolegend). For the tetramer staining, CTLs were incubated with the PE-conjugated HLA-A*0201-DEPDC1#5 or PE-conjugated HLA-A*0201-Melan-$A_{26\text{-}35*A27L}$ tetramer. Samples were analysed by LSRII flow cytometer (BD Biosciences) and evaluated with FlowJo software (TreeStar Inc.).

11. Transduction of NIH 3T3 with pBABE_puro_HLA-A*0201 retroviral vector

The pBABE_puro retroviral construct containing the human HLA-A*0201 sequence (kindly provided by Prof. Dolcetti, Aviano, Italy) was packaged using the second-generation retrovirus producers cell line Phoenix (ATCC). Packaging cells were transfected at approximately 70% of confluence with 20 µg retroviral plasmid DNA using the calcium phosphate technique. After 48 hours, the virus-containing medium was collected, filtered through a 0.45 µm filter and added to NIH 3T3 cells in presence of 8 µg/ml polybrene (Sigma-Aldrich) for 16 hours at 37°C. Fresh medium was then added and the cells were incubated for a further 24 hours in virus-free media prior to trypsinization and plating in media supplemented with 1.5 µg/ml Puromycin (Sigma-Aldrich) to select the cells expressing the HLA-A*0201 molecule. NIH 3T3 cells positive for HLA-A*0201 expression were then analyzed by flow cytometry.

12. ^{51}Cr-release assay

DEPDC1#5 peptide-specific CTL cytotoxic activity was assessed using a 6 hours ^{51}Cr-release assay. Briefly, a total of $1x10^6$ target cells were labelled with 100 µCi of $Na_2{}^{51}CrO_4$ for 1 hour at 37°C and washed twice with culture medium. Depending on the experiment, target cells were incubated with 10 µM of DEPDC1-derived or Gag-17_{77-85} peptides for 40 minutes at 37°C and then washed twice. For blocking experiments, target cells were incubated for 30 min on ice with 10 µg/ml anti-MHC-class I blocking antibody (W6/32 clone; Biolegend) or the relative isotype control (mouse IgG2a, κ isotype ctrl; Biolegend). Target and effector cells were then plated in a 96-well U-bottom plate at the indicated E/T ratio in a total volume of 200 µl. After a 6 hours incubation at 37°C, 30 µl supernatant was transferred on a scintillation plate (Perkin Elmer), and measured using a Top Count gamma counter (PerkinElmer). The percentage of lysis was calculated as follows: % Specific Lysis = (experimental release – spontaneous release) / (maximal release – spontaneous release) x 100. Spontaneous and maximal releases were obtained by incubating target cells in medium alone or in RPMI 2% SDS, respectively. Alternatively, cytotoxicity was also expressed as lytic units 30 (LU_{30}), where 1 LU_{30} was defined as the number of effector cells capable of killing 30% of target cells [179]. In this case, results were expressed in number of LU_{30} per 10^6 responder cells.

13. Outgrowth assays

Target MDA-MB-231 or NIH 3T3 cells were serially double diluted into replicate flat-bottom 96-wells plate starting from 3000 cells/well, and T cells were added where indicated at 3000 cells/well. Plates were incubated at 37°C in 5% CO_2 with weekly refeeding, and target cells outgrowth was scored after 4 weeks.

14. *In vivo* experiments of adoptive immunotherapy

On day 0, 6-8 week-old female NOD/SCID common γ chain knockout (NSG, Charles River) mice were anesthetized (1-3% isoflurane, Merial Italia), and injected into the mammary fat pad with $1x10^6$ MDA-MB-231 cells transduced with a lentiviral vector coding for the Firefly Luciferase reporter gene [180]. At day 3, mice were injected intra-tumorally with $10x10^6$ DEPDC1-specific CTLs stimulated 3 times with autologous peptide-pulsed DCs, or with Melan-A-specific CTLs in the control group. A group of mice received only PBS 1X as negative controls. The same treatment was

repeated for 2 additional times at three-four day intervals. Tumor growth was monitored over time by bioluminescence analysis. In particular, anesthetized animals were given the substrate D-Luciferin (PerkinElmer, MA, USA) by intraperitoneal injection at 150 mg/Kg in PBS (Sigma). The light emitted from the bioluminescent tumors or metastasis was detected using a cooled charge-coupled device camera mounted on a light-tight specimen box (IVIS Lumina II Imaging System; Perkin-Elmer). Imaging times ranged from 15 s to 8 min. Regions of interest from displayed images were identified around the tumor sites or lymph node metastasis region, and were quantified as total photon counts or photon/s using Living Image® software (Perkin-Elmer). In lymph node metastasis detection, the lower portion of each animal was shielded before reimaging in order to minimize the bioluminescence from primary tumor, thus allowing the signals from metastatic regions to be observed *in vivo*.

15. Statistical analysis

Results were analyzed for statistical significance by using paired or unpaired Student *t* test and ANOVA, as appropriate (**** = P< 0.0001; *** = P< 0.001; ** = P< 0.01; * = P< 0.05). Histograms represent mean values ± standard deviation (SD). In scatter-plot graphs, symbols indicate different samples or assays, and horizontal bars represent means ± SD. Statistical analysis was performed using Sigmaplot and GraphPad Prism 4.0 softwares.

16. Study approval

Anonymized human buffy coats were obtained from the Blood Bank of Padova Hospital, and donors provided their written informed consents to participate in this study. Procedures involving animals and their care were in conformity with institutional guidelines that comply with national and international laws and policies (D.L. 26/2014 and subsequent implementing circulars), and the experimental protocol (Authorization n. 1143/2015-PR) was approved by the Italian Ministry of Health.

17. 7-colors fluorescence multiplex immunohistochemistry

Four µm-thick colorectal cancer (CRC) tissue sections on slides were heated in a dry oven at 56 °C for at least two hours, to allow drainage of melting paraffin. After three washes of 5 minutes each

in clearene (Leica Biosystems) to complete the removal of paraffin, the slides were hydrated through an ethanol gradient and finally washed with distilled water. The tissues were fixed to the slides, with a 20 minutes wash in 10% neutral buffered formalin (10% formalin, 4 g/L NaH_2PO_4, 6.5 g/L Na_2HPO_4, pH7) and then rinsed with antigen retrieval pH6 (PerkinElmer) or pH9 (DAKO) solutions depending on the antigen to be detected. The antigen retrieval was brought at its boiling point using the microwave at 100% power and then left for other additional 15 minutes at 20% power. The microwave treatment served to quench endogenous peroxidase activity, for antigen retrieval and to remove antibodies after a target has been detected. After the slides were cooled at RT, they were incubated with Protein Block Serum Free (DAKO) for 10 minutes at RT and then washed with TBS 1X 0.04% Tween20 (TBST buffer). The tissue sections were completely covered with the primary antibody and incubated according to the manufacturer's instructions regarding concentration, incubation time and temperature requirements. After 3 washes with TBST buffer, slides were incubated with anti-mouse or anti-rabbit HRP-conjugated secondary antibodies (DAKO) for 10 minutes at RT, and then washed 3 times with TBST buffer. The excess of wash buffer was drained off and Opal Fluorophores (PerkinElmer) were pipetted onto the slides and incubated at RT for 10 minutes. After 3 washes, the slides were placed in antigen retrieval buffer and the microwave treatment was repeated to strip the primary/secondary-HRP complexes to allow the next antigen staining. To detect other targets, the protocol was restarted from the blocking step. When all targets had been detected, DAPI Working Solution (PerkinElmer) was added for 5 minutes at RT and the coverslips were put on the slides with mounting media. The visualization of 7-colors Opal slides was performed using Mantra Quantitative Pathology Imaging System (PerkinElmer) and the analysis was carried out with inForm™ Tissue Finder™ image analysis software (PerkinElmer).

RESULTS

1. DEPDC1 is widely expressed in tumors but not in normal tissues

Using Oncomine database and gene data analysis tools, different public available microarray studies on cancer were checked to evaluate DEPDC1 gene expression [166,168]. The analysis concerned the assessment of DEPDC1 mRNA expression levels for each of the studies considered. Fourteen independent data sets referring to different tumor histotypes showed a significant upregulation of DEPDC1 mRNA levels in primary cancers, as compared to normal counterpart tissues (P = 2.15E-7), (Figure 9 A) [181–193]. Consistent with these findings, DEPDC1 protein was found to be expressed in a large set of different human tumor cell lines, such as breast, bladder, brain, cervix, colon, stomach, leukemia, liver, lung and melanoma cell lines (Figure 9 B), thus supporting the concept that DEPDC1 can be regarded as a potential "universal" tumor-associated antigen, whose expression is strictly linked to the neoplastic status. Conversely, DEPDC1 was not found to be expressed in a set of normal different human tissues (bladder, breast, cervix, kidney, ovary, placenta, prostate, and uterus; Figure 9 B), consistently with data reported by Kanehira et al [120]. We failed, however, to visualize DEPDC1 protein in testis, while the specific mRNA had been previously detected by Northern blot, albeit at low levels, in the same normal tissue [120], likely due to the lower sensitivity of western blot.

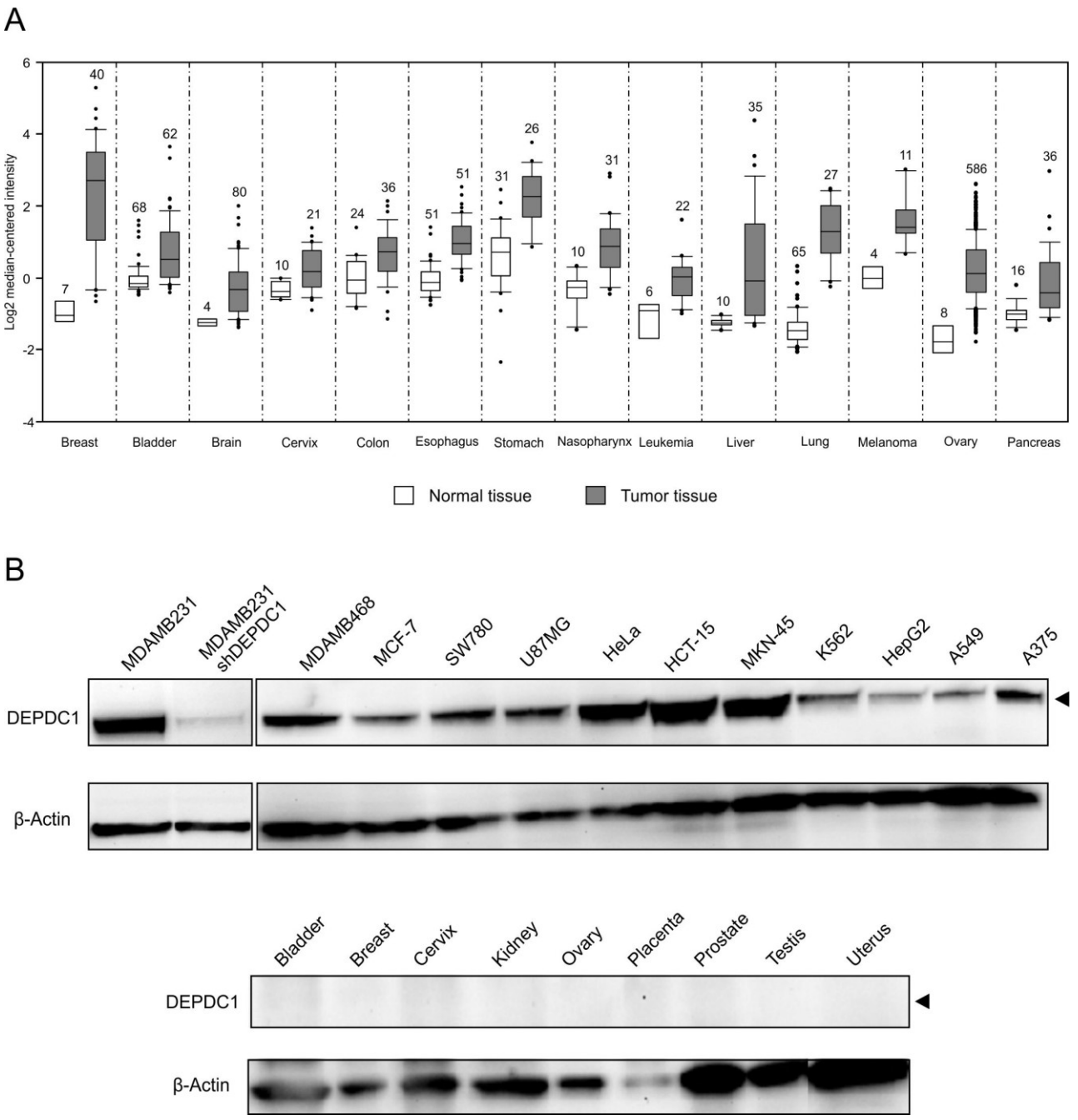

Figure 9. DEPDC1 is upregulated in different human cancers. (A) DEPDC1 mRNA expression in normal (white) and tumor tissues (grey) as reported from microarray studies in the Oncomine database. Breast: (t-test= 10.953; P-value= 1.181E-14) [181]; bladder (t-test= 6.217; P-value= 8.82E-9) [182]; brain (t-test= 9.929; P-value= 7.56E-12) [183]; cervix (t-test= 7.688; P-value= 9.13E-9; 1) [184]; colon (t-test= 3.978; P-value= 9.98E-5) [185]; esophagus (t-test= 10.994; P-value= 8.17E-19) [186]; stomach (t-test= 7.378; P-value= 4.54E-10) [187]; nasopharynx (t-test= 5.832; P-value= 1.71E-6) [188]; leukemia (t-test= 4.400; P-value= 8.57E-4) [189]; liver (t-test= 6.180; P-value= 2.18E-7) [190]; lung (t-test= 16.310; P-value= 7.19E-18; 65 lung) [191]; skin (t-test= 5.874; P-value= 3.54E-5) [192]; Ovary (t-test= 14.643; P-value= 2.12E-7) (TCGA Ovarian, No Associated Paper, 2013); Pancreas (t-test= 4.794; P-value= 8.57E-6) [193]. Numbers above each box plot refer to the number of samples reported. **(B)**

Endogenous expression of DEPDC1 protein in several human tumor cell lines (upper panels) and in different human normal tissues (lower panels), as assessed by western blot. MDA-MB-231shDEPDC1 refers to cells with DEPDC1 silenced by shRNA, used as negative control.

Moreover, DEPDC1 expression turned out to be associated with pathologic and prognostic parameters independent of the tumor type. Indeed, advanced stage (Table 1) and high grade tumors (Table 2) overexpress DEPDC1 mRNA as compared to early stage or low grade tumors, respectively.

Table 1. Upregulation of DEPDC1 mRNA levels in advanced stage cancers

Tumor type	Parameters for comparison (samples number)	P-value	Oncomine dataset	Ref
Lobular breast carcinoma	N0 (7) vs N1 (12)	3.05E-4	Lu, Breast	194
Ductal breast carcinoma	M0 (176) vs M1+ (5)	0.009	Bittner, Breast	
Large Cell Lung Carcinoma	Stage I (11) vs Stage II (5)	0.018	Hou, Lung	195
Lung Adenocarcinoma	Stage I (168) vs Stage II (58)	5.17E-5	Okayama, Lung	123
Oral Cavity Squamous Cell Carcinoma	Stage III (3) vs Stage IV (7)	0.031	Rickman, Head-Neck	196
Ductal Breast Carcinoma	Stage I (24) vs Stage II (110) vs Stage III (42) vs Stage IV (5)	0.006	Bittner, Breast	
Anaplastic Medulloblastoma	M0 (10) vs M1+ (7)	0.010	Robinson, Brain	197
Cervical Squamous Cell Carcinoma	Stage I (4) vs Stage II (11) vs Stage III (10)	0.045	Scotto, Cervix 2	198
Papillary Renal Cell Carcinoma	Stage I (17) vs Stage III (8) vs Stage IV (7)	4.57E-5	Yang, Renal	199
Hepatocellular Carcinoma	Stage I (106) vs Stage II (93) vs Stage III (39)	0.023	Jia, Liver	200
Borderline Ovarian Serous Tumor, Micropapillary Variant	Stage I (6) vs Stage III (4)	0.078	Anglesio, Ovarian	201
Pancreatic Ductal Adenocarcinoma	Stage 0 (3) vs Stage I (3) vs Stage IV (16)	0.010	Ishikawa, Pancreas	202
Endometrial Endometrioid Adenocarcinoma	Stage I (30) vs Stage II (5) vs Stage III (5)	0.006	TCGA, Uterus	203

Table 2. Upregulation of DEPDC1 mRNA levels in high grade cancers

Tumor type	Parameters for comparison (samples number)	P-value	Oncomine dataset	Ref
Peritoneal serous adenocarcinoma	Grade 2 (8) vs Grade 3 (14)	0.006	Tothill, Ovarian	204
Invasive breast carcinoma	Grade 2 (15) vs Grade 3 (16)	2.93E-6	Stickeler, Breast	205
Invasive Ductal Breast Carcinoma	Grade 1 (89) vs Grade 2 (576) vs Grade 3 (857)	1.49E-59	Curtis, Breast	206
Bladder Urothelial Carcinoma	Grade 1 (25) vs Grade 2 (37) vs Grade 3 (11)	9.43E-11	Lindgren, Bladder	207
Storiform-pleomorphic malignant fibrous histiocytoma	FNCLCC Grade 2 (16) vs FNCLCC Grade 3 (54)	1.24E-5	Gibault, Sarcoma	208
Lung Adenocarcinoma	Grade 2 (18) vs Grade 3 (14)	0.004	Ding, Lung	209
Oligodendroglioma	Grade 2 (38) vs Grade 3 (12)	4.29E-4	Sun, Brain	210
Astrocytoma	Grade 3 (24) vs Grade 4 (76)	4.07E-6	Phillips, Brain	211
Infiltrating Bladder Urothelial Carcinoma	Grade 3 (9) vs Grade 4 (3)	0.003	Dyrskjot, Bladder 3	212
Meningioma	Grade 1 (43) vs Grade 2 (19) vs Grade 3 (6)	8.39E-6	Lee, Brain 2	213
Gastric Cancer	Grade 1 (13) vs Grade 2 (18) vs Grade 3 (25)	0.035	Takeno, Gastric	214
Papillary Renal Cell Carcinoma	Grade 2 (22) vs Grade 3 (8) vs Grade 4 (3)	3.30E-6	Yang, Renal	199
Hepatocellular Carcinoma	Grade 1 (12) vs Grade 2 (9) vs Grade 3 (12)	1.76E-6	Wurmbach, Liver	190
Ovarian Serous Adenocarcinoma	Grade 1 (3) vs Grade 2 (55) vs Grade 3 (94)	8.76E-5	Tothill, Ovarian	204
Pancreatic Ductal Adenocarcinoma Epithelia	Grade 1 (4) vs Grade 2 (12) vs Grade 3 (11)	0.007	Collisson, Pancreas	215
Endometrial Endometrioid Adenocarcinoma	Grade 1 (25) vs Grade 2 (67) vs Grade 3 (25)	8.56E-5	Bittner, Endometrium	

Additionally, higher DEPDC1 mRNA levels are detected in primary tumor tissues from patients with metastatic events than in patients with no recurrence, and are related to a worst overall survival (Table 3).

Table 3. Upregulation of DEPDC1 mRNA levels in patients with the worst outcome

Tumor type	Parameters for comparison (samples number)	P-value	Oncomine dataset	Ref
Invasive breast carcinoma	No metastatic event at 1 year (191) vs metastatic event at 1 year (6)	0.004	Schmidt, Breast	216
Activated B-cell-like diffuse large B-cell lymphoma	No recurrence at 3 years (3) vs recurrence at 3 years (8)	0.021	Shaknovich, Lymphoma	217
Lung Adenocarcinoma	No Recurrence at 3 Years (26) vs Recurrence at 3 Years (30)	2.32E-4	Lee, Lung	218
Lung Adenocarcinoma	Alive at 1 Year (34) vs Dead at 1 Year (4)	0.006	Kuner, Lung	219
Clear Cell Renal Cell Carcinoma	Alive at 5 Years (34) vs Dead at 5 Years (76)	0.001	Zhao, Renal	220
Diffuse Gastric Adenocarcinoma	No Recurrence at 5 Years (6) vs Recurrence at 5 Years (12)	0.002	Forster, Gastric	221
Multiple Myeloma	Alive at 1 Year (293) vs Dead at 1 Year (33)	3.70E-6	Zhan, Myeloma 2	222
Anaplastic Oligodendroglioma	Alive at 1 Year (7) vs Dead at 1 Year (3)	0.018	Freije, Brain	223
Astrocytoma	Alive at 5 Years (13) vs Dead at 5 Years (58)	2.34E-4	Phillips, Brain	224

Noteworthy, 13 independent datasets of human triple negative breast cancers (TNBC) show an overexpression of DEPDC1 compared to other breast cancer histotypes (Table 4).

Table 4. Upregulation of DEPDC1 mRNA levels in Triple Negative Breast Cancers

Tumor type	Parameters for comparison (samples number)	P-value	Oncomine dataset	Ref
Ductal Breast Carcinoma	ERBB2/ER/PR Negative (18) vs Other Biomarker Status (19)	4.97E-5	Richardson, Breast 2	181
Invasive Ductal Breast Carcinoma	ERBB2/ER/PR Negative (46) vs Other Biomarker Status (250)	1.77E-16	TCGA, Breast	
Invasive Breast Carcinoma	ERBB2/ER/PR Negative (8) vs Other Biomarker Status (24)	1.04E-4	Stickeler, Breast	205
Ductal Breast Carcinoma	ERBB2/ER/PR Negative (39) vs Other Biomarker Status (129)	8.04E-9	Bittner, Breast	
Invasive Ductal Breast Carcinoma	ERBB2/ER/PR Negative (211) vs Other Biomarker Status (1,340)	1.83E-43	Curtis, Breast	206
Invasive Ductal Breast Carcinoma	ERBB2/ER/PR Negative (57) vs Other Biomarker Status (106)	2.09E-5	Tabchy, Breast	225
Ductal Breast Carcinoma	ERBB2/ER/PR Negative (80) vs Other Biomarker Status (32)	1.31E-6	Bonnefoi, Breast	226
Invasive Breast Carcinoma	ERBB2/ER/PR Negative (178) vs Other Biomarker Status (320)	4.45E-15	Hatzis, Breast	227
Invasive Ductal Breast Carcinoma	ERBB2/ER/PR Negative (73) vs Other Biomarker Status (495)	7.17E-7	TCGA, Breast 2	
Invasive Ductal Breast Carcinoma	ERBB2/ER/PR Negative (5) vs Other Biomarker Status (29)	0.005	Zhao, Breast	228
Breast Carcinoma	ERBB2/ER/PR Negative (19) vs Other Biomarker Status (87)	7.86E-4	Chin, Breast	229
Breast Carcinoma	ERBB2/ER/PR Negative (32) vs Other Biomarker Status (295)	2.36E-5	Kao, Breast	230
Breast Cancer Cell Line	ERBB2/ER/PR Negative (21) vs Other Biomarker Status (25)	2.35E-4	Neve, Cell Line	231

2. In silico prediction of HLA-A*0201-restricted DEPDC1-derived peptides and assessment of their MHC stabilizing properties

DEPDC1 amino acid (aa) sequence was analyzed for potential HLA-A*0201-restricted peptides using three epitope prediction algorithms available online, namely BIMAS, NetMHC and NetCTL. Different 9-aa peptides were classified according to their predicted ability to stabilize the MHC allele. The 10 peptides with the highest prediction score were chosen and synthesized for the subsequent studies (Table 5). Next, to evaluate their ability to stabilize the HLA-A*0201 allele, the DEPDC1-derived peptides were incubated with the antigen-processing deficient T2 cells. The HLA-A*0201 expression levels were measured and compared to those induced by incubation of T2 cells with an irrelevant peptide (Table 5 and Figure 10). DEPDC1-derived peptides induced different levels of HLA-A*0201 stabilization, being DEPDC1#1 and DEPDC1#5 peptides those with the highest ability to stabilize the MHC molecule.

Table 5. Candidate peptides derived from DEPDC1 sequence, their predicted binding affinities to HLA-A*0201 and stabilization ratios

Peptide	Start position	Peptide sequence	BIMAS score	NetMHC Affinity (nm)	NetCTL score	Stabilization ratio on T2 cells
DEPDC1#1	673	FLMDHHQEI	728.022	6.05	1.4641	3.7
DEPDC1#2	580	SMLTGTQSL	57.085	20.15	1.2956	2.6
DEPDC1#3	588	LLQPHLERV	133.255	47.31	1.2127	2.5
DEPDC1#4	574	SLLPASSML	79.041	37.72	1.1822	2.5
DEPDC1#5	282	FLDLPEPLL	39.307	21.60	1.1503	2.9
DEPDC1#6	289	LLTFEYYEL	54.474	41.23	1.1172	2.3
DEPDC1#7	524	YINTPVAEI	15.177	165.46	1.0234	2.0
DEPDC1#8	786	ALFGDKPTI	38.601	83.19	1.0145	1.3
DEPDC1#9	618	LLMRMISRM	71.872	58.86	1.0108	2.1
DEPDC1#10	562	RLCKSTIEL	21.362	127.36	0.9906	1.2

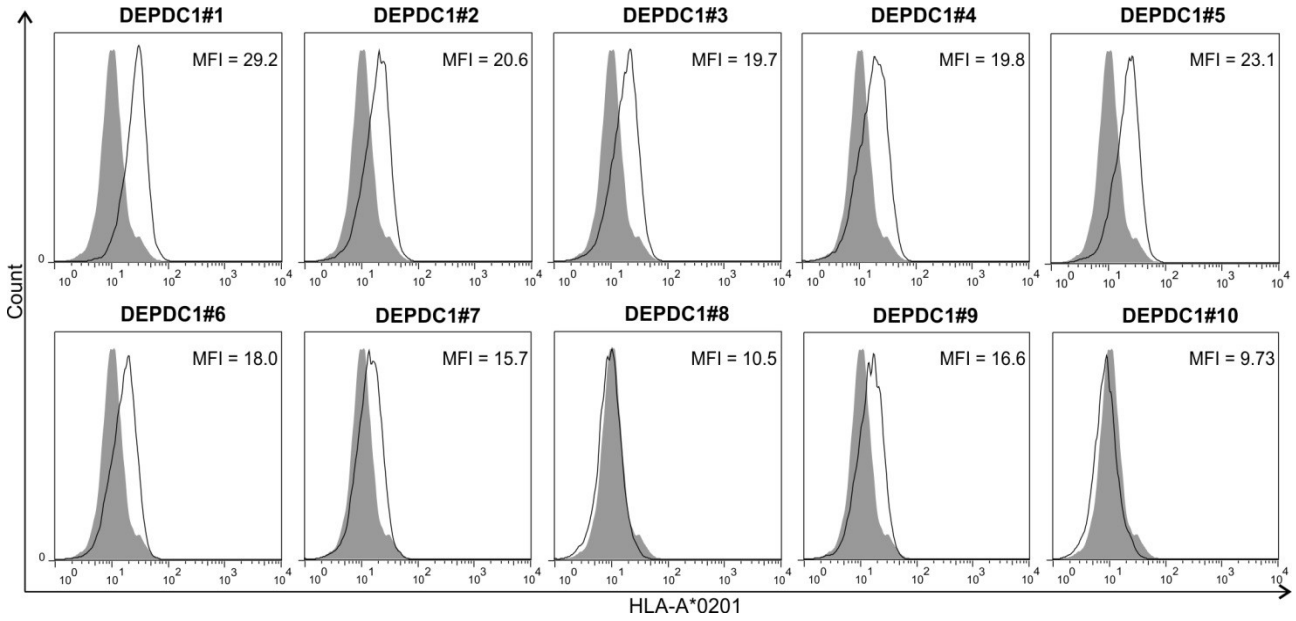

Figure 10. Comparison of the ability of different DEPDC1-derived peptides to stabilize the HLA-A*0201 allele on the surface of T2 cells. Flow cytometry analysis reports the expression of HLA-A*0201 on T2 cells (black line and related Mean Fluorescence Intensity, MFI) induced by the selected DEPDC1-derived peptides. An HLA-A*24-restricted DEPDC1-derived peptide was used as negative control (filled grey; MFI = 7.71).

3. Generation of DEPDC1-derived peptide-specific T cell cultures

Lymphocytes and monocytes were obtained from PBMCs of healthy donors. Monocytes were induced to differentiate into mature DCs to act as antigen-presenting cells for T cell stimulation. By flow cytometry, we first confirmed the DC maturation by the expression of CD83 and the absence of CD14 expressing cells; the increase expression levels of the co-stimulatory molecules CD80 (also known as B7.1) and CD86 (also known as B7.2), both upregulated during the DC activation and fundamental for the interaction with naïve T cells and, finally, the expression levels of MHC-class I (HLA-ABC) and class II (HLA-DR) molecules and the chemokine receptor CCR7 (Figure 11).

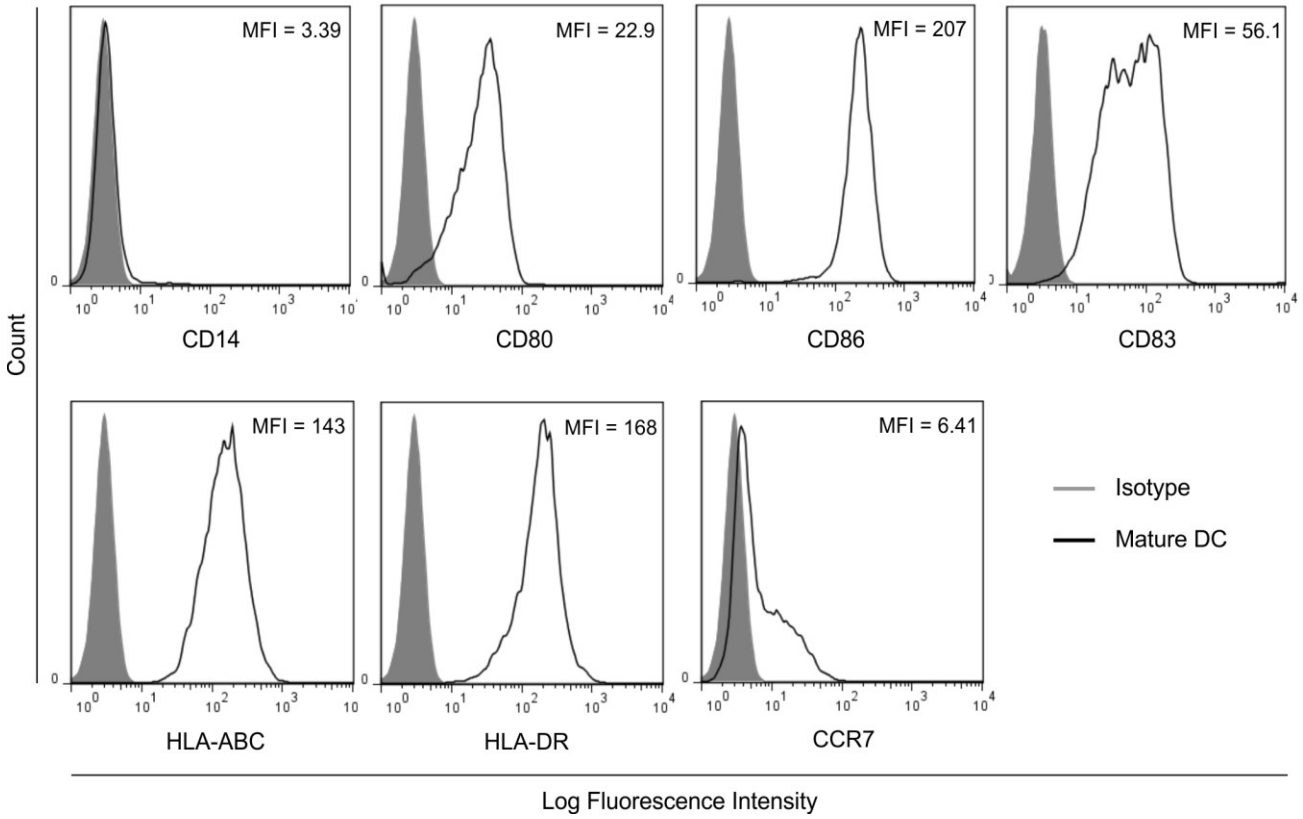

Figure 11. Phenotypic characterization of monocytes-derived mature DC. Mean fluorescence intensity (MFI) of mature dendritic cells markers generated from human monocytes cultured in presence of GM-CSF, IL-4 and LPS (black line) and the isotype control (filled grey) assessed by flow cytometry analysis.

The lymphocytes were immunomagnetically enriched for $CD8^+$ T cells (80 ± 1.5% of total lymphocytes), being the remaining contaminant $CD4^+$ T cell subset only fractional (7.6 ± 5.9%; Figure 12). To induce the expansion of antigen-reactive T cell populations, $CD8^+$ T cells were stimulated weekly with the autologous DCs pulsed with the DEPDC1-derived peptides.

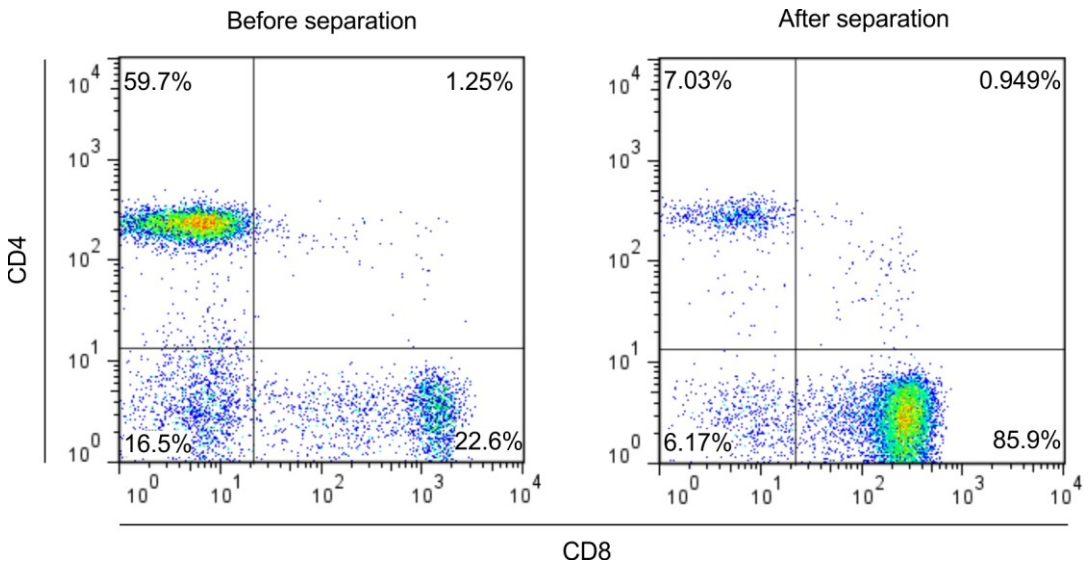

Figure 12. Assessment of immunomagnetic enrichment of CD8⁺ T cell populations. Representative flow cytometry analysis of lymphocytes isolated from PBMC of healthy donors before and after the enrichment with MACS CD8 microbeads, as described in Materials and Methods. Within each gate, the percentage of cells is reported.

4. DEPDC1#5 peptide induces IFN-γ production in peptide-stimulated T cell cultures

To evaluate which DEPDC1-derived peptide was able to induce a CTL functional response, at the third round of stimulation, T cell cultures were screened for IFN-γ production in response to HLA-A*0201-positive lymphoblastoid cell line (LCL) cells pre-loaded with the different DEPDC1-derived peptides. The most responsive $CD8^+$ population was observed after stimulation with DEPDC1#5 peptide. LCL cells loaded with an irrelevant peptide (HLA-A*0201-restricted Gag-17_{77-85}, SLYNTVATL) or left unpulsed did not induce IFN-γ production (Figure 13 A-B).

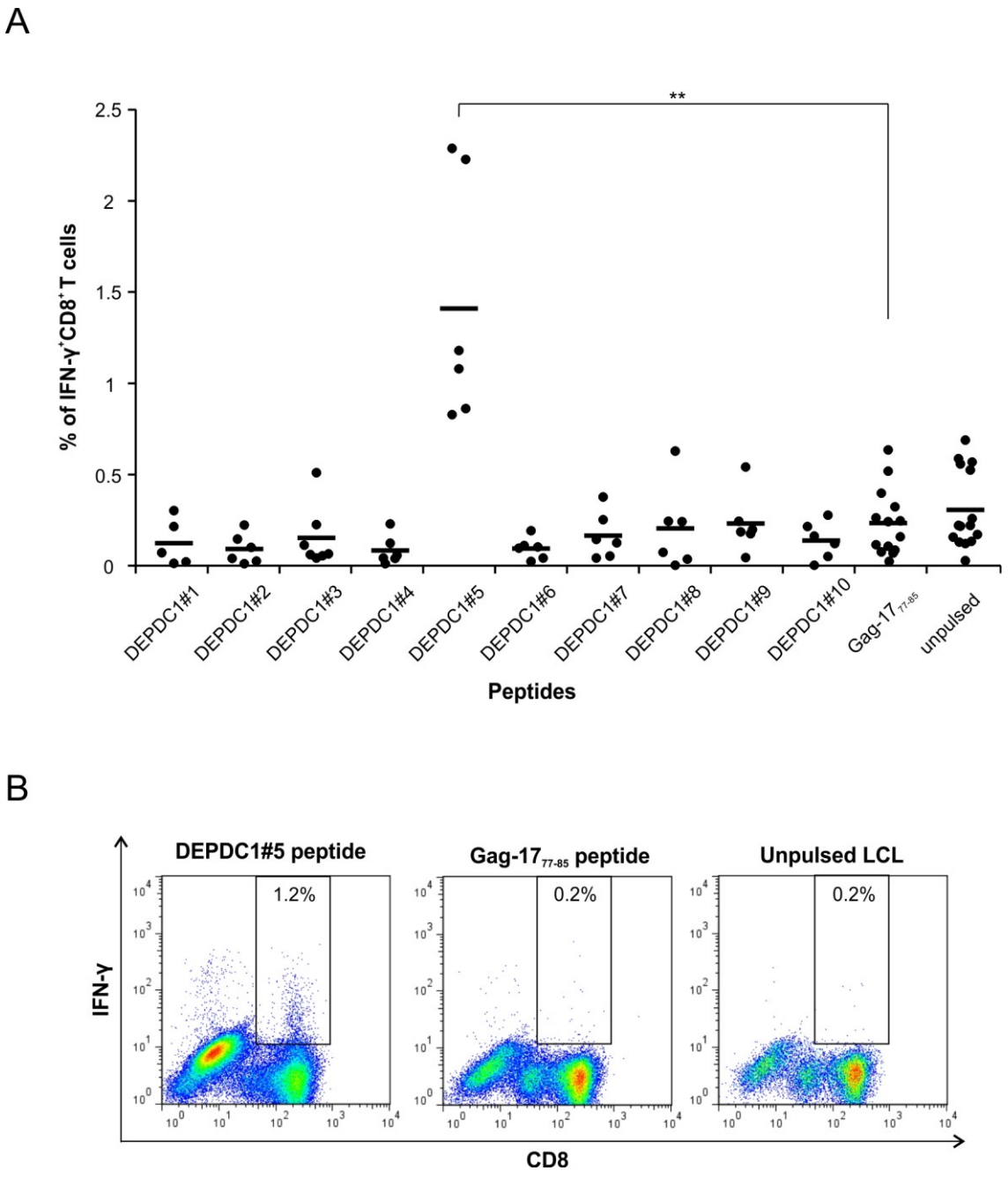

Figure 13. Identification of DEPDC1-derived immunogenic epitopes. (A) IFN-γ production from $CD8^+$ T cells stimulated for 3 times with autologous DCs pulsed with each DEPDC1-derived peptide was measured in response to unpulsed or pulsed LCL cells, by cytokine intracellular staining. LCL cells loaded with Gag-$17_{77\text{-}85}$ peptide served as a negative control. Data are presented as the percentage of $CD8^+$ T cells positive for IFN-γ staining [** = P< 0.01; not statistically significant (p > 0.05) if not indicated]. **(B)** Flow cytometry dot plots of intracellular IFN-γ detection in a DEPDC1#5 peptide-derived T cell culture upon challenge with LCL cells pulsed with either DEPDC1#5 or Gag-$17_{77\text{-}85}$ peptide, or unpulsed. Within each gate, the percentage of IFN-γ producing $CD8^+$ T cells is reported. The panel shows one representative experiment out of 6 performed.

5. Phenotypical characterization of DEPDC1#5-stimulated T cell populations

The results from the intracellular staining for IFN-γ detection lead us to focus on and further characterize DEPDC1#5 peptide-restimulated T cell cultures. Figure 14A displays the flow cytometry gating strategy for phenotypical characterization of the cell cultures. In particular, after three stimulation rounds the bulk population was essentially composed of $CD8^+$ T cells (79.4 ± 1.5%; n = 24 donors), but a small fraction of $CD4^+$ T cells was still present in the cultures (7.5 ± 5.9%; n = 24 donors; Figure 14 B). Because of the different contribution of memory subsets in mediating antitumor immune responses [232], the differentiation state of T cells was investigated through the combined analysis of the chemokine receptor CCR7 and the CD45RA isoform, to distinguish $CCR7^+CD45RA^+$ naïve, $CCR7^+CD45^-$ central memory (CM), $CCR7^-CD45RA^-$ effector memory (EM) and $CCR7^-CD45RA^+$ terminally differentiated (Temra) cells [233]. The majority of $CD8^+$ lymphocytes after 3 weeks of cultures had an effector memory phenotype (78.48 ± 7%; n = 11 donors; Figure 14 C), mainly with the lack of expression of both the lymphoid-homing marker CD62L and the co-stimulatory molecule CD28 (58.8 ± 17% $CD62L^-CD28^-$ among $CCR7^-CD45RA^-$ $CD8^+$ T cells; n = 11 donors; Figure 14 D). A small group of $CCR7^-CD45RA^-$ $CD8^+$ T cells were $CD62L^-CD28^+$ (20.0 ± 16% $CD62L^-CD28^+$ among $CCR7^-CD45RA^-$ $CD8^+$ T cells; n = 11 donors) or $CD62L^+CD28^+$ (11.1 ± 8% $CD62L^+CD28^+$ among $CCR7^-CD45RA^-$ $CD8^+$ T cells; n = 11 donors; Figure 14 D), indicating subsets of “transitional” memory T cells, more differentiated than CM T cells but not as fully differentiated as EM T cells in terms of phenotype [234]. NK cells ($CD3^-CD16^+CD56^+$) and NKT cells ($CD3^+CD16^+CD56^+$) were essentially undetectable in the cultures (data not shown).

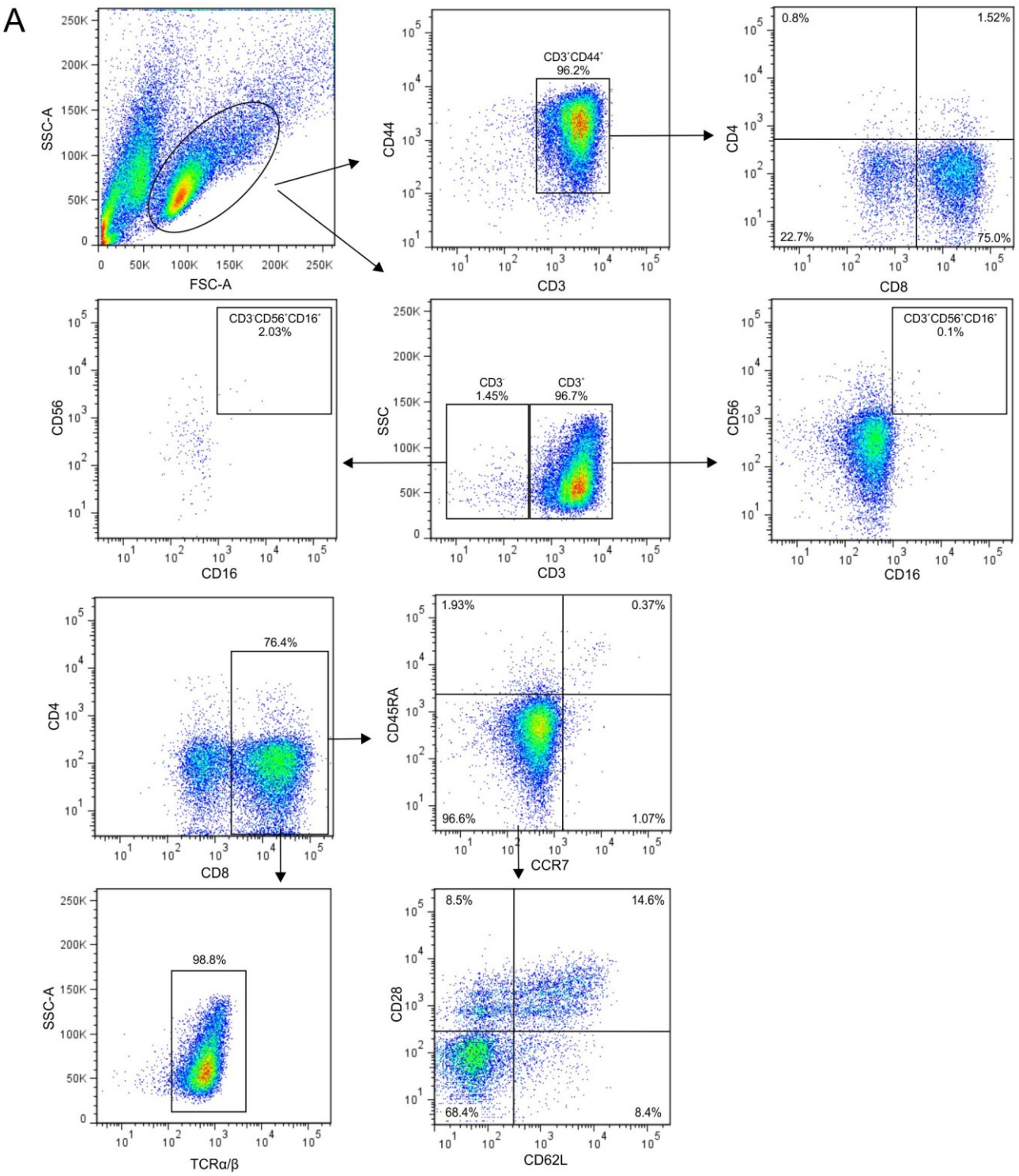
A
SSC-A
FSC-A
CD3+CD44+
96.2%
CD44
CD3
CD4
CD8
0.8%
1.52%
22.7%
75.0%
CD3-CD56+CD16+
2.03%
CD56
CD16
SSC
CD3-
1.45%
CD3+
96.7%
CD3-CD56+CD16+
0.1%
76.4%
CD4
CD8
1.93%
0.37%
96.6%
1.07%
CD45RA
CCR7
98.8%
TCRα/β
8.5%
14.6%
68.4%
8.4%
CD28
CD62L

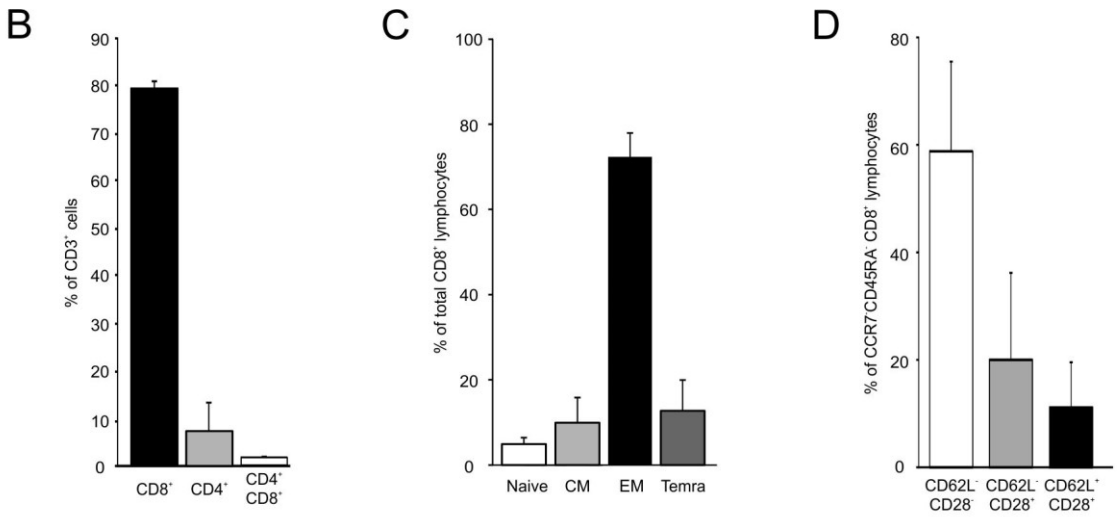

Figure 14. Characterization of DEPDC1#5 peptide-specific T cell cultures. (A) Flow cytometry gating strategy for T cell subsets analysis. Numbers refer to percentage of positive cells. **(B)** Flow cytometry analysis of T cells subsets in cell cultures after 3 stimulations with autologous DCs pulsed with DEPDC1#5 peptide. The mean percentage and standard deviation are shown (n = 24 healthy donors). **(C)** Percentages of $CD8^+$ T cells within subsets defined by the expression of CD45RA and CCR7 differentiation markers [$CD45RA^+CCR7^+$ naïve, $CD45RA^-CCR7^+$ central memory (CM), $CD45RA^-CCR7^-$ effector memory (EM) and $CD45RA^+CCR7^-$ terminally differentiated effector memory (Temra) cells]. The mean percentage and standard deviation are shown (n = 11 healthy donors). **(D)** Percentages of $CCR7^-CD45RA^-$ effector memory $CD8^+$ T cells within subsets defined by the expression of CD62L and CD28 markers The mean percentage and standard deviation are shown (n = 11 healthy donors).

To evaluate the presence of antigen-specific T cells in culture, we took advantage of the tetramer technology in use in our laboratory. HLA-A*0201/DEPDC1#5-specific biomonomers were purified by HPLC to separate the fraction from unconjugated MHC heavy chains, β2-microglobulins and epitope peptides (Figure 15 A), and subsequently biotinylated. The biotinylated monomers obtained were then purified by HPLC (Figure 15 B) and the tetramers were obtained by the addition of Extravidin-PE. Finally, the efficiency of tetramerization was assessed by ELISA. As shown in Figure 15C, free biomonomers were undetectable in tetramer preparation, indicating that the tetramerization process was carried out with optimal efficiency. DEPDC1#5 peptide-specific $CD8^+$ T cells were then quantified by tetramer staining throughout the culture period. The amount of $CD8^+$ T cells expressing a DEPDC1#5/HLA-A*0201-specific TCR reached a peak (1 ± 0.5%)

after three *in vitro* stimulations, and then slightly declined after the fourth stimulation (Figure 15 D-E).

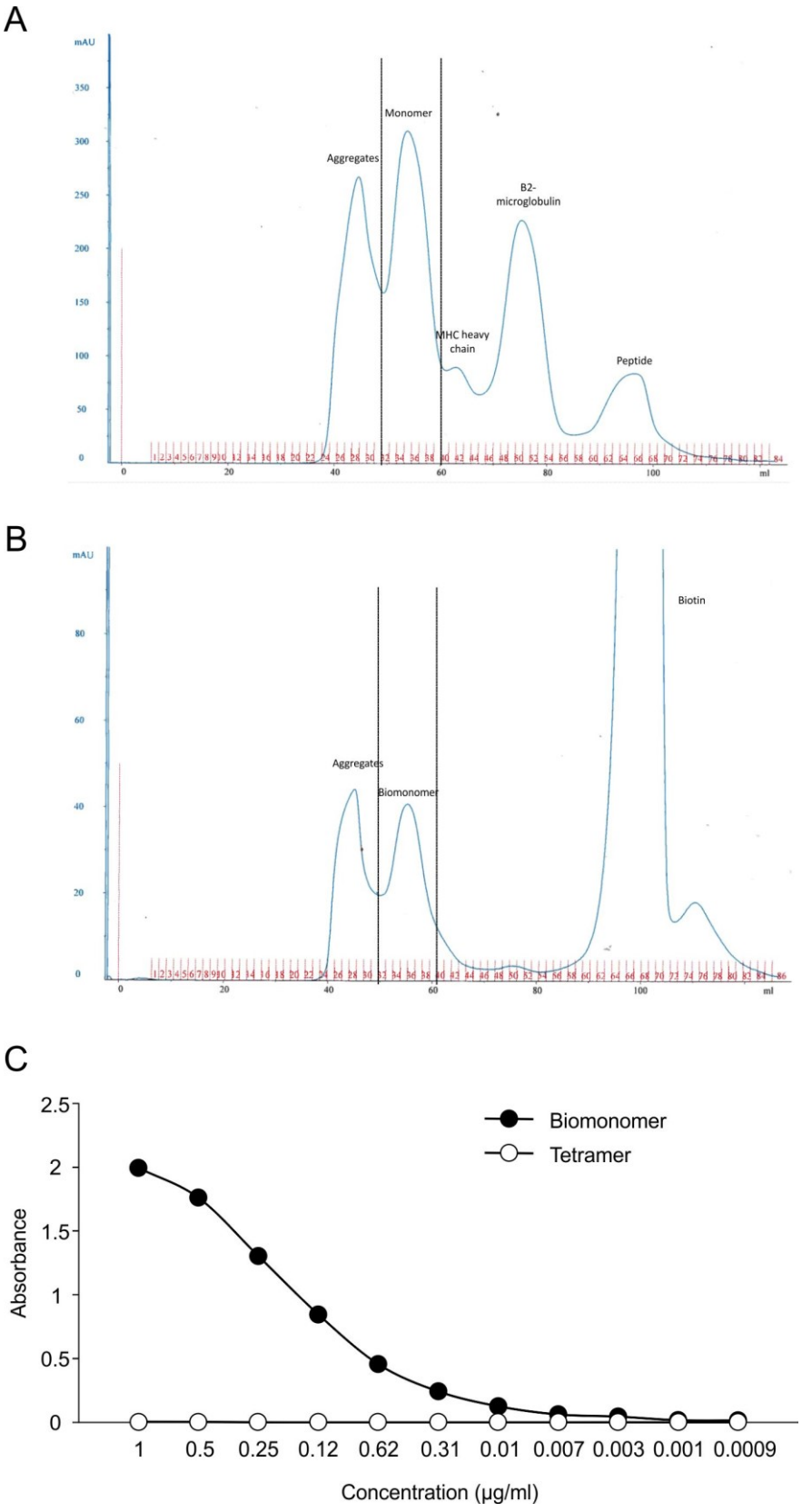

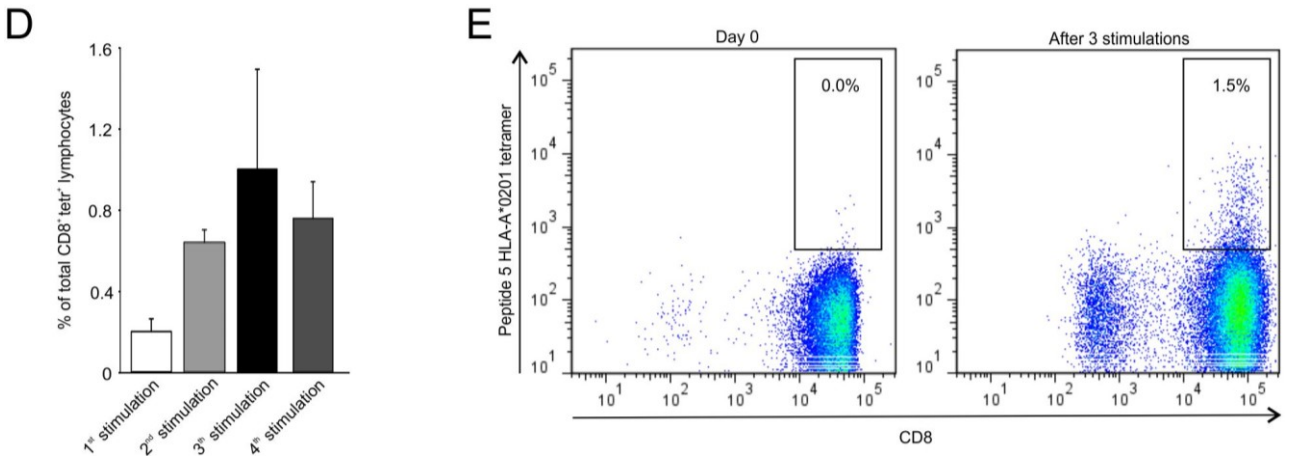

Figure 15. Tetramer staining of DEPDC1#5-specific T cell cultures. (A) HPLC purification of HLA-A*0201/DEPDC1#5 monomers from unconjugated components. Vertical bars refer to the monomer fractions collected. **(B)** HPLC purification of biotinylated HLA-A*0201/DEPDC1#5 monomers from free biotin. Vertical bars refer to the biomonomer fractions collected. **(C)** Tetramerization efficiency of DEPDC1#5-specific tetramer, as assessed by ELISA. The absorbance at 490 nm of different dilutions (starting from 1 µg/ml) of the tetramer preparation (open circles) and biomonomer (filled circles) were compared. **(D)** Tetramer staining of $CD8^+$ T cells after sequential rounds of stimulation. The mean percentage ± SD of $CD8^+$/$tetramer^+$ lymphocytes in cultures is shown for each stimulation. **(E)** Representative tetramer staining of DEPDC1#5 peptide-stimulated T cell culture at day 0 (left) and after 3 stimulations (right), out of the 8 experiments performed.

6. DEPDC1#5 peptide-stimulated CTL are HLA-A*0201-restricted, strictly antigen-specific and recognize an endogenously processed epitope in tumor cells

Antigen specificity of CTLs stimulated with DEPDC1#5 peptide was assessed against the MDA-MB-231 TNBC cell line, which is HLA-A*0201-positive and endogenously express DEPDC1 (Figure 16 A). Upon challenge with these cells, a consistent fraction of DEPDC1#5 peptide-induced CTL was stimulated to produce IFN-γ; on the other hand, the percentage of cytokine-producing $CD8^+$ CTLs sharply dropped in response to MDA-MB-231 cells either pretreated with the anti-MHC class I W6/32 blocking antibody, or silenced for DEPDC1 expression by a specific short hairpin RNA (shDEPDC1). A control scrambled siRNA (shCTRL) produced no relevant effects on recognition (Figure 16 B). Additionally, a very limited IFN-γ response was observed against the human embryonic kidney 293 cell line, which endogenously express DEPDC1 (Figure 16 A) but is devoid of

the HLA-A*0201 molecule. Conversely, their stable transfection with the HLA-A*0201 allele (Figure 16 C) led to a prompt and sustained recognition of target cells, and increased the percentage of IFN-γ^+ responding $CD8^+$ T cells (Figure 16 B).

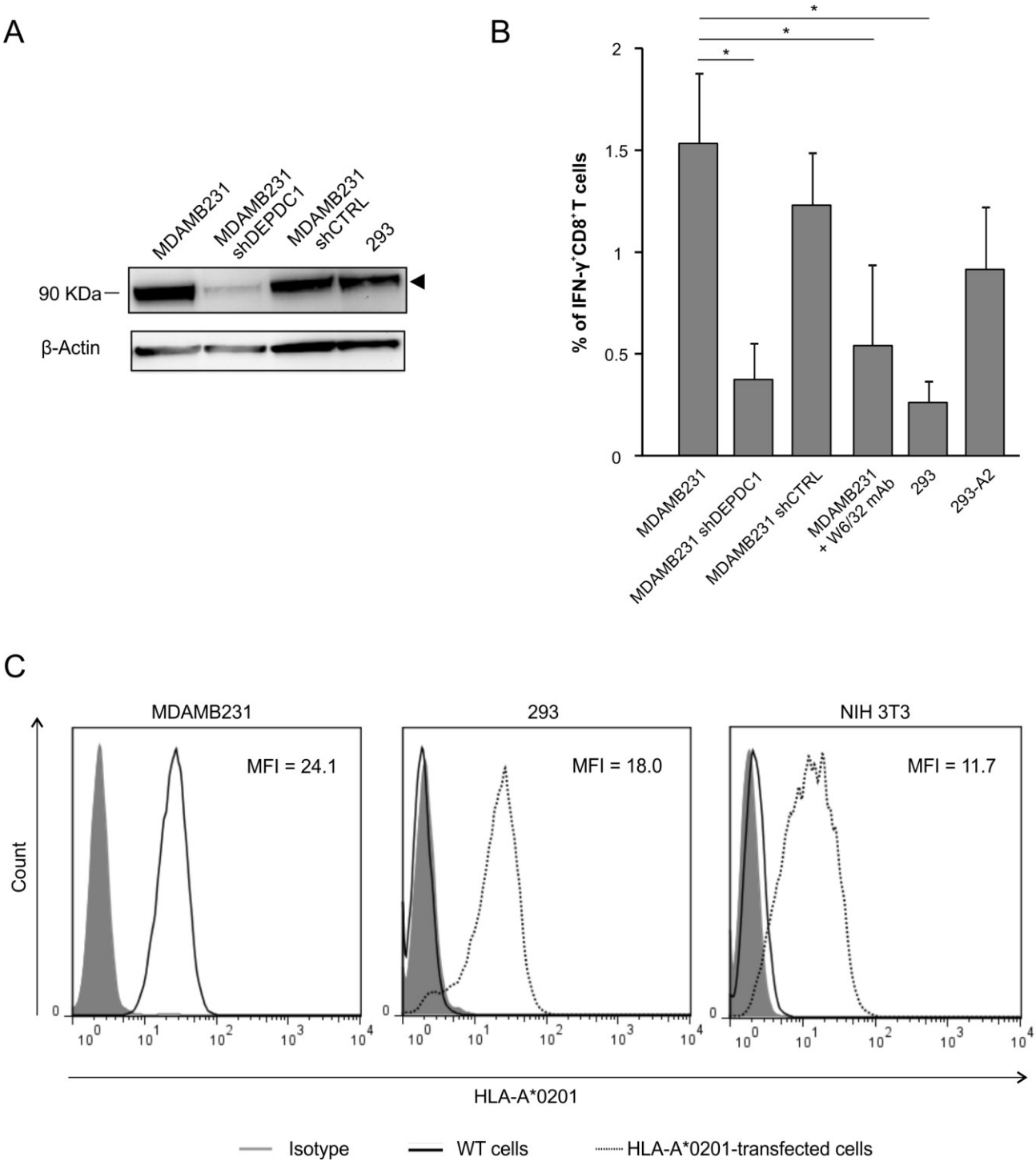

Figure 16. Specific functional response of DEPDC1#5 peptide-stimulated CTLs. (A) Western blot analysis of DEPDC1 protein expression in MDA-MB-231 and 293 cell lines. MDA-MB-231shDEPDC1 are silenced for DEPDC1, while shCTRL refer to cells silenced with a scrambled control siRNA. **(B)** Intracellular IFN-γ staining of DEPDC1#5 peptide-specific $CD8^+$ T cells stimulated for 3 times with autologous DEPDC1#5 peptide-pulsed DC. Data are presented as the mean percentage ± SD of $CD8^+$ T cells positive for intracellular IFN-γ staining (* = P< 0.05; n = 3 healthy donors). **(C)** HLA-A*0201 expression on transfected (dotted lines) and untransfected (dark lines) 293 and NIH 3T3 cell lines. MDA-MB-231 were used as positive control.

In support of these data, the cytotoxic activity of DEPDC1#5 peptide-stimulated CTLs was assessed in a classical ^{51}Cr-release assay. CTLs exerted a high cytotoxic activity against MDA-MB-231 cell line; such lysis was significantly reduced by DEPDC1 silencing, while the shCTRL did not affect the cytotoxicity, thus confirming antigen specificity (Figure 17 A).

To further demonstrate that the CTL activity was specific for the DEPDC1#5 peptide, MDA-MB-231 cells were pulsed with DEPDC1#5 or Gag-$17_{77\text{-}85}$ peptides, and tested for susceptibility to lysis. In this condition, exogenous peptides bind to HLA-A*0201 and replace the endogenously presented peptides. CTLs exhibited a significantly higher lytic activity against DEPDC1#5-pulsed MDA-MB-231 cells as compared to the same cells pulsed with the irrelevant HLA-A*0201-restricted peptide (Figure 17 B). As a confirmation of the HLA-A*0201 restriction, the incubation of MDA-MB-231 cells with the W6/32 blocking antibody led to a significant reduction of cytotoxicity, an effect that was not observed with the addition of an isotype control antibody (Figure 17 C). Furthermore, DEPDC1#5 peptide-stimulated CTLs were significantly more cytotoxic against HLA-A*0201 transfected 293 cells, which acquire the ability to present DEPDC1-derived peptides in the context of the HLA-A*0201 molecule, compared to wild type 293 cells that lack the expression of this allele (Figure17 D).

The critical aspects of peptide specificity and HLA recognition were further confirmed by assessing the lytic activity of DEPDC1#5 peptide-stimulated CTLs against the NIH 3T3 murine fibroblast cell line, which does not express endogenously both human DEPDC1 and HLA-A*0201. CTLs did not disclose any relevant activity against wild type NIH 3T3 cells, but cytotoxicity significantly increased when target cells were simultaneously transfected with HLA-A*0201 (Figure 16 C) and pulsed with DEPDC1#5 peptide; HLA-A*0201-transfected NIH 3T3 cells unloaded or pulsed with an irrelevant peptide were essentially not recognized (Figure 17 E).

The differences in cytotoxic activity among experimental and control samples can be further appreciated when data are expressed in terms of LU_{30} (Figure 17 F-G).

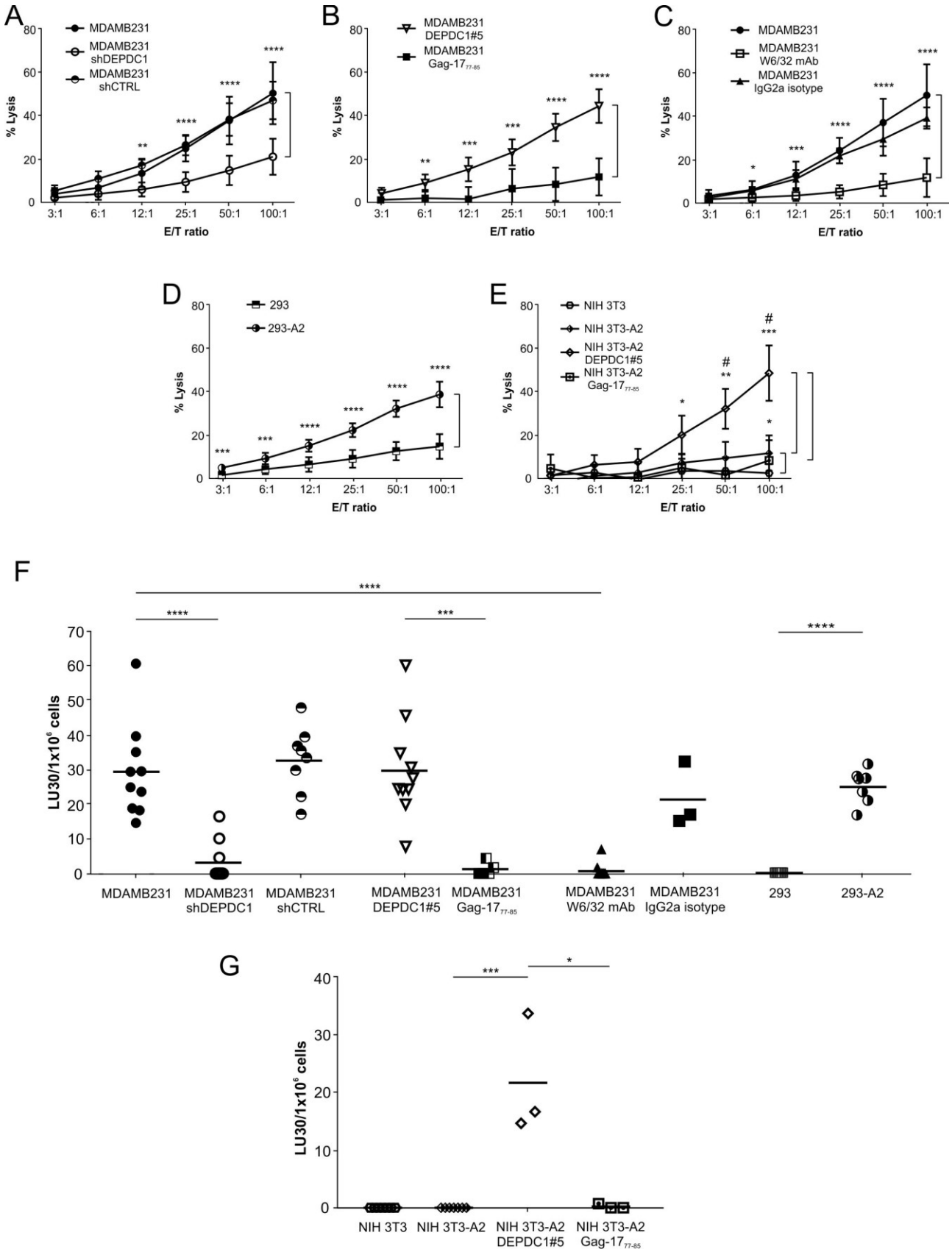

Figure 17. Functional characterization of DEPDC1#5 peptide-stimulated CTLs. (A-E) Lytic activity and specificity of DEPDC1#5 peptide-stimulated CTL. Cytotoxicity of $CD8^+$ T cells stimulated for 3 times with autologous DEPDC1#5 peptide-pulsed DC was analyzed by a 6-h chromium release assays against the reported targets. Results are expressed as percentage of specific lysis at different effector-to-target (E/T) ratio [* = P< 0.05; ** = P< 0.01; *** = P< 0.001; **** = P<0.0001; # = P< 0.05, as referred to NIH 3T3-A2 DEPDC1#5 *vs.* NIH 3T3-A2 Gag-17_{77-85}; not statistically significant (P > 0.05) if not indicated]. **(F-G)** Cytotoxicity data of curves in A-E are expressed as LU_{30} [* = P< 0.05; *** = P< 0.001; **** = P<0.0001; not statistically significant (P > 0.05) if not indicated].

7. DEPDC1#5 peptide-stimulated CTL restrain tumor growth *in vitro*

To investigate the ability to induce long-term effects *in vitro*, DEPDC1#5 peptide-stimulated CTLs were co-cultured with MDA-MB-231 or NIH 3T3 in an outgrowth assay. After 4 weeks, both MDA-MB-231 and NIH 3T3 reached the full confluency in the absence of lymphocytes. Conversely, the addition of DEPDC1#5 peptide-stimulated CTLs completely inhibited the growth of MDA-MB-231 cells (Figure 18), even at very low effector/target ratios. Control CTLs represented by T cells redirected to the prostate-specific membrane antigen (PSMA) by transduction with a PSMA-specific chimeric antigen receptor (CAR) [235], were not able to repress MDA-MB-231 growth, and served as control for antigen specificity (Ctrl-CTL). No effects were observed on NIH 3T3 cell growth (Figure 18).

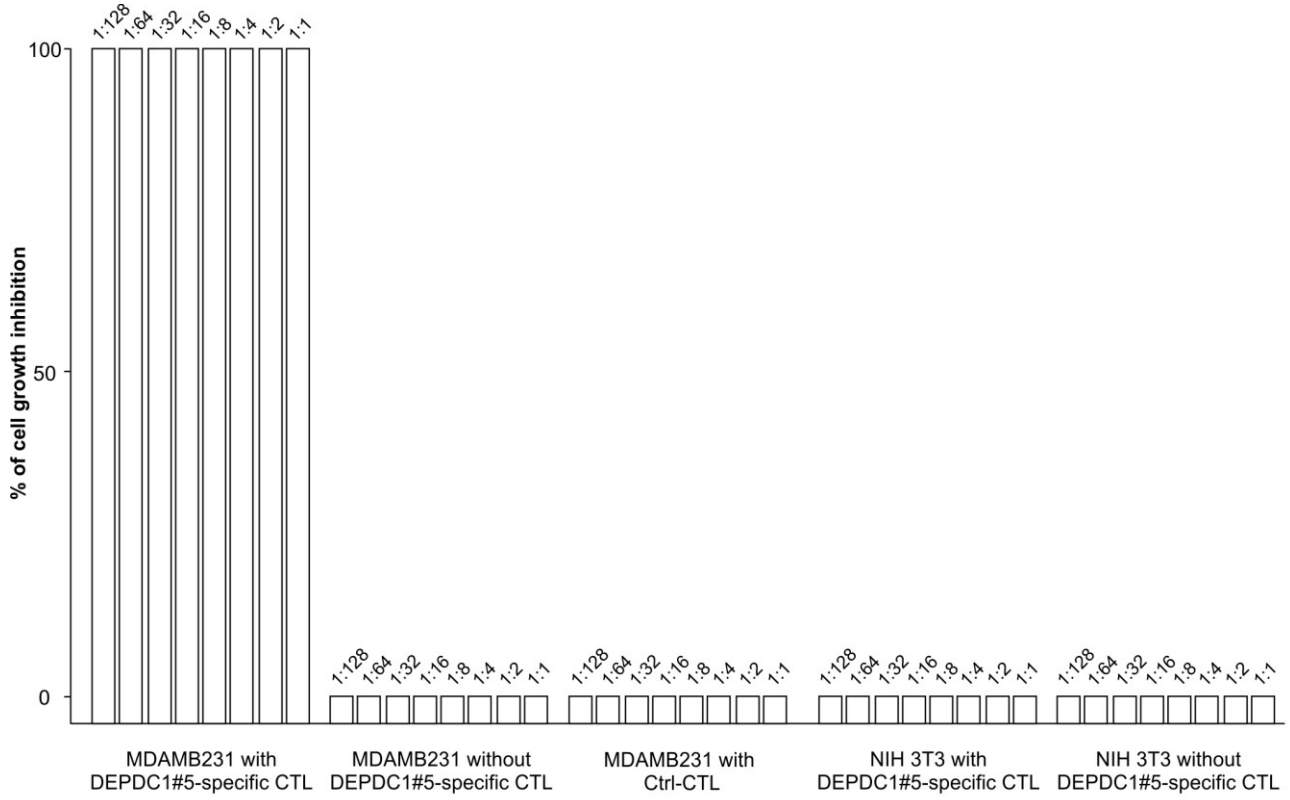

Figure 18. *In vitro* tumor growth restraining activity by DEPDC1#5 peptide-specific CTLs. The figure reports the inhibition of MDA-MB-231 outgrowth by DEPDC1#5 peptide-specific T cells. MDA-MB-231 cultured alone or in presence of non-specific CTL (Ctrl-CTL), and NIH 3T3 cells alone or co-cultured with DEPDC1#5 peptide-specific CTL were used as negative controls. Results are expressed as percentage of target cell growth inhibition, and the numbers above each bar refer to the target:CTL ratio (n = 3 healthy donors).

8. Set up of DEPDC1-unrelated peptide-stimulated T cell cultures as proper controls for adoptive immunotherapy

Before proceeding with experiments aimed at assessing the *in vivo* therapeutic efficacy of anti-DEPDC1 T cells upon adoptive transfer, unrelated control effectors were generated. Thus, CTL populations directed against the HLA-A2-restricted Melan-$A_{26\text{-}35*A27L}$ peptide were obtained following the same protocol used to generate DEPDC1#5 peptide-stimulated CTL, and the amount of $CD8^+$ T cells expressing a Melan-$A_{26\text{-}35*A27L}$/HLA-A*0201-specific TCR was quantified using tetramer staining throughout the culture period (25.7 ± 19.44% at the third round of stimulation, n = 3 healthy donors; Figure 19 A-B). The cytotoxic activity of Melan-$A_{26\text{-}35*A27L}$ peptide-stimulated CTL was assessed in a classical ^{51}Cr-release assay to confirm that they didn't recognize MDA-MB-231 cells alone or pre-loaded with the DEPDC1#5 peptide. Conversely, if breast cancer cells were

pulsed with the Melan-$A_{26\text{-}35*A27L}$ peptide, the cytotoxicity was significantly increased (Figure 19 C-D).

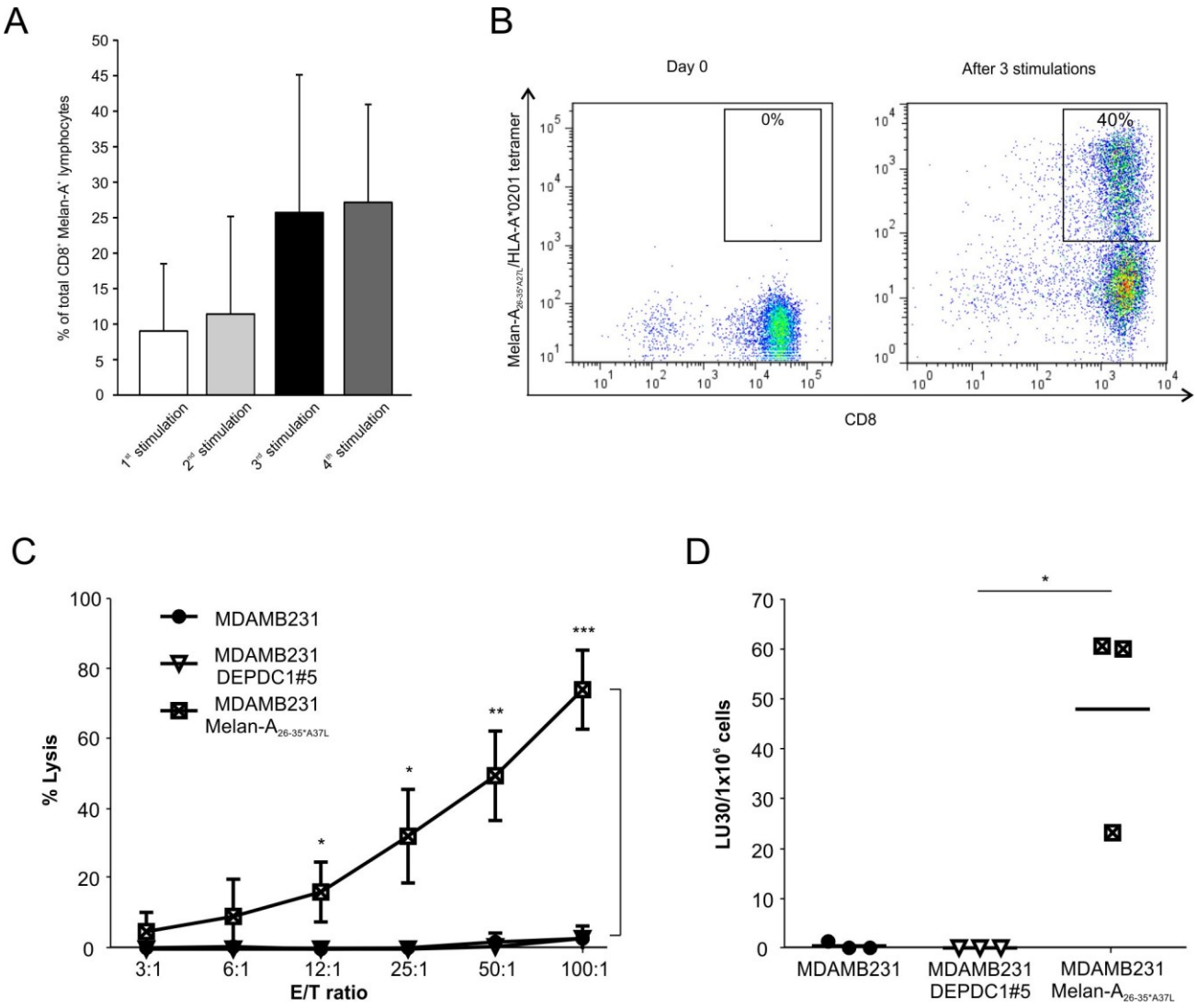

Figure 19. Characterization of Melan-$A_{26\text{-}35*A27L}$-stimulated CTL populations. (A) Tetramer staining of $CD8^+$ T cells in cultures undergoing sequential rounds of stimulation. The mean percentage ± SD of $CD8^+$/$tetramer^+$ lymphocytes in cultures is shown for each stimulation. **(B)** The panel shows the tetramer staining of a representative Melan-$A_{26\text{-}35*A27L}$ peptide-stimulated T cell culture at day 0 (left) and after 3 stimulations (right), out of the 3 experiments performed. **(C)** Lytic activity of Melan-$A_{26\text{-}35*A27L}$ peptide-stimulated CTL analyzed by a 6-h chromium release assays against the reported targets. Results are expressed as percentage of specific lysis at different effector-to-target (E/T) ratio [* = P< 0.05; ** = P< 0.01; *** = P< 0.001; not statistically significant (P > 0.05) if not indicated]. **(D)** Cytotoxic activity as in (C) was expressed in terms of LU30 [* = P< 0.05; not statistically significant (P > 0.05) if not indicated].

9. Adoptively transferred DEPDC1#5 peptide-stimulated CTLs inhibit breast cancer growth and restrain metastasis process

The *in vivo* therapeutic efficacy of DEPDC1#5 peptide-stimulated and control CTL was evaluated against MDA-MB-231 cells stably transduced with the firefly luciferase (luc) reporter gene, and injected into the mammary fat pad of NSG female mice. Three days after inoculation, the tumor was detected by BLI and a group of mice (n = 9) received intra-tumor injections of DEPDC1#5 peptide-stimulated CTLs for a total of 3 doses, whereas another group (n = 8) received CTL cultures stimulated against the irrelevant Melan-$A_{26\text{-}35*A27L}$ peptide; the untreated mice (n = 18) were injected with PBS (Figure 20 A). While a progressive increase in tumor growth was observed in the two groups of control mice, DEPDC1#5 peptide-stimulated CTL treatment was able to delay the primary tumor growth (Figure 20 B).

When MDA-MB-231 cells are injected orthotopically into mammary fat pad in NSG mice, metastases are frequently observed 3-4 weeks later in the axillary lymph nodes and lungs [236–238]. In this regard, mice treated with CTLs showed a significant reduction in peripheral metastatic colonization as compared to untreated mice and to mice treated with Melan-A-specific CTLs, when examined at the same primary tumor size (Figure 20 C), thus clearly indicating that DEPDC1#5 peptide-stimulated CTLs were also effective in inhibiting metastases.

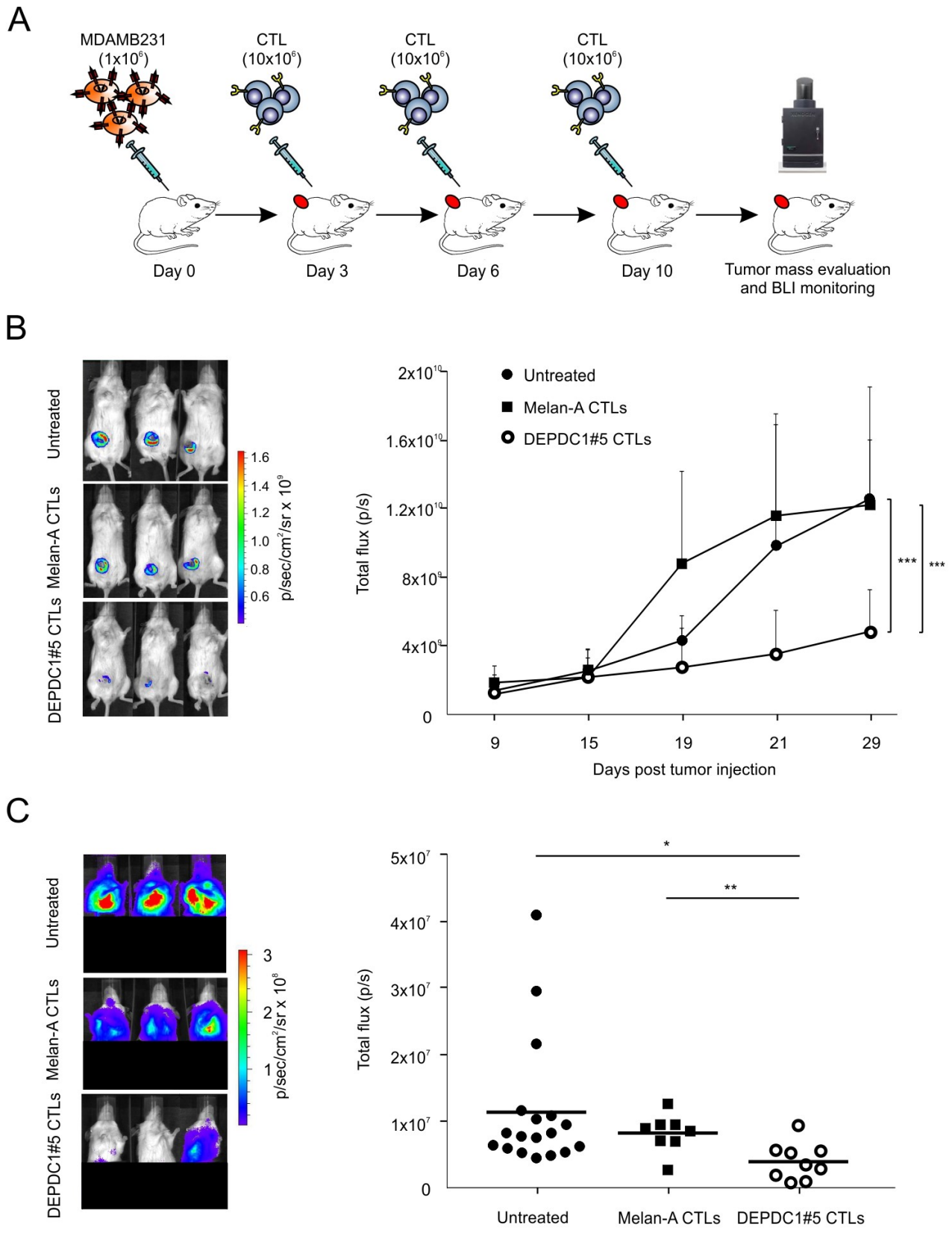

Figure 20. Assessment of therapeutic efficacy *in vivo* of DEPDC1#5 peptide-specific CTL. (A) On day 0, NSG mice were injected into the mammary fat pad with $1x10^6$ luc-transduced MDA-MB-231 cells, and were treated intra-tumorally at days 3, 6 and 10 with $1x10^7$ DEPDC1#5 peptide-specific

CTLs (n = 9) or Melan-A peptide-specific CTL (n = 8). The untreated group of mice received 3 injections of PBS1X (n = 18). **(B)** Tumor growth was monitored by BLI measurement as photon flux. Left panels show the primary tumor BLI of 3 representative mice for each group after 29 days from tumor injection, while right panel reports tumor growth of all animals at different time points (mean of photons/second ± SD; *** = $P < 0.001$; the ANOVA was used for statistical analysis). **(C)** Distant metastatic colonization was evaluated by BLI when a primary tumor size of about 700 mm^3 was reached in each group. The left panels show the BLI of distant metastases in 3 representative mice for each group, while right panel reports the photons/second detected in each individual mouse belonging to the different groups (* = $P < 0.05$; ** = $P < 0.01$).

10. Multispectral imaging and optimization of 7-colors fluorescence multiplex immunohistochemistry with Opal staining

During my three-months training in Paris at the Prof. Galon's laboratory, I learned the fundamentals of multispectral imaging using the PerkinElmer's Opal multiplex immunohistochemistry (mIHC) technique on colorectal cancer (CRC) and adenoma tissue sections, an expertise that will be instrumental for further studies in the context of the current TNBC project. The mIHC enables simultaneous detection of multiple proteins of interest of formalin-fixed paraffin-embedded (FFPE) tissue sections. In my protocol, an HRP-conjugated secondary antibody binds to an unconjugated primary antibody specific for the target/antigen of interest, and the detection is ultimately achieved with a fluorophore-conjugated tyramide molecule, allowing for serial stripping of the primary/secondary antibody pairs, while preserving the antigen-associated fluorescence signal. PerkinElmer's Phenoptics workflow enables imaging and analysis of up to six immunofluorescence markers, plus counterstaining, within intact FFPE tissue sections, saving valuable tissues and enabling full contextual exploration of multiple cell types, functional states and cell-to-cell interactions that are difficult or impossible to obtain by other methods. There are a number of considerations that can impact the success of a fluorescent mIHC experiment and, in Prof. J. Galon's laboratory, I learned how to successfully optimize 7-colors multiplex assays. In this regard, a critical aspect of multispectral imaging and an essential component to obtain quantitative results is the generation of correct spectral libraries for each fluorophore, including any background or tissue autofluorescence, that means the correct separation of all of the fluorescence signals within the sample. Therefore, the optimal concentration of primary antibodies of the multiplex panels, by performing titrations for each individual component, and the optimal antibody-fluorophore pairing, in order to achieve the best

possible signal intensity and signal to noise ratio for each target of the panels, have to be evaluated. The final aim is to obtain a complete spectral library, including all the fluorescence signals present in the multiplex panel, necessary for accurate unmixing of Opal fluorophores and analysis of multiplex slides (Figure 21).

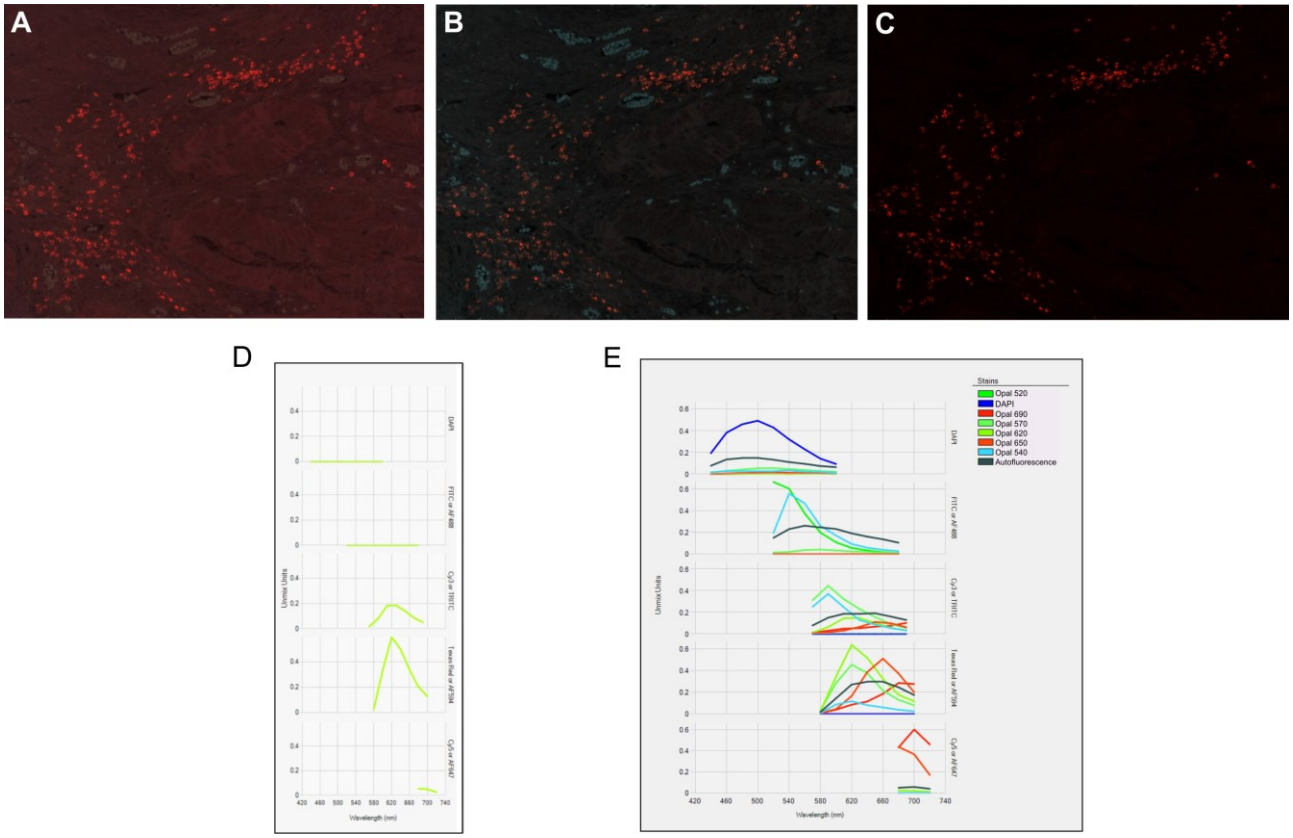

Figure 21. Spectral library from a mIHC assay. An example of a CRC tissue slide with single staining for CD4-Opal620 and the extraction of the corresponding spectrum. **(A)** Original color (RGB) image; **(B)** unmixed Opal620 image showing CD4 expression; **(C)** unmixed image without tissue autofluorescence obtained from an unstained tissue section; **(D)** extracted spectrum of Opal620; **(E)** complete extracted spectral library, which include Opal520, Opal690, Opal570, Opal620, Opal650, Opal540, DAPI and tissue autofluorescence spectra.

Once built an optimized spectral library, including the complete spectral proprieties of each independent signal necessary for spectral unmixing, multiplex staining of CRC and adenoma tissue slides had to be set up. In this regard, it is critical to optimize the order in which the antibodies in a

multiplex panel are applied to the tissue section, to ensure that multiple rounds of heating do not compromise target-specific epitopes. Once found the optimal antibodies order, I analyzed the multiplex stained slides with the Mantra quantitative pathology workstation, which enables isolation of individual colors to allow independent, noninterfering and precise measurement of protein expression, while eliminating background (Figure 22).

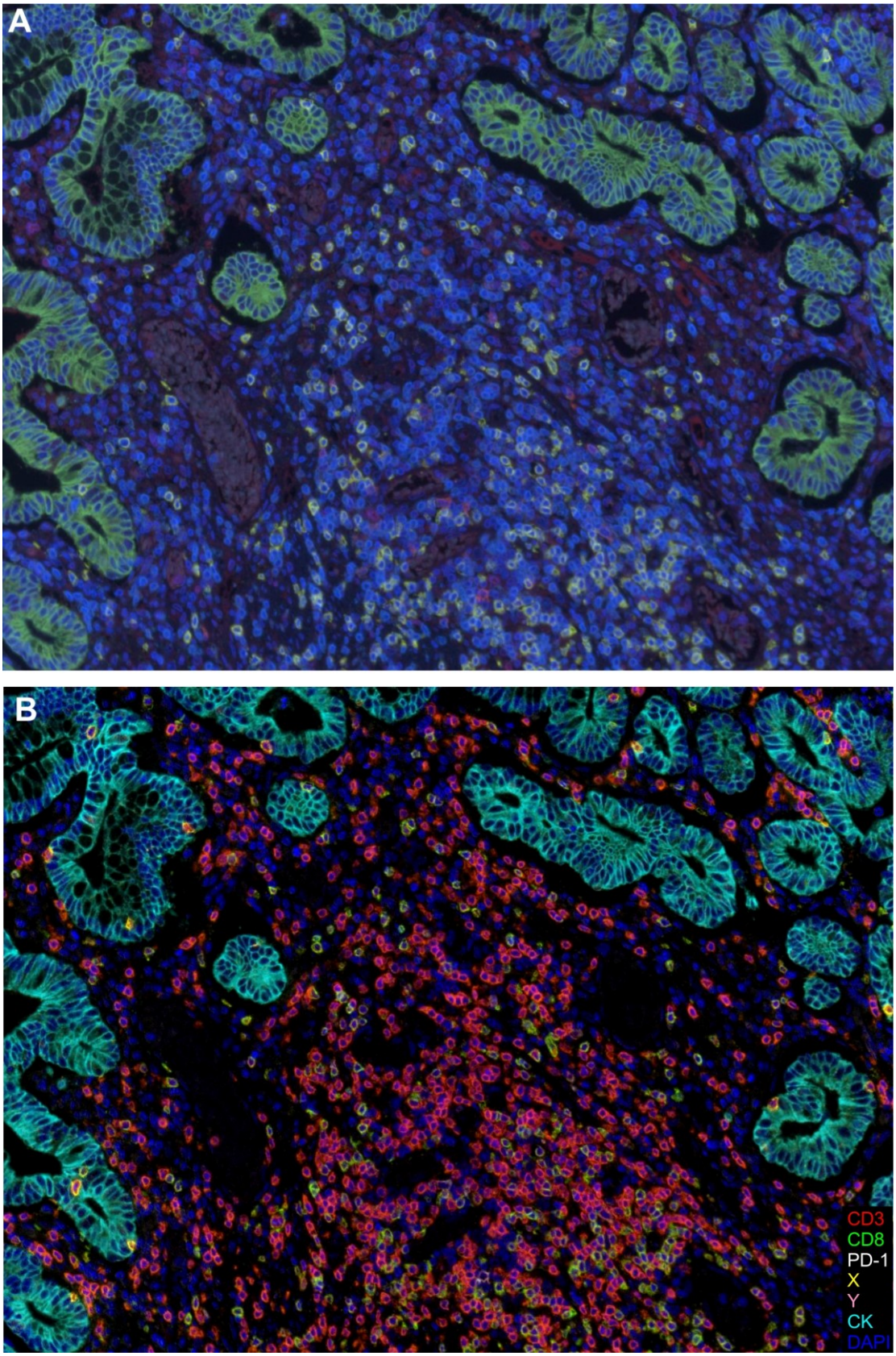

Figure 22. Example of 7-colors multiplex staining of CRC tissue sample. (A) Original RGB image; **(B)** unmixed image stained with CD3 (red), CD8 (green), PD-1 (white), X marker (yellow), Y marker (pink), cytokeratin (cyan), nuclei (blue).

Another important advance afforded by the imaging software, is the ability to take fluorescent IHC images and create simulated brightfield images. Since all images retain multispectral information, elements of the spectra can be used to simulate various brightfield views, such as H&E, or hematoxylin with DAB chromogen (Figure 23).

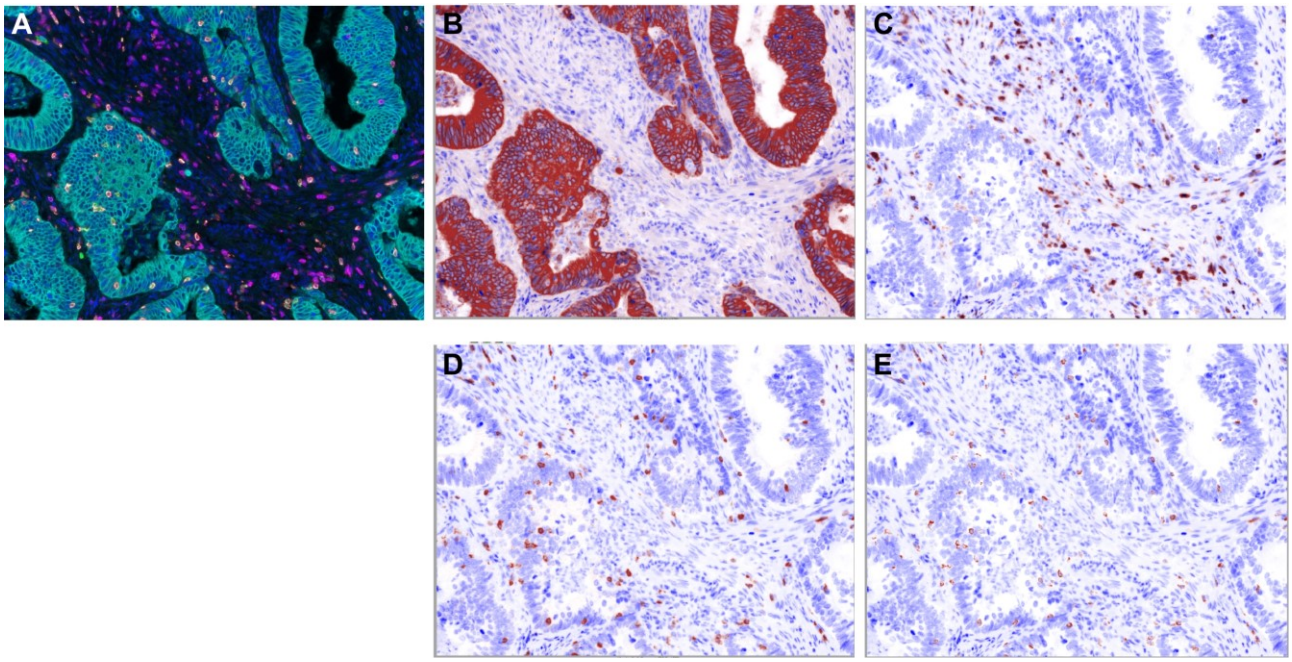

Figure 23. Simulated IHC images. (A) Unmixed mIHC examining the expression of CD3 (magenta), CD8 (red), PD-1 (white), X marker (green), cytokeratin (cyan) and nuclei (blue) in CRC tissue. **(B)** Subsequent simulated hematoxylin and DAB staining indicating cytokeratin expression, **(C)** CD3 expression, **(D)** CD8 expression and **(E)** PD-1 expression.

Using the inForm™ Tissue Finder™ image analysis software, the image analysis starts with an automated tissue segmentation into regions of morphologically distinct architectures, such as tumor and stroma. Trainable pattern recognition makes this possible and avoids often prohibitively laborious manual identification of regions of interest (Figure 24 A). The training of morphologic software was done by drawing representative training regions on some images of the cohort, allowing the software to “learn” to recognize the morphologies of interest. The resulting image segmentation algorithm is then applied to each image. The next step is the identification and segmentation of individual cells, starting with nuclear and then membranous or cytoplasmic

segmentation. The expression of markers can be then read out on a per-cell and per-cell-compartment basis (Figure 24 B). Once the parameters are known for each cell, further advanced machine learning approaches can then automatically “phenotype” cells into user-defined categories and, as Figure 24C shows, it is possible to visualize functional states, cell-to-cell interaction and the location of single cells within the tumor and in the stroma. Since the xy coordinates and the tissue context are preserved, a wide range of spatial and cellular interaction metrics can be explored: Figure 24D displays an example of a possible analysis that can be achieved with the exported data, allowing the quantification of different cell types in distinct morphological areas of the tumor microenvironment.

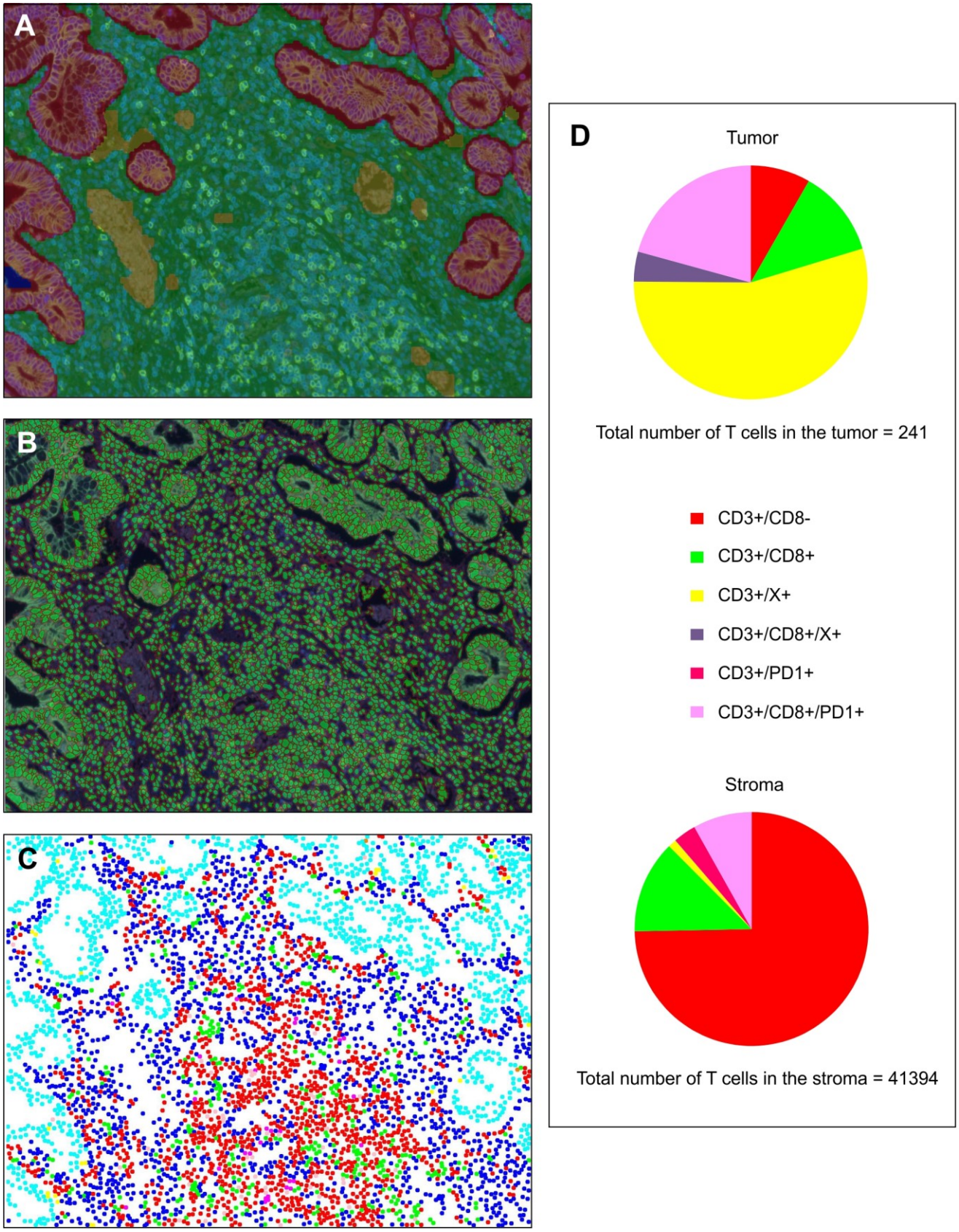

Figure 24. Image analysis of multiplex immunohistochemically stained sections. (A) Tissue segmentation. Tumor regions are shown in red, stroma in green, blood vessels in yellow and no tissue in blue. **(B)** Cell segmentation. Membranes are shown in red and nuclei in green. **(C)**

Phenotyping. $CD3^+/CD8^-$ cells are shown in red, $CD3^+/CD8^+$ cells in green, $CD3^+/PD1^+$ cells in magenta, $CD3^+/CD8^+/PD1^+$ cells in pink, $CD3^+/X^+$ cells in yellow, $CD3^+/CD8^+/X^+$ cells in orange, CK^+ cells in cyan and other cells in blue. **(D)** Example of a possible analysis resulted from exported data, in which specific cell types are quantified in different morphologically distinct regions of the tumor microenvironment.

DISCUSSION

Generally, tumor-specific mutations represent ideal targets for cancer immunotherapy, since they are not present in healthy tissues and can potentially be recognized as neo-antigens by the T-cell repertoire. However, personalized vaccines against these specific mutated proteins are hampered by the fact that every patient's tumor possesses a unique set of mutations, which must be first identified with enormous time-consuming and expensive molecular screenings. Therefore, the identification of tumor-specific antigens shared by multiple patients and by different types of cancers, is crucial to overcome these problems and to make immunotherapy universally applicable. The involvement of DEPDC1 in many aspects of cancer traits suggests its key role in tumor cell growth and survival [120,121], hence supporting a low possibility of antigen down-regulation. Therefore, we investigated DEPDC1 gene expression among human cancer tissues using the Oncomine database, and found that it is overexpressed almost ubiquitously in human cancers as compared to the healthy counterpart tissues. This aspect, together with its involvement in the oncogenic process, strongly indicate that DEPDC1 can be regarded as a novel universal oncoantigen, potentially suitable for targeting many different tumors.

Additionally, the pathologic and prognostic value of DEPDC1 up-regulation is consistently supported by its association with the most common clinic-pathological variables associated to cancer aggressiveness, such as the presence of regional nodal metastasis, invasion of distant organs and presence of poorly differentiated or undifferentiated abnormal-looking cells, and a significant correlation was demonstrated with both overall and disease-free survival. According to the predominant DEPDC1 overexpression in most aggressive tumors, its up-regulation was found to be particularly relevant in TNBCs, which are characterized by a poorer prognosis respect other forms of breast cancer, and associated with an increased risk of recurrence within 3 years from diagnosis and an increased 5-year mortality rate [140]. In this regard, our study showed that a HLA-A*0201-restricted DEPDC1-derived peptide could be exploited for immunotherapy against TNBCs, since nowadays no hormonal treatments or targeted therapies are available for such tumor as it lacks the appropriate targets for these drugs [164].

We decided to focus on the HLA-A*0201 allele as it is the most common HLA class I subtype in the Caucasian population and the second most common in the Japanese population [165,239]. Therefore, ten HLA-A*0201-restricted DEPDC1-derived peptides were identified by integrating the results of

three epitope prediction programs based on the prediction of peptide binding affinity to MHC, the probability of peptide proteasomal cleavage and the efficiency of peptide transport trough the endoplasmic reticulum. One of the peptides tested had the ability to induce a specific and relevant functional CTL response against target cells; indeed, DEPDC1#5-stimulated CTLs produced IFN-γ in presence of both target cells artificially loaded with the DEPDC1#5 peptide, and tumor cells endogenously expressing the DEPDC1 protein. Furthermore, despite the small percentage of tetramer-positive T cells, the DEPDC1#5-stimulated CTL populations exerted a relevant and specific cytotoxic activity against human triple negative breast cancer cells, indicating that TNBC cells naturally process the DEPDC1 antigen and present the epitope in association with the HLA-A*0201 molecules, thus becoming susceptible to the CTL attack. These findings suggest that even a small fraction of antigen-specific T cells can exert a significant lytic function, likely due to the recycling potentialities of the effectors, ultimately leading to a marked enhancement of the overall activity of DEPDC1#5-specific lymphocytes. Nonetheless, the antigen specificity and HLA-restricted nature of the cytotoxicity were confirmed using target cells lacking the protein or the HLA-A*0201 allele or both, which were not recognized by the CTL cultures.

In an attempt to have access to a more representative and consistent effector population, we repeatedly tried to sort the DEPDC1#5 tetramer-positive subset from cultures; however, because of the lower sensitivity of the available instrument (MoFlo Astrios Cell Sorter, Beckman Coulter) as compared to the LSRII flow cytometry, we always failed in detecting and sorting any tetramer-positive cell population. We also tried to isolate DEPDC1#5-specific T cell clones, but the number of T cells obtained was always largely insufficient to perform any additional experiment, in particular *in vivo*. The major problem for expansion was due to the limited availability of autologous dendritic cells required for T cell stimulation. Nonetheless, such material could be useful to isolate DEPDC1#5-specific TCRs for subsequent T cell engineering, even though the long steps of TCR gene cloning, expression in suitable viral vectors, transduction of activated T lymphocytes and assessment of their *in vitro* and *in vivo* functional activity were out of the scope of present work.

Adoptive immunotherapy attempts to circumvent the insufficient T cell responsiveness to tumors by collecting the tumor infiltrating lymphocytes (TIL), providing them with the necessary stimulatory conditions for an optimal activation, and reinfusing into the patient. However, there is no certainty about the type of $CD8^+$ T cells that would be the optimal for the treatment of cancer. Terminal effector T cells provide variable and often very short-lived protection against tumors in

both humans and mice [240,241]. Therefore, the *ex vivo* enhanced survival and proliferative potential of memory T cells, as well as their ability to rapidly become reactivated upon secondary challenge, makes them a more promising choice for generating protective immunity against cancer. However, it remains uncertain whether their protective capacity can be attributed to one particular subset of memory T cells. Central memory T cells expand well in response to a secondary activation and survive for long periods, and hence they are likely to be good at protecting against large tumor burdens, metastasis and relapse [242]. Conversely, effector memory T cells are able to exert immediate cytotoxic activity and should act rapidly to restrain the growth of existing tumors in isolated peripheral sites [243]. After three *in vitro* stimulations with autologous peptide-pulsed DC, we obtained heterogeneous $CD8^+$ T cell cultures, mainly composed by effector memory T cells, and in part by central memory and terminal effector T cells; it is not currently known whether just one or the other of the memory cell subsets is superior in providing protection against cancer, but a heterogeneous T cell population has the benefit to contribute the useful properties of both activated effector memory T cells that can immediately traffic to the tumor and destroy the cells, and central memory T cells that home to the lymph node where they can proliferate and be restimulated by incoming DC from the tumor site, leading to an expansion of the anti-tumor immune response.

The functional response mediated by DEPDC1#5-stimulated CTL was not apparently a short-term effect, as completely inhibited *in vitro* breast cancer cell growth even at very low effector to target ratios. Moreover, in a TNBC mouse model DEPDC1-stimulated CTL delayed breast primary tumor growth and reduced peripheral colonization despite the apparently limited number of DEPDC1#5-specific $CD8^+$ T cells injected, thus demonstrating the effectiveness of the CTL therapy also in restraining of the metastasis process. Conversely, CTL populations directed against the well-known immunogenic Melan-A protein [175], which is not expressed in MDA-MB-231 cells [244], had no therapeutic effects despite the higher amount of Melan-$A_{26\text{-}35*A27L}$ specific $CD8^+$ T cells infused, thus excluding a possible therapeutic effect of non-specific lymphocytes.

In conclusion, we demonstrated that the HLA-A*0201-restricted DEPDC1#5 peptide is a putative tumor epitope that could be exploited in immunotherapy against different tumors overexpressing the DEPDC1 protein. Data from literature show that such results are *per se* sufficient to justify the transfer to the clinical setting and the starting of a vaccination clinical trial. With the specific regard to DEPDC1, Obara and colleagues [137] identified a HLA-A24-restricted epitope from DEPDC1 through a genome-wide expression profile analysis of bladder cancer, and used it for vaccinating

patients. Notably, the overall preclinical assumptions were based on the *in vitro* establishment of four DEPDC1-specific CTL clones, which were simply tested for IFN-γ production and cytotoxicity against suitable targets. Thereafter, authors moved directly *in vivo* in bladder cancer patients, where they proved the immunogenicity of the peptide also following vaccination. Currently, we cannot advance a clinical trial with the identified DEPDC1#5 peptide, and therefore the only possibility we foresee to demonstrate its immunogenicity *in vivo* would be the identification of the potential mouse counterpart (if existing), and the carrying out of vaccination studies in mice. An alternative could be represented by immunization studies in HLA-A2-transgenic mice, but previous experiences in the lab with HHD mice (a transgenic strain carrying a hybrid K^b/HLA-A2 molecule) have been always quite unsuccessful.

This is the main reason we decided to perform adoptive transfer experiments *in vivo* in tumor-bearing mice, to provide insights about the potentiality of the identified antigenic epitope in eliciting a functional T cell population; indeed, since CTL proved to maintain a tumoricidal potential, this approach suggest that DEPDC1#5-expanded CTL cultures could be potentially suitable for ACT in TNBC patients and/or patients carrying DEPDC1-expressing tumors. A major problem for this approach, however, might be represented by the limited number of DEPDC1#5-specific T cells obtained after the *in vitro* stimulations. Nonetheless, this might be due to the fact that our DEPDC1#5-specific CTL cultures were generated from healthy donor PBMC, in which DEPDC1-specific precursors were essentially undetectable at day 0. In this regard, it would be interesting to try to stimulate a potentially primed DEPDC1-specific T cell population derived from the peripheral blood or neoplasia of cancer patients with DEPDC1-positive tumors. This approach is currently ongoing in collaboration with colleagues at the National Cancer Institute in Aviano (CRO-IRCCS), and involves the stimulation of PMBC from TNBC patients, even though preliminary results are still elusive. Alternatively, a Rapid Expansion Protocol approach [245] could be tried, even though such technology is currently not set up in our laboratory.

Moreover, as recent studies showed that therapy with immune-checkpoint inhibitors enhanced neoantigen-specific T cell reactivity, a possible shortcut to bypass the availability of limited amounts of expanded DEPDC1#5-specific CTL populations for adoptive transfer in patients, could rely on combination therapeutic approaches with immune-checkpoint inhibitors currently in clinical use, such as the monoclonal antibodies Ipilimumab (anti-CTLA-4), MDX-1106 (anti-PD-1) or BMS-936559 (anti-PD-ligand1 [PD-L1]) [246], capable of enhancing antigen-specific T cell reactivity and inducing more effective antitumor immune responses.

As an alternative, cloning the TCR from DEPDC1#5-reactive T cells to be used for genetically engineering patient T cells could represent an option to generate large amounts of effectors, even though the requirement of specialized GMP facilities and the strong safety problems associated to the genetic manipulation of donor lymphocytes represent serious constrains for this approach.

Nonetheless and taking together, the results of this study support the concept that DEPDC1 can be considered as a universal tumor antigen, and might represent a potential and safe target for treating many human tumor subtypes through immunotherapy, as its overexpression is confined only in tumor cells and not in normal tissues.

As further advances in immunotherapy approaches require a detailed understanding of the tumor microenvironment, including the characterization of functional states of different immune cells, their spatial distribution and their interactions with tumor cells, we plan to employ an approach of multiplexing digital pathology to study the intimate relationships that adoptively transferred lymphocytes can establish with TNBC cells in tumor-bearing mice. Until recently, flow cytometry was the best methodology to obtain multicolor analysis required for the accurate characterization of the surface antigen profile of multiple cells simultaneously. However, flow cytometry can be less effective in the detection of extremely rare cell populations, and does not allow to assess the architectural relationships as the tissues must be disaggregated. To overcome this limitation, classical IHC can be used on FFPE tissue section, maintaining cellular spatial relationships. However, while chromogenic IHC is compatible with a limited number of antigen staining in the same slide, there are numerous benefits to adopt a multiplexing approach, which relies on tyramide-based fluorescent detection. Firstly, concurrent examination of 7 or more proteins/biomarkers, their spatial relationship and frequency of co-expression, all in the context of preserved tissue architecture, can offer insights into disease progression. Secondly, thanks to the covalent bond formation between multiple fluorophore-conjugated tyramide molecules and the tyrosine residues of the antigen of interest, the level of signal amplification is markedly enhanced, allowing the detection of extremely low expressed proteins. In addition, multiple primary antibodies of the same species can be used in a sequential fashion, simplifying the multiplex panel design. Notably, multiplex detection of 7 or more proteins relies on the unmixing of overlapping fluorophore emission spectra, which not only ensures that the signal from each protein of interest is differentiated from the rest, but also provides the ability to take into account and subtract the signal arising from tissue autofluorescence, enabling accurate fluorescence intensity quantitation in FFPE samples. Furthermore, the combination of multispectral imaging with software for

morphologic tissue area segmentation and cellular segmentation to perform quantitative per-cell and per-cell compartment intensity quantitation, provides researchers with phenotypic data about individual cells within particular morphologic regions of an image, rendering the cancer immunology knowledges more complete as compare to the multimarker information obtained with only the flow cytometry. Importantly, reliable image analysis can be controlled through standardization of the imaging protocols and fluorescent signal threshold imposition, as the same algorithm is used to analyze all the cohort slides. Finally, with mIHC and multispectral analysis integrated into the pathologists workflow, it is of great value collecting maximal information from a single tissue slide, as patient cancer tissue samples are rare. The benefits of this methodology, combined with the development of software for quantitation, are making fluorescent mIHC an increasingly powerful tool in the analysis and characterization of disease progression, enabling deeper insight into tissue and cellular processes, and ultimately supporting diagnostic potential in order to improve clinical care. The knowledge of this methodology, which provides phenotyping of immune and cancer cells combined with the cytoarchitectonics of the tumor, opens additional opportunities to further understand the tumor microenvironment dynamics and this will then be leveraged in analyses of multiple cancer types, both in human and in mouse.

ABBREVIATIONS

TSA	tumor-specific antigens
DEPDC1	DEP domain containing 1
CTL	cytotoxic T lymphocytes
TNBC	triple negative breast cancer
NK cells	natural killer cells
IFN-γ	interferon-γ
HLA	human leucocyte antigen
TCR	T-cell receptor
MHC	major histocompatibility complex
TGF-β	transforming growth factor β
MDSC	myeloid-derived suppressor cells
Treg	regulatory T cells
CTLA-4	cytotoxic T-lymphocyte antigen 4
PD-1	programmed cell death protein 1
TAA	tumor-associated antigen
PSA	prostate specific antigen
CEA	carcinoembryonic antigen
WT1	Wilms tumor 1
HPV	human papilloma virus
IL	interleukin
FDA	food and drug administration
mAbs	monoclonal antibodies
DC	dendritic cells
APC	antigen-presenting cells
GM-CSF	granulocyte-macrophage colony-stimulating factor
PD-L1	programmed cell death ligand 1
EGFR	epidermal growth factor receptor
ADCC	antibody-dependent cytotoxicity
CDC	complement-dependent cytotoxicity
ACT	adoptive cell therapy
TIL	tumor-infiltrating lymphocytes
CAR	chimeric-antigen receptor
CIK	cytokine-induced killer cells
LAK	lymphokine-activated killer cells
EEC	endometrial endometrioid carcinoma
ER	estrogen receptor
PR	progesterone receptor
HER2	human epidermal growth factor receptor type 2
FFPE	formalin-fixed paraffin-embedded
mIHC	multispectral immunohistochemistry
HRP	horseradish peroxidase
TSA	tyramide signal amplification
MWT	microwave treatment

aa	amino acid
PBMC	peripheral blood mononuclear cells
LCL	lymphoblastoid cell line
NSG	NOD/SCID gamma
BLI	bioluminescence
rhIL-2	recombinant human interleukin 2
SD	standard deviation

BIBLIOGRAPHY

1. Hanahan D, Weinberg RA. Hallmarks of cancer: The next generation. *Cell*. 2011;144(5):646-674. doi:10.1016/j.cell.2011.02.013.
2. Smyth MJ, Dunn GP, Schreiber RD. Cancer immunosurveillance and immunoediting: the roles of immunity in suppressing tumor development and shaping tumor immunogenicity. *Adv Immunol*. 2006;90:1-50. doi:10.1016/S0065-2776(06)90001-7.
3. Dranoff G. Cytokines in cancer pathogenesis and cancer therapy. *Nat Rev Cancer*. 2004;4(1):11-22. doi:10.1038/nrc1252.
4. Dunn GP, Bruce AT, Ikeda H, Old LJ, Schreiber RD. Cancer immunoediting: from immunosurveillance to tumor escape. *Nat Immunol*. 2002;3(11):991-998. doi:10.1038/ni1102-991.
5. Schreiber RD, Old LJ, Smyth MJ. Cancer immunoediting: integrating immunity's roles in cancer suppression and promotion. *Science*. 2011;331(6024):1565-1570. doi:10.1126/science.1203486.
6. Spiotto MT, Rowley DA, Schreiber H. Bystander elimination of antigen loss variants in established tumors. *Nat Med*. 2004;10(3):294-298. doi:10.1038/nm999.
7. Ostrand-Rosenberg S. Immune surveillance: a balance between protumor and antitumor immunity. *Curr Opin Genet Dev*. 2008;18(1):11-18. doi:10.1016/j.gde.2007.12.007.
8. Lurquin C, Van Pel A, Mariamé B, et al. Structure of the gene of tum− transplantation antigen P91A: The mutated exon encodes a peptide recognized with Ld by cytolytic T cells. *Cell*. 1989;58(2):293-303. doi:10.1016/0092-8674(89)90844-1.
9. Rammensee HG, Falk K, Rötzschke O. Peptides Naturally Presented by MHC Class I Molecules. *Annu Rev Immunol*. 1993;11(1):213-244. doi:10.1146/annurev.iy.11.040193.001241.
10. Vigneron N, Van den Eynde BJ. Insights into the processing of MHC class I ligands gained from the study of human tumor epitopes. *Cell Mol Life Sci*. 2011;68(9):1503-1520. doi:10.1007/s00018-011-0658-x.
11. Caspi RR. Immunotherapy of autoimmunity and cancer: the penalty for success. *Nat Rev Immunol*. 2008;8(12):970-976. doi:10.1038/nri2438.
12. Coulie PG, Van den Eynde BJ, van der Bruggen P, Boon T. Tumour antigens recognized by T lymphocytes: at the core of cancer immunotherapy. *Nat Rev Cancer*. 2014;14(2):135-146. doi:10.1038/nrc3670.
13. Hoek KS, Schlegel NC, Eichhoff OM, et al. Novel MITF targets identified using a two-step DNA microarray strategy. *Pigment Cell Melanoma Res*. 2008;21(6):665-676. doi:10.1111/j.1755-148X.2008.00505.x.
14. Wölfel T, Van Pel A, Brichard V, et al. Two tyrosinase nonapeptides recognized on HLA-A2 melanomas by autologous cytolytic T lymphocytes. *Eur J Immunol*. 1994;24(3):759-764. doi:10.1002/eji.1830240340.
15. Kawakami Y, Eliyahu S, Jennings C, et al. Recognition of multiple epitopes in the human

melanoma antigen gp100 by tumor-infiltrating T lymphocytes associated with in vivo tumor regression. *J Immunol*. 1995;154(8):3961-3968. http://www.ncbi.nlm.nih.gov/pubmed/7706734. Accessed June 10, 2016.

16. Kawakami Y, Eliyahu S, Sakaguchi K, et al. Identification of the immunodominant peptides of the MART-1 human melanoma antigen recognized by the majority of HLA-A2-restricted tumor infiltrating lymphocytes. *J Exp Med*. 1994;180(1):347-352. doi:10.1084/jem.180.1.347.

17. Wang RF, Parkhurst MR, Kawakami Y, Robbins PF, Rosenberg SA. Utilization of an alternative open reading frame of a normal gene in generating a novel human cancer antigen. *J Exp Med*. 1996;183(3):1131-1140. doi:10.1084/jem.183.3.1131.

18. Pittet MJ, Valmori D, Dunbar PR, et al. High Frequencies of Naive Melan-a/Mart-1–Specific Cd8 $^{+}$ T Cells in a Large Proportion of Human Histocompatibility Leukocyte Antigen (Hla)-A2 Individuals. *J Exp Med*. 1999;190(5):705-716. doi:10.1084/jem.190.5.705.

19. Yee C, Thompson JA, Roche P, et al. Melanocyte Destruction after Antigen-Specific Immunotherapy of Melanoma. *J Exp Med*. 2000;192(11):1637-1644. doi:10.1084/jem.192.11.1637.

20. Correale P, Nieroda C, Zaremba S, et al. In Vitro Generation of Human Cytotoxic T Lymphocytes Specific for Peptides Derived From Prostate-Specific Antigen. *JNCI J Natl Cancer Inst*. 1997;89(4):293-300. doi:10.1093/jnci/89.4.293.

21. Olson BM, Frye TP, Johnson LE, et al. HLA-A2-restricted T-cell epitopes specific for prostatic acid phosphatase. *Cancer Immunol Immunother*. 2010;59(6):943-953. doi:10.1007/s00262-010-0820-6.

22. Hammarström S. The carcinoembryonic antigen (CEA) family: structures, suggested functions and expression in normal and malignant tissues. *Semin Cancer Biol*. 1999;9(2):67-81. doi:10.1006/scbi.1998.0119.

23. Akhtar NH, Pail O, Saran A, Tyrell L, Tagawa ST. Prostate-specific membrane antigen-based therapeutics. *Adv Urol*. 2012;2012:973820. doi:10.1155/2012/973820.

24. Bright RK, Bright JD, Byrne JA. Overexpressed oncogenic tumor-self antigens New vaccine targets. doi:10.4161/hv.29475.

25. Schmidt SM, Schag K, Müller MR, et al. Survivin is a shared tumor-associated antigen expressed in a broad variety of malignancies and recognized by specific cytotoxic T cells. *Blood*. 2003;102(2):571-576. doi:10.1182/blood-2002-08-2554.

26. Barfoed, Petersen, Kirkin, Thor Straten T, Claesson, Zeuthen. Cytotoxic T-Lymphocyte Clones, Established by Stimulation with the HLA-A2 Binding p5365-73 Wild Type Peptide Loaded on Dendritic Cells In Vitro, Specifically Recognize and Lyse HLA-A2 Tumour Cells Overexpressing the p53 Protein. *Scand J Immunol*. 2000;51(2):128-133. doi:10.1046/j.1365-3083.2000.00668.x.

27. Kraus MH, Popescu NC, Amsbaugh SC, King CR. Overexpression of the EGF receptor-related proto-oncogene erbB-2 in human mammary tumor cell lines by different molecular mechanisms. *EMBO J*. 1987;6(3):605-610. http://www.ncbi.nlm.nih.gov/pubmed/3034598. Accessed June 10, 2016.

28. Asemissen AM, Keilholz U, Tenzer S, et al. Identification of a Highly Immunogenic HLA-A*01-Binding T Cell Epitope of WT1. *Clin Cancer Res*. 2006;12(24):7476-7482. doi:10.1158/1078-

0432.CCR-06-1337.

29. Chapuis AG, Ragnarsson GB, Nguyen HN, et al. Transferred WT1-reactive CD8+ T cells can mediate antileukemic activity and persist in post-transplant patients. *Sci Transl Med*. 2013;5(174):174ra27. doi:10.1126/scitranslmed.3004916.

30. Gilboa E. The makings of a tumor rejection antigen. *Immunity*. 1999;11(3):263-270. http://www.ncbi.nlm.nih.gov/pubmed/10514004. Accessed April 23, 2016.

31. Iacovides D, Michael S, Achilleos C, Strati K. Shared mechanisms in stemness and carcinogenesis: lessons from oncogenic viruses. *Front Cell Infect Microbiol*. 2013;3:66. doi:10.3389/fcimb.2013.00066.

32. Welters MJP, Kenter GG, Piersma SJ, et al. Induction of Tumor-Specific CD4+ and CD8+ T-Cell Immunity in Cervical Cancer Patients by a Human Papillomavirus Type 16 E6 and E7 Long Peptides Vaccine. *Clin Cancer Res*. 2008;14(1):178-187. doi:10.1158/1078-0432.CCR-07-1880.

33. Kawakami Y, Wang X, Shofuda T, et al. Isolation of a New Melanoma Antigen, MART-2, Containing a Mutated Epitope Recognized by Autologous Tumor-Infiltrating T Lymphocytes. *J Immunol*. 2001;166(4):2871-2877. doi:10.4049/jimmunol.166.4.2871.

34. Linnebacher M, Gebert J, Rudy W, et al. Frameshift peptide-derived T-cell epitopes: A source of novel tumor-specific antigens. *Int J Cancer*. 2001;93(1):6-11. doi:10.1002/ijc.1298.

35. Wölfel T, Hauer M, Schneider J, et al. A p16INK4a-insensitive CDK4 mutant targeted by cytolytic T lymphocytes in a human melanoma. *Science*. 1995;269(5228):1281-1284. doi:10.1126/science.7652577.

36. Lennerz V, Fatho M, Gentilini C, et al. The response of autologous T cells to a human melanoma is dominated by mutated neoantigens. *Proc Natl Acad Sci*. 2005;102(44):16013-16018. doi:10.1073/pnas.0500090102.

37. Yotnda P, Firat H, Garcia-Pons F, et al. Cytotoxic T cell response against the chimeric p210 BCR-ABL protein in patients with chronic myelogenous leukemia. *J Clin Invest*. 1998;101(10):2290-2296. doi:10.1172/JCI488.

38. Yotnda P, Garcia F, Peuchmaur M, et al. Cytotoxic T cell response against the chimeric ETV6-AML1 protein in childhood acute lymphoblastic leukemia. *J Clin Invest*. 1998;102(2):455-462. doi:10.1172/JCI3126.

39. Lucas S, De Smet C, Arden KC, et al. Identification of a new MAGE gene with tumor-specific expression by representational difference analysis. *Cancer Res*. 1998;58(4):743-752. http://www.ncbi.nlm.nih.gov/pubmed/9485030. Accessed June 10, 2016.

40. Boël P, Wildmann C, Sensi ML, et al. BAGE: a new gene encoding an antigen recognized on human melanomas by cytolytic T lymphocytes. *Immunity*. 1995;2(2):167-175. doi:10.1016/S1074-7613(95)80053-0.

41. Ehrlich M, Gama-Sosa MA, Huang L-H, et al. Amount and distribution of 5-methylcytosine in human DNA from different types of tissues or cells. *Nucleic Acids Res*. 1982;10(8):2709-2721. doi:10.1093/nar/10.8.2709.

42. HAAS GG, D'CRUZ OJ, DE BAULT LE. Distribution of Human Leukocyte Antigen-ABC and -D/DR Antigens in the Unfixed Human Testis. *Am J Reprod Immunol Microbiol*. 1988;18(2):47-51. doi:10.1111/j.1600-0897.1988.tb00234.x.

43. Finn OJ. Cancer immunology. *N Engl J Med*. 2008;358(25):2704-2715. doi:10.1056/NEJMra072739.

44. Rosenberg SA, Lotze MT. Cancer immunotherapy using interleukin-2 and interleukin-2-activated lymphocytes. *Annu Rev Immunol*. 1986;4:681-709. doi:10.1146/annurev.iy.04.040186.003341.

45. Fyfe G, Fisher RI, Rosenberg SA, Sznol M, Parkinson DR, Louie AC. Results of treatment of 255 patients with metastatic renal cell carcinoma who received high-dose recombinant interleukin-2 therapy. *J Clin Oncol*. 1995;13(3):688-696. http://www.ncbi.nlm.nih.gov/pubmed/7884429. Accessed June 13, 2016.

46. Atkins MB, Lotze MT, Dutcher JP, et al. High-dose recombinant interleukin 2 therapy for patients with metastatic melanoma: analysis of 270 patients treated between 1985 and 1993. *J Clin Oncol*. 1999;17(7):2105-2116. http://www.ncbi.nlm.nih.gov/pubmed/10561265. Accessed June 13, 2016.

47. Sharma P, Wagner K, Wolchok JD, Allison JP. Novel cancer immunotherapy agents with survival benefit: recent successes and next steps. *Nat Rev Cancer*. 2011;11(11):805-812. doi:10.1038/nrc3153.

48. Vanneman M, Dranoff G. Combining immunotherapy and targeted therapies in cancer treatment. *Nat Rev Cancer*. 2012;12(4):237-251. doi:10.1038/nrc3237.

49. Lesterhuis WJ, Haanen JBAG, Punt CJA. Cancer immunotherapy--revisited. *Nat Rev Drug Discov*. 2011;10(8):591-600. doi:10.1038/nrd3500.

50. Melief CJM, van der Burg SH. Immunotherapy of established (pre)malignant disease by synthetic long peptide vaccines. *Nat Rev Cancer*. 2008;8(5):351-360. doi:10.1038/nrc2373.

51. Pardoll DM. The blockade of immune checkpoints in cancer immunotherapy. *Nat Rev Cancer*. 2012;12(4):252-264. doi:10.1038/nrc3239.

52. Maus M V, Fraietta JA, Levine BL, Kalos M, Zhao Y, June CH. Adoptive immunotherapy for cancer or viruses. *Annu Rev Immunol*. 2014;32:189-225. doi:10.1146/annurev-immunol-032713-120136.

53. Rader C. Monoclonal Antibody Therapy for Cancer. In: *Experimental and Applied Immunotherapy*. Totowa, NJ: Humana Press; 2011:59-83. doi:10.1007/978-1-60761-980-2_3.

54. Palucka K, Banchereau J. Cancer immunotherapy via dendritic cells. *Nat Rev Cancer*. 2012;12(4):265-277. doi:10.1038/nrc3258.

55. Mayordomo JI, Zorina T, Storkus WJ, et al. Bone marrow-derived dendritic cells pulsed with synthetic tumour peptides elicit protective and therapeutic antitumour immunity. *Nat Med*. 1995;1(12):1297-1302. http://www.ncbi.nlm.nih.gov/pubmed/7489412. Accessed June 14, 2016.

56. Zeis M, Siegel S, Wagner A, et al. Generation of cytotoxic responses in mice and human individuals against hematological malignancies using survivin-RNA-transfected dendritic cells. *J Immunol*. 2003;170(11):5391-5397. http://www.ncbi.nlm.nih.gov/pubmed/12759413. Accessed June 14, 2016.

57. Blalock LT, Landsberg J, Messmer M, et al. Human dendritic cells adenovirally-engineered to express three defined tumor antigens promote broad adaptive and innate immunity. *Oncoimmunology*. 2012;1(3):287-357. doi:10.4161/onci.18628.

58. Kandalaft LE, Powell DJ, Chiang CL, et al. Autologous lysate-pulsed dendritic cell vaccination followed by adoptive transfer of vaccine-primed ex vivo co-stimulated T cells in recurrent ovarian cancer. *Oncoimmunology*. 2013;2(1):e22664. doi:10.4161/onci.22664.

59. Schmidt T, Ziske C, Märten A, et al. Intratumoral immunization with tumor RNA-pulsed dendritic cells confers antitumor immunity in a C57BL/6 pancreatic murine tumor model. *Cancer Res*. 2003;63(24):8962-8967. http://www.ncbi.nlm.nih.gov/pubmed/14695214. Accessed June 14, 2016.

60. Koido S, Homma S, Okamoto M, et al. Fusions between dendritic cells and whole tumor cells as anticancer vaccines. *Oncoimmunology*. 2013;2(5):e24437. doi:10.4161/onci.24437.

61. Schreibelt G, Klinkenberg LJJ, Cruz LJ, et al. The C-type lectin receptor CLEC9A mediates antigen uptake and (cross-)presentation by human blood BDCA3+ myeloid dendritic cells. *Blood*. 2012;119(10):2284-2292. doi:10.1182/blood-2011-08-373944.

62. Tacken PJ, de Vries IJM, Gijzen K, et al. Effective induction of naive and recall T-cell responses by targeting antigen to human dendritic cells via a humanized anti-DC-SIGN antibody. *Blood*. 2005;106(4):1278-1285. doi:10.1182/blood-2005-01-0318.

63. van Broekhoven CL, Parish CR, Demangel C, Britton WJ, Altin JG. Targeting dendritic cells with antigen-containing liposomes: a highly effective procedure for induction of antitumor immunity and for tumor immunotherapy. *Cancer Res*. 2004;64(12):4357-4365. doi:10.1158/0008-5472.CAN-04-0138.

64. Hangalapura BN, Oosterhoff D, de Groot J, et al. Potent antitumor immunity generated by a CD40-targeted adenoviral vaccine. *Cancer Res*. 2011;71(17):5827-5837. doi:10.1158/0008-5472.CAN-11-0804.

65. Kantoff PW, Higano CS, Shore ND, et al. Sipuleucel-T immunotherapy for castration-resistant prostate cancer. *N Engl J Med*. 2010;363(5):411-422. doi:10.1056/NEJMoa1001294.

66. DeFrancesco L. Landmark approval for Dendreon's cancer vaccine. *Nat Biotechnol*. 2010;28(6):531-532. doi:10.1038/nbt0610-531.

67. Yaddanapudi K, Mitchell RA, Eaton JW. Cancer vaccines: Looking to the future. *Oncoimmunology*. 2013;2(3):e23403. doi:10.4161/onci.23403.

68. Aruga A. Vaccination of biliary tract cancer patients with four peptides derived from cancer-testis antigens. *Oncoimmunology*. 2013;2(7):e24882. doi:10.4161/onci.24882.

69. Bijker MS, van den Eeden SJF, Franken KL, Melief CJM, Offringa R, van der Burg SH. CD8+ CTL priming by exact peptide epitopes in incomplete Freund's adjuvant induces a vanishing CTL response, whereas long peptides induce sustained CTL reactivity. *J Immunol*. 2007;179(8):5033-5040. http://www.ncbi.nlm.nih.gov/pubmed/17911588. Accessed June 16, 2016.

70. Ciocca DR, Cayado-Gutierrez N, Maccioni M, Cuello-Carrion FD. Heat shock proteins (HSPs) based anti-cancer vaccines. *Curr Mol Med*. 2012;12(9):1183-1197. http://www.ncbi.nlm.nih.gov/pubmed/22804241. Accessed June 16, 2016.

71. Fioretti D, Iurescia S, Fazio VM, Rinaldi M. DNA vaccines: developing new strategies against cancer. *J Biomed Biotechnol*. 2010;2010:174378. doi:10.1155/2010/174378.

72. Pol JG, Zhang L, Bridle BW, et al. Maraba virus as a potent oncolytic vaccine vector. *Mol Ther*. 2014;22(2):420-429. doi:10.1038/mt.2013.249.

73. FUTURE II Study Group. Quadrivalent vaccine against human papillomavirus to prevent high-grade cervical lesions. *N Engl J Med*. 2007;356(19):1915-1927. doi:10.1056/NEJMoa061741.

74. Vacchelli E, Eggermont A, Fridman WH, et al. Trial Watch: Immunostimulatory cytokines. *Oncoimmunology*. 2013;2(7):e24850. doi:10.4161/onci.24850.

75. Robertson MJ, Kline J, Struemper H, et al. A dose-escalation study of recombinant human interleukin-18 in combination with rituximab in patients with non-Hodgkin lymphoma. *J Immunother*. 36(6):331-341. doi:10.1097/CJI.0b013e31829d7e2e.

76. Asmana Ningrum R, Asmana Ningrum R. Human Interferon Alpha-2b: A Therapeutic Protein for Cancer Treatment. *Scientifica (Cairo)*. 2014;2014:1-8. doi:10.1155/2014/970315.

77. Antony GK, Dudek AZ. Interleukin 2 in cancer therapy. *Curr Med Chem*. 2010;17(29):3297-3302. http://www.ncbi.nlm.nih.gov/pubmed/20712575. Accessed June 16, 2016.

78. Melero I, Grimaldi AM, Perez-Gracia JL, Ascierto PA. Clinical development of immunostimulatory monoclonal antibodies and opportunities for combination. *Clin Cancer Res*. 2013;19(5):997-1008. doi:10.1158/1078-0432.CCR-12-2214.

79. Waitz R, Fassò M, Allison JP. CTLA-4 blockade synergizes with cryoablation to mediate tumor rejection. *Oncoimmunology*. 2012;1(4):544-546. http://www.ncbi.nlm.nih.gov/pubmed/22754781. Accessed June 16, 2016.

80. Zitvogel L, Kroemer G. Targeting PD-1/PD-L1 interactions for cancer immunotherapy. *Oncoimmunology*. 2012;1(8):1223-1225. doi:10.4161/onci.21335.

81. Curiel TJ, Wei S, Dong H, et al. Blockade of B7-H1 improves myeloid dendritic cell-mediated antitumor immunity. *Nat Med*. 2003;9(5):562-567. doi:10.1038/nm863.

82. Melero I, Hirschhorn-Cymerman D, Morales-Kastresana A, Sanmamed MF, Wolchok JD. Agonist antibodies to TNFR molecules that costimulate T and NK cells. *Clin Cancer Res*. 2013;19(5):1044-1053. doi:10.1158/1078-0432.CCR-12-2065.

83. Schnurr M, Duewell P. Breaking tumor-induced immunosuppression with 5'-triphosphate siRNA silencing TGFβ and activating RIG-I. *Oncoimmunology*. 2013;2(5):e24170. doi:10.4161/onci.24170.

84. Mavilio D, Lugli E. Inhibiting the inhibitors: Checkpoints blockade in solid tumors. *Oncoimmunology*. 2013;2(9):e26535. doi:10.4161/onci.26535.

85. Wolchok JD, Neyns B, Linette G, et al. Ipilimumab monotherapy in patients with pretreated advanced melanoma: a randomised, double-blind, multicentre, phase 2, dose-ranging study. *Lancet Oncol*. 2010;11(2):155-164. doi:10.1016/S1470-2045(09)70334-1.

86. PD-1 Inhibitor Approved for Melanoma. *Cancer Discov*. 2014;4(11):1249-1249. doi:10.1158/2159-8290.CD-NB2014-144.

87. Wei H, Zhao L, Hellstrom I, Hellstrom KE, Guo Y. Dual targeting of CD137 co-stimulatory and PD-1 co-inhibitory molecules for ovarian cancer immunotherapy. *Oncoimmunology*. 2014;3:e28248. doi:10.4161/onci.28248.

88. Vacchelli E, Aranda F, Eggermont A, et al. Trial Watch: Tumor-targeting monoclonal antibodies in cancer therapy. *Oncoimmunology*. 2014;3(1):e27048. doi:10.4161/onci.27048.

89. Pol Specenier JBV. Cetuximab: its unique place in head and neck cancer treatment. *Biologics*. 2013;7:77.

90. Jonker DJ, O'Callaghan CJ, Karapetis CS, et al. Cetuximab for the Treatment of Colorectal Cancer. *N Engl J Med*. 2007;357(20):2040-2048. doi:10.1056/NEJMoa071834.

91. Forero-Torres A, Infante JR, Waterhouse D, et al. Phase 2, multicenter, open-label study of tigatuzumab (CS-1008), a humanized monoclonal antibody targeting death receptor 5, in combination with gemcitabine in chemotherapy-naive patients with unresectable or metastatic pancreatic cancer. *Cancer Med*. 2013;2(6):925-932. doi:10.1002/cam4.137.

92. Leal M, Sapra P, Hurvitz SA, et al. Antibody-drug conjugates: an emerging modality for the treatment of cancer. *Ann N Y Acad Sci*. 2014;1321(1):41-54. doi:10.1111/nyas.12499.

93. Hubert P, Amigorena S. Antibody-dependent cell cytotoxicity in monoclonal antibody-mediated tumor immunotherapy. *Oncoimmunology*. 2012;1(1):103-105. doi:10.4161/onci.1.1.17963.

94. Winiarska M. Molecular mechanisms of the antitumor effects of anti-CD20 antibodies. *Front Biosci*. 2011;16(1):277. doi:10.2741/3688.

95. Introna M, Golay J, Golay J, et al. Complement in antibody therapy: friend or foe? *Blood*. 2009;114(26):5247-5248. doi:10.1182/blood-2009-10-249532.

96. Jaeger U, Trneny M, Melzer H, et al. Rituximab maintenance for patients with aggressive B-cell lymphoma in first remission: results of the randomized NHL13 trial. *Haematologica*. 2015;100(7):955-963. doi:10.3324/haematol.2015.125344.

97. Scott SD. Rituximab: A New Therapeutic Monoclonal Antibody for Non-Hodgkin's Lymphoma. *Cancer Pract*. 1998;6(3):195-197. doi:10.1046/j.1523-5394.1998.006003195.x.

98. Topp MS, Gökbuget N, Zugmaier G, et al. Long-term follow-up of hematologic relapse-free survival in a phase 2 study of blinatumomab in patients with MRD in B-lineage ALL. *Blood*. 2012;120(26):5185-5187. doi:10.1182/blood-2012-07-441030.

99. Scott AM, Wolchok JD, Old LJ. Antibody therapy of cancer. *Nat Rev Cancer*. 2012;12(4):278-287. doi:10.1038/nrc3236.

100. Vacchelli E, Vitale I, Eggermont A, et al. Trial watch: Dendritic cell-based interventions for cancer therapy. *Oncoimmunology*. 2013;2(10):e25771. doi:10.4161/onci.25771.

101. Jenq RR, van den Brink MRM. Allogeneic haematopoietic stem cell transplantation: individualized stem cell and immune therapy of cancer. *Nat Rev Cancer*. 2010;10(3):213-221. doi:10.1038/nrc2804.

102. Rosenberg SA, Yang JC, Sherry RM, et al. Durable Complete Responses in Heavily Pretreated Patients with Metastatic Melanoma Using T-Cell Transfer Immunotherapy. *Clin Cancer Res*. 2011;17(13):4550-4557. doi:10.1158/1078-0432.CCR-11-0116.

103. Woo EY, Yeh H, Chu CS, et al. Cutting edge: Regulatory T cells from lung cancer patients directly inhibit autologous T cell proliferation. *J Immunol*. 2002;168(9):4272-4276. http://www.ncbi.nlm.nih.gov/pubmed/11970966. Accessed June 23, 2016.

104. Tran E, Turcotte S, Gros A, et al. Cancer immunotherapy based on mutation-specific CD4+ T cells in a patient with epithelial cancer. *Science*. 2014;344(6184):641-645. doi:10.1126/science.1251102.

105. Ho WY, Nguyen HN, Wolfl M, Kuball J, Greenberg PD. In vitro methods for generating CD8+ T-cell clones for immunotherapy from the naïve repertoire. *J Immunol Methods*. 2006;310(1-2):40-52. doi:10.1016/j.jim.2005.11.023.

106. Chapuis AG, Thompson JA, Margolin KA, et al. Transferred melanoma-specific CD8+ T cells persist, mediate tumor regression, and acquire central memory phenotype. *Proc Natl Acad Sci U S A*. 2012;109(12):4592-4597. doi:10.1073/pnas.1113748109.

107. Wright SE, Rewers-Felkins KA, Quinlin IS, et al. Cytotoxic T-lymphocyte immunotherapy for ovarian cancer: a pilot study. *J Immunother*. 35(2):196-204. doi:10.1097/CJI.0b013e318243f213.

108. Rosenberg SA. Cell transfer immunotherapy for metastatic solid cancer--what clinicians need to know. *Nat Rev Clin Oncol*. 2011;8(10):577-585. doi:10.1038/nrclinonc.2011.116.

109. Liu K, Rosenberg SA. Transduction of an IL-2 gene into human melanoma-reactive lymphocytes results in their continued growth in the absence of exogenous IL-2 and maintenance of specific antitumor activity. *J Immunol*. 2001;167(11):6356-6365. http://www.ncbi.nlm.nih.gov/pubmed/11714800. Accessed June 23, 2016.

110. Bellone M, Calcinotto A, Corti A. Won't you come on in? How to favor lymphocyte infiltration in tumors. *Oncoimmunology*. 2012;1(6):986-988. doi:10.4161/onci.20213.

111. Kershaw MH, Teng MWL, Smyth MJ, Darcy PK. Supernatural T cells: genetic modification of T cells for cancer therapy. *Nat Rev Immunol*. 2005;5(12):928-940. doi:10.1038/nri1729.

112. Robbins PF, Morgan RA, Feldman SA, et al. Tumor regression in patients with metastatic synovial cell sarcoma and melanoma using genetically engineered lymphocytes reactive with NY-ESO-1. *J Clin Oncol*. 2011;29(7):917-924. doi:10.1200/JCO.2010.32.2537.

113. Porter DL, Levine BL, Kalos M, Bagg A, June CH. Chimeric antigen receptor-modified T cells in chronic lymphoid leukemia. *N Engl J Med*. 2011;365(8):725-733. doi:10.1056/NEJMoa1103849.

114. Kershaw MH, Westwood JA, Slaney CY, Darcy PK. Clinical application of genetically modified T cells in cancer therapy. *Clin Transl Immunol*. 2014;3(5):e16. doi:10.1038/cti.2014.7.

115. Besser MJ, Shoham T, Harari-Steinberg O, et al. Development of allogeneic NK cell adoptive transfer therapy in metastatic melanoma patients: in vitro preclinical optimization studies. *PLoS One*. 2013;8(3):e57922. doi:10.1371/journal.pone.0057922.

116. Parkhurst MR, Riley JP, Dudley ME, Rosenberg SA. Adoptive transfer of autologous natural killer cells leads to high levels of circulating natural killer cells but does not mediate tumor regression. *Clin Cancer Res*. 2011;17(19):6287-6297. doi:10.1158/1078-0432.CCR-11-1347.

117. Schmidt-Wolf IG, Negrin RS, Kiem HP, Blume KG, Weissman IL. Use of a SCID mouse/human lymphoma model to evaluate cytokine-induced killer cells with potent antitumor cell activity. *J Exp Med*. 1991;174(1):139-149. http://www.ncbi.nlm.nih.gov/pubmed/1711560. Accessed June 23, 2016.

118. Guo Y, Han W, Schmidt-Wolf I, et al. Cytokine-induced killer (CIK) cells: from basic research to clinical translation. *Chin J Cancer*. 2015;34(3):6. doi:10.1186/s40880-015-0002-1.

119. Cappuzzello E, Tosi A, Zanovello P, Sommaggio R, Rosato A. Redirecting Cytokine induced killer cell activity by CD16 engagement with clinical grade antibodies. *Oncoimmunology*. 2016;in press(8):1-10. doi:10.1080/2162402X.2016.1199311.

120. Kanehira M, Harada Y, Takata R, et al. Involvement of upregulation of DEPDC1 (DEP domain containing 1) in bladder carcinogenesis. *Oncogene*. 2007;26(44):6448-6455. doi:10.1038/sj.onc.1210466.

121. Kassambara A, Schoenhals M, Moreaux J, et al. Inhibition of DEPDC1A, a bad prognostic marker in multiple myeloma, delays growth and induces mature plasma cell markers in malignant plasma cells. Galardy PJ, ed. *PLoS One*. 2013;8(4):e62752. doi:10.1371/journal.pone.0062752.

122. Kretschmer C, Sterner-Kock A, Siedentopf F, Schoenegg W, Schlag PM, Kemmner W. Identification of early molecular markers for breast cancer. *Mol Cancer*. 2011;10(1):15. doi:10.1186/1476-4598-10-15.

123. Okayama H, Kohno T, Ishii Y, et al. Identification of genes upregulated in ALK-positive and EGFR/KRAS/ALK-negative lung adenocarcinomas. *Cancer Res*. 2012;72(1):100-111. doi:10.1158/0008-5472.CAN-11-1403.

124. Stangeland B, Mughal AA, Grieg Z, et al. Combined expressional analysis, bioinformatics and targeted proteomics identify new potential therapeutic targets in glioblastoma stem cells. *Oncotarget*. 2015;6(28):26192-26215. doi:10.18632/oncotarget.4613.

125. Yuan S-G, Liao W-J, Yang J-J, Huang G-J, Huang Z-Q. DEP domain containing 1 is a novel diagnostic marker and prognostic predictor for hepatocellular carcinoma. *Asian Pac J Cancer Prev*. 2014;15(24):10917-10922. http://www.ncbi.nlm.nih.gov/pubmed/25605201. Accessed March 24, 2016.

126. Salhia B, Kiefer J, Ross JTD, et al. Integrated genomic and epigenomic analysis of breast cancer brain metastasis. *PLoS One*. 2014;9(1):e85448. doi:10.1371/journal.pone.0085448.

127. Boutros M, Mlodzik M. Dishevelled: at the crossroads of divergent intracellular signaling pathways. *Mech Dev*. 1999;83(1-2):27-37. http://www.ncbi.nlm.nih.gov/pubmed/10507837. Accessed June 2, 2016.

128. Koelle MR, Horvitz HR. EGL-10 regulates G protein signaling in the C. elegans nervous system and shares a conserved domain with many mammalian proteins. *Cell*. 1996;84(1):115-125. http://www.ncbi.nlm.nih.gov/pubmed/8548815. Accessed June 2, 2016.

129. Kharrat A, Millevoi S, Baraldi E, Ponting CP, Bork P, Pastore A. Conformational stability studies of the pleckstrin DEP domain: definition of the domain boundaries. *Biochim Biophys Acta*. 1998;1385(1):157-164. http://www.ncbi.nlm.nih.gov/pubmed/9630596. Accessed June 2, 2016.

130. Heyninck K, Beyaert R. A20 inhibits NF-kappaB activation by dual ubiquitin-editing functions. *Trends Biochem Sci*. 2005;30(1):1-4. doi:10.1016/j.tibs.2004.11.001.

131. Harada Y, Kanehira M, Fujisawa Y, et al. Cell-permeable peptide DEPDC1-ZNF224 interferes with transcriptional repression and oncogenicity in bladder cancer cells. *Cancer Res*. 2010;70(14):5829-5839. doi:10.1158/0008-5472.CAN-10-0255.

132. Mi Y, Zhang C, Bu Y, et al. DEPDC1 is a novel cell cycle related gene that regulates mitotic progression. *BMB Rep*. 2015;48(7):413-418. http://www.pubmedcentral.nih.gov/articlerender.fcgi?artid=4577292&tool=pmcentrez&rendertype=abstract. Accessed May 2, 2016.

133. Yang Y, Jiang Y, Jiang M, et al. Protocadherin 10 inhibits cell proliferation and induces apoptosis via regulation of DEP domain containing 1 in endometrial endometrioid carcinoma. *Exp Mol Pathol*. 2016;100(2):344-352. doi:10.1016/j.yexmp.2016.03.002.

134. Chung S, Kijima K, Kudo A, et al. Preclinical evaluation of biomarkers associated with

antitumor activity of MELK inhibitor. *Oncotarget*. February 2016. doi:10.18632/oncotarget.7685.

135. Pickard MR, Green AR, Ellis IO, et al. Dysregulated expression of Fau and MELK is associated with poor prognosis in breast cancer. *Breast Cancer Res*. 2009;11(4):R60. doi:10.1186/bcr2350.

136. Choi S, Ku J-L. Resistance of colorectal cancer cells to radiation and 5-FU is associated with MELK expression. *Biochem Biophys Res Commun*. 2011;412(2):207-213. doi:10.1016/j.bbrc.2011.07.060.

137. Obara W, Ohsawa R, Kanehira M, et al. Cancer peptide vaccine therapy developed from oncoantigens identified through genome-wide expression profile analysis for bladder cancer. *Jpn J Clin Oncol*. 2012;42(7):591-600. doi:10.1093/jjco/hys069.

138. Murahashi M, Hijikata Y, Yamada K, et al. Phase I clinical trial of a five-peptide cancer vaccine combined with cyclophosphamide in advanced solid tumors. *Clin Immunol*. April 2016. doi:10.1016/j.clim.2016.03.015.

139. Bauer KR, Brown M, Cress RD, Parise CA, Caggiano V. Descriptive analysis of estrogen receptor (ER)-negative, progesterone receptor (PR)-negative, and HER2-negative invasive breast cancer, the so-called triple-negative phenotype: a population-based study from the California cancer Registry. *Cancer*. 2007;109(9):1721-1728. doi:10.1002/cncr.22618.

140. Boyle P. Triple-negative breast cancer: epidemiological considerations and recommendations. *Ann Oncol*. 2012;23 Suppl 6(suppl_6):vi7-12. doi:10.1093/annonc/mds187.

141. Dietze EC, Sistrunk C, Miranda-Carboni G, O'Regan R, Seewaldt VL. Triple-negative breast cancer in African-American women: disparities versus biology. *Nat Rev Cancer*. 2015;15(4):248-254. doi:10.1038/nrc3896.

142. Carey LA, Dees EC, Sawyer L, et al. The triple negative paradox: primary tumor chemosensitivity of breast cancer subtypes. *Clin Cancer Res*. 2007;13(8):2329-2334. doi:10.1158/1078-0432.CCR-06-1109.

143. Heitz F, Harter P, Traut A, Lueck HJ, Beutel B, du Bois A. Cerebral metastases (CM) in breast cancer (BC) with focus on triple-negative tumors. *ASCO Meet Abstr*. 2008;26(15_suppl):1010. http://hwmaint.meeting.ascopubs.org/cgi/content/abstract/26/15_suppl/1010. Accessed April 27, 2016.

144. Ott PA, Hodi FS, Robert C. CTLA-4 and PD-1/PD-L1 Blockade: New Immunotherapeutic Modalities with Durable Clinical Benefit in Melanoma Patients. *Clin Cancer Res*. 2013;19(19).

145. Schreiber RD, Old LJ, Smyth MJ. Cancer immunoediting: integrating immunity's roles in cancer suppression and promotion. *Science*. 2011;331(6024):1565-1570. doi:10.1126/science.1203486.

146. Galon J, Costes A, Sanchez-Cabo F, et al. Type, Density, and Location of Immune Cells Within Human Colorectal Tumors Predict Clinical Outcome. *Science (80-)*. 2006;313(5795).

147. Zhang L, Conejo-Garcia JR, Katsaros D, et al. Intratumoral T cells, recurrence, and survival in epithelial ovarian cancer. *N Engl J Med*. 2003;348(3):203-213. doi:10.1056/NEJMoa020177.

148. Liu H, Zhang T, Ye J, et al. Tumor-infiltrating lymphocytes predict response to chemotherapy in patients with advance non-small cell lung cancer. *Cancer Immunol Immunother*.

2012;61(10):1849-1856. doi:10.1007/s00262-012-1231-7.

149. Shah W, Yan X, Jing L, Zhou Y, Chen H, Wang Y. A reversed CD4/CD8 ratio of tumor-infiltrating lymphocytes and a high percentage of CD4(+)FOXP3(+) regulatory T cells are significantly associated with clinical outcome in squamous cell carcinoma of the cervix. *Cell Mol Immunol*. 2011;8(1):59-66. doi:10.1038/cmi.2010.56.

150. Nielsen JS, Sahota RA, Milne K, et al. CD20+ tumor-infiltrating lymphocytes have an atypical CD27- memory phenotype and together with CD8+ T cells promote favorable prognosis in ovarian cancer. *Clin Cancer Res*. 2012;18(12):3281-3292. doi:10.1158/1078-0432.CCR-12-0234.

151. Mansfield JR. Multispectral imaging: a review of its technical aspects and applications in anatomic pathology. *Vet Pathol*. 2014;51(1):185-210. doi:10.1177/0300985813506918.

152. Vasaturo A, Halilovic A, Bol KF, et al. T cell landscape in a primary melanoma predicts the survival of patients with metastatic disease after their treatment with dendritic cell vaccines. *Cancer Res*. 2016.

153. Hoyt C, Wang C, Roman K, Johnson K, Miller P, Mittendorf E. Characterizing immune evasion in FFPE tissue sections - a new method for measuring cellular interactions via multiplexed phenotype mapping and spatial point patterns. *J Immunother Cancer*. 2014;2(Suppl 3):P259. doi:10.1186/2051-1426-2-S3-P259.

154. Oguejiofor K, Hall J, Slater C, et al. Stromal infiltration of CD8 T cells is associated with improved clinical outcome in HPV-positive oropharyngeal squamous carcinoma. *Br J Cancer*. 2015;113(6):886-893. doi:10.1038/bjc.2015.277.

155. Stack EC, Wang C, Roman KA, Hoyt CC. Multiplexed immunohistochemistry, imaging, and quantitation: a review, with an assessment of Tyramide signal amplification, multispectral imaging and multiplex analysis. *Methods*. 2014;70(1):46-58. doi:10.1016/j.ymeth.2014.08.016.

156. Dickinson ME, Bearman G, Tille S, Lansford R, Fraser SE. Multi-spectral imaging and linear unmixing add a whole new dimension to laser scanning fluorescence microscopy. *Biotechniques*. 2001;31(6):1272, 1274-1276, 1278. http://www.ncbi.nlm.nih.gov/pubmed/11768655. Accessed October 7, 2016.

157. Neves H, Kwok HF. Recent advances in the field of anti-cancer immunotherapy. *BBA Clin*. 2015;3:280-288. doi:10.1016/j.bbacli.2015.04.001.

158. Mahoney KM, Rennert PD, Freeman GJ. Combination cancer immunotherapy and new immunomodulatory targets. *Nat Rev Drug Discov*. 2015;14(8):561-584. doi:10.1038/nrd4591.

159. Taube JM, Klein A, Brahmer JR, et al. Association of PD-1, PD-1 ligands, and other features of the tumor immune microenvironment with response to anti-PD-1 therapy. *Clin Cancer Res*. 2014;20(19):5064-5074. doi:10.1158/1078-0432.CCR-13-3271.

160. Rizvi NA, Hellmann MD, Snyder A, et al. Cancer immunology. Mutational landscape determines sensitivity to PD-1 blockade in non-small cell lung cancer. *Science*. 2015;348(6230):124-128. doi:10.1126/science.aaa1348.

161. Melero I, Berman DM, Aznar MA, Korman AJ, Pérez Gracia JL, Haanen J. Evolving synergistic combinations of targeted immunotherapies to combat cancer. *Nat Rev Cancer*. 2015;15(8):457-472. doi:10.1038/nrc3973.

162. Geynisman DM, Chien C-R, Smieliauskas F, Shen C, Shih Y-CT. Economic evaluation of therapeutic cancer vaccines and immunotherapy: a systematic review. *Hum Vaccin Immunother*. 2014;10(11):3415-3424. doi:10.4161/hv.29407.

163. Coulie PG, Van den Eynde BJ, van der Bruggen P, Boon T. Tumour antigens recognized by T lymphocytes: at the core of cancer immunotherapy. *Nat Rev Cancer*. 2014;14(2):135-146. doi:10.1038/nrc3670.

164. Foulkes WD, Smith IE, Reis-Filho JS. Triple-negative breast cancer. *N Engl J Med*. 2010;363(20):1938-1948. doi:10.1056/NEJMra1001389.

165. Cao K, Hollenbach J, Shi X, Shi W, Chopek M, Fernández-Viña MA. Analysis of the frequencies of HLA-A, B, and C alleles and haplotypes in the five major ethnic groups of the United States reveals high levels of diversity in these loci and contrasting distribution patterns in these populations. *Hum Immunol*. 2001;62(9):1009-1030. http://www.ncbi.nlm.nih.gov/pubmed/11543903. Accessed March 24, 2016.

166. Rhodes DR, Yu J, Shanker K, et al. ONCOMINE: a cancer microarray database and integrated data-mining platform. *Neoplasia*. 6(1):1-6. http://www.pubmedcentral.nih.gov/articlerender.fcgi?artid=1635162&tool=pmcentrez&rendertype=abstract. Accessed November 5, 2015.

167. Rhodes DR, Kalyana-Sundaram S, Mahavisno V, et al. Oncomine 3.0: genes, pathways, and networks in a collection of 18,000 cancer gene expression profiles. *Neoplasia*. 2007;9(2):166-180. http://www.pubmedcentral.nih.gov/articlerender.fcgi?artid=1813932&tool=pmcentrez&rendertype=abstract. Accessed October 25, 2015.

168. Rhodes DR, Yu J, Shanker K, et al. Large-scale meta-analysis of cancer microarray data identifies common transcriptional profiles of neoplastic transformation and progression. *Proc Natl Acad Sci U S A*. 2004;101(25):9309-9314. doi:10.1073/pnas.0401994101.

169. Parker KC, Bednarek MA, Coligan JE. Scheme for ranking potential HLA-A2 binding peptides based on independent binding of individual peptide side-chains. *J Immunol*. 1994;152(1):163-175. http://www.ncbi.nlm.nih.gov/pubmed/8254189. Accessed January 29, 2016.

170. Andreatta M, Nielsen M. Gapped sequence alignment using artificial neural networks: application to the MHC class I system. *Bioinformatics*. October 2015. doi:10.1093/bioinformatics/btv639.

171. Larsen M V, Lundegaard C, Lamberth K, Buus S, Lund O, Nielsen M. Large-scale validation of methods for cytotoxic T-lymphocyte epitope prediction. *BMC Bioinformatics*. 2007;8:424. doi:10.1186/1471-2105-8-424.

172. Tsomides TJ, Walker BD, Eisen HN. An optimal viral peptide recognized by CD8+ T cells binds very tightly to the restricting class I major histocompatibility complex protein on intact cells but not to the purified class I protein. *Proc Natl Acad Sci U S A*. 1991;88(24):11276-11280. http://www.ncbi.nlm.nih.gov/pubmed/1722325. Accessed February 1, 2016.

173. Tsomides TJ, Aldovini A, Johnson RP, Walker BD, Young RA, Eisen HN. Naturally processed viral peptides recognized by cytotoxic T lymphocytes on cells chronically infected by human immunodeficiency virus type 1. *J Exp Med*. 1994;180(4):1283-1293. http://www.pubmedcentral.nih.gov/articlerender.fcgi?artid=2191672&tool=pmcentrez&rendertype=abstract. Accessed February 1, 2016.

174. Recognition of the highly conserved YMDD region in the human immunodeficiency virus type 1 reverse transcriptase by HLA-A2-restricted cytotoxic T l... - PubMed - NCBI. http://www.ncbi.nlm.nih.gov/pubmed/8568316. Accessed February 1, 2016.

175. Christensen O, Lupu A, Schmidt S, et al. Melan-A/MART1 analog peptide triggers anti-myeloma T-cells through crossreactivity with HM1.24. *J Immunother*. 32(6):613-621. doi:10.1097/CJI.0b013e3181a95198.

176. Nijman HW, Houbiers JG, Vierboom MP, et al. Identification of peptide sequences that potentially trigger HLA-A2.1-restricted cytotoxic T lymphocytes. *Eur J Immunol*. 1993;23(6):1215-1219. doi:10.1002/eji.1830230603.

177. Vikman S, Giandomenico V, Sommaggio R, Oberg K, Essand M, Tötterman TH. CD8+ T cells against multiple tumor-associated antigens in peripheral blood of midgut carcinoid patients. *Cancer Immunol Immunother*. 2008;57(3):399-409. doi:10.1007/s00262-007-0382-4.

178. Roskrow MA, Suzuki N, Gan Y, et al. Epstein-Barr Virus (EBV)-Specific Cytotoxic T Lymphocytes for the Treatment of Patients With EBV-Positive Relapsed Hodgkin's Disease. *Blood*. 1998;91(8).

179. Bryant J, Day R, Whiteside TL, Herberman RB. Calculation of lytic units for the expression of cell-mediated cytotoxicity. *J Immunol Methods*. 1992;146(1):91-103. http://www.ncbi.nlm.nih.gov/pubmed/1735786. Accessed January 20, 2017.

180. Keyaerts M, Verschueren J, Bos TJ, et al. Dynamic bioluminescence imaging for quantitative tumour burden assessment using IV or IP administration of D: -luciferin: effect on intensity, time kinetics and repeatability of photon emission. *Eur J Nucl Med Mol Imaging*. 2008;35(5):999-1007. doi:10.1007/s00259-007-0664-2.

181. Richardson AL, Wang ZC, De Nicolo A, et al. X chromosomal abnormalities in basal-like human breast cancer. *Cancer Cell*. 2006;9(2):121-132. doi:10.1016/j.ccr.2006.01.013.

182. Lee J-S, Leem S-H, Lee S-Y, et al. Expression signature of E2F1 and its associated genes predict superficial to invasive progression of bladder tumors. *J Clin Oncol*. 2010;28(16):2660-2667. doi:10.1200/JCO.2009.25.0977.

183. Murat A, Migliavacca E, Gorlia T, et al. Stem cell-related "self-renewal" signature and high epidermal growth factor receptor expression associated with resistance to concomitant chemoradiotherapy in glioblastoma. *J Clin Oncol*. 2008;26(18):3015-3024. doi:10.1200/JCO.2007.15.7164.

184. Zhai Y, Kuick R, Nan B, et al. Gene expression analysis of preinvasive and invasive cervical squamous cell carcinomas identifies HOXC10 as a key mediator of invasion. *Cancer Res*. 2007;67(21):10163-10172. doi:10.1158/0008-5472.CAN-07-2056.

185. Skrzypczak M, Goryca K, Rubel T, et al. Modeling oncogenic signaling in colon tumors by multidirectional analyses of microarray data directed for maximization of analytical reliability. *PLoS One*. 2010;5(10):e13091. doi:10.1371/journal.pone.0013091.

186. Su H, Hu N, Yang HH, et al. Global gene expression profiling and validation in esophageal squamous cell carcinoma and its association with clinical phenotypes. *Clin Cancer Res*. 2011;17(9):2955-2966. doi:10.1158/1078-0432.CCR-10-2724.

187. D'Errico M, de Rinaldis E, Blasi MF, et al. Genome-wide expression profile of sporadic gastric cancers with microsatellite instability. *Eur J Cancer*. 2009;45(3):461-469. doi:10.1016/j.ejca.2008.10.032.

188. Sengupta S, den Boon JA, Chen I-H, et al. Genome-wide expression profiling reveals EBV-associated inhibition of MHC class I expression in nasopharyngeal carcinoma. *Cancer Res*. 2006;66(16):7999-8006. doi:10.1158/0008-5472.CAN-05-4399.

189. Choi YL, Tsukasaki K, O'Neill MC, et al. A genomic analysis of adult T-cell leukemia. *Oncogene*. 2007;26(8):1245-1255. doi:10.1038/sj.onc.1209898.

190. Wurmbach E, Chen Y, Khitrov G, et al. Genome-wide molecular profiles of HCV-induced dysplasia and hepatocellular carcinoma. *Hepatology*. 2007;45(4):938-947. doi:10.1002/hep.21622.

191. Hou J, Aerts J, den Hamer B, et al. Gene expression-based classification of non-small cell lung carcinomas and survival prediction. *PLoS One*. 2010;5(4):e10312. doi:10.1371/journal.pone.0010312.

192. Riker AI, Enkemann SA, Fodstad O, et al. The gene expression profiles of primary and metastatic melanoma yields a transition point of tumor progression and metastasis. *BMC Med Genomics*. 2008;1:13. doi:10.1186/1755-8794-1-13.

193. Pei H, Li L, Fridley BL, et al. FKBP51 affects cancer cell response to chemotherapy by negatively regulating Akt. *Cancer Cell*. 2009;16(3):259-266. doi:10.1016/j.ccr.2009.07.016.

194. Lu X, Lu X, Wang ZC, Iglehart JD, Zhang X, Richardson AL. Predicting features of breast cancer with gene expression patterns. *Breast Cancer Res Treat*. 2008;108(2):191-201. doi:10.1007/s10549-007-9596-6.

195. Hou J, Aerts J, den Hamer B, et al. Gene expression-based classification of non-small cell lung carcinomas and survival prediction. *PLoS One*. 2010;5(4):e10312. doi:10.1371/journal.pone.0010312.

196. Rickman DS, Millon R, De Reynies A, et al. Prediction of future metastasis and molecular characterization of head and neck squamous-cell carcinoma based on transcriptome and genome analysis by microarrays. *Oncogene*. 2008;27(51):6607-6622. doi:10.1038/onc.2008.251.

197. Robinson G, Parker M, Kranenburg TA, et al. Novel mutations target distinct subgroups of medulloblastoma. *Nature*. 2012;488(7409):43-48. doi:10.1038/nature11213.

198. Scotto L, Narayan G, Nandula S V, et al. Identification of copy number gain and overexpressed genes on chromosome arm 20q by an integrative genomic approach in cervical cancer: potential role in progression. *Genes Chromosomes Cancer*. 2008;47(9):755-765. doi:10.1002/gcc.20577.

199. Yang XJ, Tan M-H, Kim HL, et al. A molecular classification of papillary renal cell carcinoma. *Cancer Res*. 2005;65(13):5628-5637. doi:10.1158/0008-5472.CAN-05-0533.

200. Jia H-L, Ye Q-H, Qin L-X, et al. Gene expression profiling reveals potential biomarkers of human hepatocellular carcinoma. *Clin Cancer Res*. 2007;13(4):1133-1139. doi:10.1158/1078-0432.CCR-06-1025.

201. Anglesio MS, Arnold JM, George J, et al. Mutation of ERBB2 provides a novel alternative mechanism for the ubiquitous activation of RAS-MAPK in ovarian serous low malignant potential tumors. *Mol Cancer Res*. 2008;6(11):1678-1690. doi:10.1158/1541-7786.MCR-08-0193.

202. Ishikawa M, Yoshida K, Yamashita Y, et al. Experimental trial for diagnosis of pancreatic ductal carcinoma based on gene expression profiles of pancreatic ductal cells. *Cancer Sci*.

2005;96(7):387-393. doi:10.1111/j.1349-7006.2005.00064.x.

203. Cancer Genome Atlas Research Network, Kandoth C, Schultz N, et al. Integrated genomic characterization of endometrial carcinoma. *Nature*. 2013;497(7447):67-73. doi:10.1038/nature12113.

204. Tothill RW, Tinker A V., George J, et al. Novel Molecular Subtypes of Serous and Endometrioid Ovarian Cancer Linked to Clinical Outcome. *Clin Cancer Res*. 2008;14(16):5198-5208. doi:10.1158/1078-0432.CCR-08-0196.

205. Stickeler E, Pils D, Klar M, et al. Basal-like molecular subtype and HER4 up-regulation and response to neoadjuvant chemotherapy in breast cancer. *Oncol Rep*. 2011;26(4):1037-1045. doi:10.3892/or.2011.1392.

206. Curtis C, Shah SP, Chin S-F, et al. The genomic and transcriptomic architecture of 2,000 breast tumours reveals novel subgroups. *Nature*. 2012;486(7403):346-352. doi:10.1038/nature10983.

207. Lindgren D, Liedberg F, Andersson A, et al. Molecular characterization of early-stage bladder carcinomas by expression profiles, FGFR3 mutation status, and loss of 9q. *Oncogene*. 2006;25(18):2685-2696. doi:10.1038/sj.onc.1209249.

208. Gibault L, Pérot G, Chibon F, et al. New insights in sarcoma oncogenesis: a comprehensive analysis of a large series of 160 soft tissue sarcomas with complex genomics. *J Pathol*. 2011;223(1):64-71. doi:10.1002/path.2787.

209. Ding L, Getz G, Wheeler DA, et al. Somatic mutations affect key pathways in lung adenocarcinoma. *Nature*. 2008;455(7216):1069-1075. doi:10.1038/nature07423.

210. Sun L, Hui A-M, Su Q, et al. Neuronal and glioma-derived stem cell factor induces angiogenesis within the brain. *Cancer Cell*. 2006;9(4):287-300. doi:10.1016/j.ccr.2006.03.003.

211. Phillips HS, Kharbanda S, Chen R, et al. Molecular subclasses of high-grade glioma predict prognosis, delineate a pattern of disease progression, and resemble stages in neurogenesis. *Cancer Cell*. 2006;9(3):157-173. doi:10.1016/j.ccr.2006.02.019.

212. Dyrskjøt L, Kruhøffer M, Thykjaer T, et al. Gene expression in the urinary bladder: a common carcinoma in situ gene expression signature exists disregarding histopathological classification. *Cancer Res*. 2004;64(11):4040-4048. doi:10.1158/0008-5472.CAN-03-3620.

213. Lee Y, Liu J, Patel S, et al. Genomic landscape of meningiomas. *Brain Pathol*. 2010;20(4):751-762. doi:10.1111/j.1750-3639.2009.00356.x.

214. Takeno A, Takemasa I, Seno S, et al. Gene expression profile prospectively predicts peritoneal relapse after curative surgery of gastric cancer. *Ann Surg Oncol*. 2010;17(4):1033-1042. doi:10.1245/s10434-009-0854-1.

215. Collisson EA, Sadanandam A, Olson P, et al. Subtypes of pancreatic ductal adenocarcinoma and their differing responses to therapy. *Nat Med*. 2011;17(4):500-503. doi:10.1038/nm.2344.

216. Schmidt M, Böhm D, von Törne C, et al. The humoral immune system has a key prognostic impact in node-negative breast cancer. *Cancer Res*. 2008;68(13):5405-5413. doi:10.1158/0008-5472.CAN-07-5206.

217. Shaknovich R, Geng H, Johnson NA, et al. DNA methylation signatures define molecular

subtypes of diffuse large B-cell lymphoma. *Blood*. 2010;116(20):e81-9. doi:10.1182/blood-2010-05-285320.

218. Lee E-S, Son D-S, Kim S-H, et al. Prediction of recurrence-free survival in postoperative non-small cell lung cancer patients by using an integrated model of clinical information and gene expression. *Clin Cancer Res*. 2008;14(22):7397-7404. doi:10.1158/1078-0432.CCR-07-4937.

219. Kuner R, Muley T, Meister M, et al. Global gene expression analysis reveals specific patterns of cell junctions in non-small cell lung cancer subtypes. *Lung Cancer*. 2009;63(1):32-38. doi:10.1016/j.lungcan.2008.03.033.

220. Zhao H, Ljungberg B, Grankvist K, Rasmuson T, Tibshirani R, Brooks JD. Gene expression profiling predicts survival in conventional renal cell carcinoma. *PLoS Med*. 2006;3(1):e13. doi:10.1371/journal.pmed.0030013.

221. Förster S, Gretschel S, Jöns T, Yashiro M, Kemmner W. THBS4, a novel stromal molecule of diffuse-type gastric adenocarcinomas, identified by transcriptome-wide expression profiling. *Mod Pathol*. 2011;24(10):1390-1403. doi:10.1038/modpathol.2011.99.

222. Zhan F, Huang Y, Colla S, et al. The molecular classification of multiple myeloma. *Blood*. 2006;108(6):2020-2028. doi:10.1182/blood-2005-11-013458.

223. Freije WA, Castro-Vargas FE, Fang Z, et al. Gene expression profiling of gliomas strongly predicts survival. *Cancer Res*. 2004;64(18):6503-6510. doi:10.1158/0008-5472.CAN-04-0452.

224. Phillips HS, Kharbanda S, Chen R, et al. Molecular subclasses of high-grade glioma predict prognosis, delineate a pattern of disease progression, and resemble stages in neurogenesis. *Cancer Cell*. 2006;9(3):157-173. doi:10.1016/j.ccr.2006.02.019.

225. Tabchy A, Valero V, Vidaurre T, et al. Evaluation of a 30-gene paclitaxel, fluorouracil, doxorubicin, and cyclophosphamide chemotherapy response predictor in a multicenter randomized trial in breast cancer. *Clin Cancer Res*. 2010;16(21):5351-5361. doi:10.1158/1078-0432.CCR-10-1265.

226. Bonnefoi H, Potti A, Delorenzi M, et al. Validation of gene signatures that predict the response of breast cancer to neoadjuvant chemotherapy: a substudy of the EORTC 10994/BIG 00-01 clinical trial. *Lancet Oncol*. 2007;8(12):1071-1078. doi:10.1016/S1470-2045(07)70345-5.

227. Hatzis C, Pusztai L, Valero V, et al. A genomic predictor of response and survival following taxane-anthracycline chemotherapy for invasive breast cancer. *JAMA*. 2011;305(18):1873-1881. doi:10.1001/jama.2011.593.

228. Zhao H, Langerød A, Ji Y, et al. Different gene expression patterns in invasive lobular and ductal carcinomas of the breast. *Mol Biol Cell*. 2004;15(6):2523-2536. doi:10.1091/mbc.E03-11-0786.

229. Chin K, DeVries S, Fridlyand J, et al. Genomic and transcriptional aberrations linked to breast cancer pathophysiologies. *Cancer Cell*. 2006;10(6):529-541. doi:10.1016/j.ccr.2006.10.009.

230. Kao K-J, Chang K-M, Hsu H-C, et al. Correlation of microarray-based breast cancer molecular subtypes and clinical outcomes: implications for treatment optimization. *BMC Cancer*. 2011;11(1):143. doi:10.1186/1471-2407-11-143.

231. Neve RM, Chin K, Fridlyand J, et al. A collection of breast cancer cell lines for the study of functionally distinct cancer subtypes. *Cancer Cell*. 2006;10(6):515-527.

doi:10.1016/j.ccr.2006.10.008.

232. Perret R, Ronchese F. Memory T cells in cancer immunotherapy: which CD8 T-cell population provides the best protection against tumours? *Tissue Antigens*. 2008;72(3):187-194. doi:10.1111/j.1399-0039.2008.01088.x.

233. Sallusto F, Lenig D, Förster R, Lipp M, Lanzavecchia A. Two subsets of memory T lymphocytes with distinct homing potentials and effector functions. *Nature*. 1999;401(6754):708-712. doi:10.1038/44385.

234. Mahnke YD, Brodie TM, Sallusto F, Roederer M, Lugli E. The who's who of T-cell differentiation: Human memory T-cell subsets. *Eur J Immunol*. 2013;43(11):2797-2809. doi:10.1002/eji.201343751.

235. Zuccolotto G, Fracasso G, Merlo A, et al. PSMA-Specific CAR-Engineered T Cells Eradicate Disseminated Prostate Cancer in Preclinical Models. Lapteva N, ed. *PLoS One*. 2014;9(10):e109427. doi:10.1371/journal.pone.0109427.

236. Iorns E, Drews-Elger K, Ward TM, et al. A New Mouse Model for the Study of Human Breast Cancer Metastasis. Kyprianou N, ed. *PLoS One*. 2012;7(10):e47995. doi:10.1371/journal.pone.0047995.

237. Di Minin G, Bellazzo A, Dal Ferro M, et al. Mutant p53 Reprograms TNF Signaling in Cancer Cells through Interaction with the Tumor Suppressor DAB2IP. *Mol Cell*. 2014;56(5):617-629. doi:10.1016/j.molcel.2014.10.013.

238. Rustighi A, Zannini A, Tiberi L, et al. Prolyl-isomerase Pin1 controls normal and cancer stem cells of the breast. *EMBO Mol Med*. 2014;6(1):99-119. doi:10.1002/emmm.201302909.

239. Itoh Y, Mizuki N, Shimada T, et al. High-throughput DNA typing of HLA-A, -B, -C, and -DRB1 loci by a PCR-SSOP-Luminex method in the Japanese population. *Immunogenetics*. 2005;57(10):717-729. doi:10.1007/s00251-005-0048-3.

240. Gattinoni L, Klebanoff CA, Palmer DC, et al. Acquisition of full effector function in vitro paradoxically impairs the in vivo antitumor efficacy of adoptively transferred CD8+ T cells. *J Clin Invest*. 2005;115(6):1616-1626. doi:10.1172/JCI24480.

241. Robbins PF, Dudley ME, Wunderlich J, et al. Cutting edge: persistence of transferred lymphocyte clonotypes correlates with cancer regression in patients receiving cell transfer therapy. *J Immunol*. 2004;173(12):7125-7130. http://www.ncbi.nlm.nih.gov/pubmed/15585832. Accessed November 2, 2016.

242. Roberts AD, Ely KH, Woodland DL. Differential contributions of central and effector memory T cells to recall responses. *J Exp Med*. 2005;202(1):123-133. doi:10.1084/jem.20050137.

243. Speiser DE, Baumgaertner P, Barbey C, et al. A novel approach to characterize clonality and differentiation of human melanoma-specific T cell responses: spontaneous priming and efficient boosting by vaccination. *J Immunol*. 2006;177(2):1338-1348. doi:10.4049/JIMMUNOL.177.2.1338.

244. Nerlich AG, Bachmeier BE. Density-dependent lineage instability of MDA-MB-435 breast cancer cells. *Oncol Lett*. 2013;5(4):1370-1374. doi:10.3892/ol.2013.1157.

245. Jin J, Sabatino M, Somerville R, et al. Simplified method of the growth of human tumor infiltrating lymphocytes in gas-permeable flasks to numbers needed for patient treatment. *J Immunother*. 2012;35(3):283-292. doi:10.1097/CJI.0b013e31824e801f.

246. Callahan MK, Wolchok JD. At the bedside: CTLA-4- and PD-1-blocking antibodies in cancer immunotherapy. *J Leukoc Biol*. 2013;94(1):41-53. doi:10.1189/jlb.1212631.

RINGRAZIAMENTI

Un ringraziamento particolare al **Prof. Antonio Rosato**,

per il contributo teorico, professionale e umano a questo progetto.

Grazie anche a tutte le mie colleghe di laboratorio, per i preziosi consigli e tutto l'aiuto dato.

Infine, un immenso grazie va al Prof. Jerome Galon, per avermi accettata nel suo laboratorio,

e alla Dr.ssa Angela Vasaturo, per tutti gli inestimabili insegnamenti.